

OPEN FILE REPORT O-15-04

**GEOLOGIC MAP OF THE SOUTHERN OREGON COAST BETWEEN
BANDON, COQUILLE, AND SUNSET BAY, COOS COUNTY, OREGON**

by Thomas J. Wiley¹, Jason D. McClaughry², Clark A. Niewendorp¹, Lina Ma¹,
Heather H. Herinckx³, and Katherine A. Mickelson¹



2015

¹ Oregon Department of Geology and Mineral Industries, 800 NE Oregon Street, Suite 965, Portland, OR 97232

² Oregon Department of Geology and Mineral Industries, Baker City Field Office, Baker County Courthouse, 1995 3rd Street, Suite 130, Baker City, OR 97814

³ Department of Geology, Portland State University, 17 Cramer Hall, 1721 SW Broadway Street, Portland, OR 97201

NOTICE

This manuscript is submitted for publication with the understanding that the United States Government is authorized to reproduce and distribute reprints for governmental use. The views and conclusions contained in this document are those of the authors and should not be interpreted as necessarily representing the official policies, either expressed or implied, of the U.S. government.

This product is for informational purposes and may not have been prepared for or be suitable for legal, engineering, or surveying purposes. Users of this information should review or consult the primary data and information sources to ascertain the usability of the information. This publication cannot substitute for site-specific investigations by qualified practitioners. Site-specific data may give results that differ from the results shown in the publication.

Cover photograph: East-dipping beds of concretion-bearing sandstone that make up the lower Coaledo Formation at Shore Acres State Park in the northwest part of the map area. The view is looking north along the coast, from the parking area viewpoint (WGS84 geographic coordinates: 387536mE., 4797781mN.).

Photo credit: Jason McClaughry, 2014

Oregon Department of Geology and Mineral Industries Open-File Report O-15-04
Published in conformance with ORS 516.030

For additional information:
Administrative Offices
800 NE Oregon Street, Suite 965
Portland, OR 97232
Telephone (971) 673-1555
Fax (971) 673-1562
<http://www.oregongeology.org>
<http://www.oregon.gov/dogami>

TABLE OF CONTENTS

| | |
|--|----|
| INTRODUCTION | 1 |
| GEOGRAPHIC AND GEOLOGIC SETTING | 4 |
| Siletz terrane | 6 |
| Sixes River terrane. | 6 |
| Paleogene overlap sequence. | 7 |
| Lower Pleistocene and Miocene rocks. | 7 |
| Surficial deposits. | 7 |
| PREVIOUS WORK. | 8 |
| METHODOLOGY | 10 |
| EXPLANATION OF MAP UNITS | 11 |
| Overview of map units along the southwest Oregon coast. | 12 |
| Upper Cenozoic surficial deposits | 15 |
| Lower Cenozoic and Mesozoic rocks. | 25 |
| STRUCTURAL GEOLOGY | 35 |
| Sixes River terrane. | 35 |
| Siletz terrane | 36 |
| Terrane bounding faults. | 36 |
| Younger (post-amalgamation) deformation | 37 |
| Elevated marine platforms | 40 |
| ACKNOWLEDGMENTS | 40 |
| REFERENCES. | 41 |
| APPENDIX—GEOGRAPHIC INFORMATION SYSTEMS (GIS) DATABASE | 49 |
| Geodatabase specifications | 49 |
| Geologic maps | 52 |
| Geochemical analytical methods | 53 |
| Geochronology analytical methods | 54 |
| Bedding (strike and dip). | 55 |
| Water well logs | 56 |

LIST OF FIGURES

| | | |
|-------------------|---|----|
| Figure 1. | Location of the southern coast study area in Oregon | 2 |
| Figure 2. | Current project area. | 3 |
| Figure 3. | Tectonic setting of the Pacific Northwest region of the United States | 4 |
| Figure 4. | Tectonostratigraphic terranes in southwestern Oregon | 5 |
| Figure 5. | Sources of geologic mapping used during the preparation of this report | 9 |
| Figure 6. | Time-rock chart showing the 51 geologic units in the Bandon, Coquille, and Sunset Bay areas | 14 |
| Figure 7. | High water on the flood plain of Coquille River Valley southwest of Highway 42S near Coquille, Oregon | 15 |
| Figure 8. | Sandstone of Fivemile Point | 30 |
| Figure 9. | Distinctive light-colored clasts in quarry blocks of sandstone of Fivemile Point | 32 |
| Figure 10. | Recumbent fold in beds at Sacchi Beach | 39 |
| Figure A1. | Southern Oregon coast geodatabase feature data sets. | 49 |
| Figure A2. | Relationships between tables and MapUnitPolys feature class in the geodatabase | 49 |
| Figure A3. | Southern Oregon coast geodatabase feature classes | 50 |
| Figure A4. | Southern Oregon coast geodatabase relationships | 51 |
| Figure A5. | Thumbnails of map plates accompanying this report. | 52 |

LIST OF TABLES

| | | |
|-----------------|--|----|
| Table 1. | Partial chronological listing of maps and reports on which this study builds | 8 |
| Table 2. | Correlation of marine terraces along the southern and central Oregon coast. | 22 |
| Table 3. | Representative X-ray fluorescence analyses for rocks in the Bandon, Coquille, and Sunset Bay areas | 31 |

MAP PLATES

| | |
|-----------------|---|
| Plate 1. | Geologic map of the Bill Peak 7.5' quadrangle, Coos County, Oregon, scale 1:24,000 |
| Plate 2. | Geologic map of the Coquille 7.5' quadrangle, Coos County, Oregon, scale 1:24,000 |
| Plate 3. | Geologic map of the Bullards and Riverton 7.5' quadrangles, Coos County, Oregon, scale 1:24,000 |
| Plate 4. | Geologic map of the Cape Arago 7.5' quadrangle, Coos County, Oregon, scale 1:24,000 |

GEODATABASE, SHAPE FILES, AND SPREADSHEETS (ALSO SEE APPENDIX)

Esri v. 10.1 formatted geodatabase: SC2015_v10.1_v2.gdb

| | | |
|---|--------------------------|--------------------------|
| Geochemistry spreadsheet and shapefile: | SC2015_Geochemistry.xls | SC2015_Geochemistry.shp |
| Geochronology spreadsheet and shapefile: | SC2015_Geochronology.xls | SC2015_Geochronology.shp |
| includes subfolder NEW_UPB_ANALYTICALDATA: TableDR1 LA-ICPMS Final_FY14.xls | | |
| Bedding spreadsheet and shapefile: | SC2015_Bedding.xls | SC2015_Bedding.shp |
| Water well spreadsheet and shapefile: | SC2015_WaterWells.xls | SC2015_WaterWells.shp |
| Reference map shapefile: | | SC2015_RefMap.shp |

INTRODUCTION

This report, digital geodatabase, and the accompanying set of plottable geologic maps were prepared to provide an updated and spatially accurate geologic framework for the southern Oregon coast between Bandon, Coquille, and Sunset Bay in western Coos County (Figure 1). Geologic mapping summarized here represents one part of a multi-year project to map the Oregon coast from the California border north to Coos Bay (Figure 2). The project is a high priority of the Oregon Geologic Map Advisory Committee (OGMAC) and was supported in part during 2014 and 2015 by the U.S. Geological Survey (USGS) STATEMAP component of the National Cooperative Geologic Mapping Program under assistance award G14AC00165. Matching funds were provided by the Oregon Department of Geology and Mineral Industries (DOGAMI). The core product of this study is an Esri ArcGIS® ArcMap® 10.1 format geodatabase that combines new and existing mapping in a digital format consistent with the digital statewide Oregon Geologic Data Compilation database (OGDC-5, Ma and others, 2009). Both bedrock and surficial geologic interpretations can be recovered from the geodatabase. It contains spatial

information about geologic units and structures, and basic data about each geologic unit such as age, lithology, mineralogy, and structure. Digitization at scales of 1:8,000 or better was accomplished using georeferenced lidar base layers. The geodatabase is supported by this report describing the geology in detail and by digital appendices with geochemical, geochronological, structural, and water well data. Four plottable geologic maps, showing the distribution of contrasting bedrock lithologies, critical structural relationships, and surficial geology, cover the Bill Peak 7.5' quadrangle (Plate 1), the Coquille 7.5' quadrangle (Plate 2), the Bullards and Riverton 7.5' quadrangles (Plate 3), and the Cape Arago 7.5' quadrangle (Plate 4) at a scale of 1:24,000. These maps refine our understanding of geologic conditions that control the distribution, quantity, and quality of groundwater resources, the distribution of terrain susceptible to landslides, the nature of seismic hazards, and the distribution of potential aggregate sources and other mineral resources. The geodatabase provides a basis for future geologic, geohydrologic, and geohazard studies in this part of the southern Oregon coast.

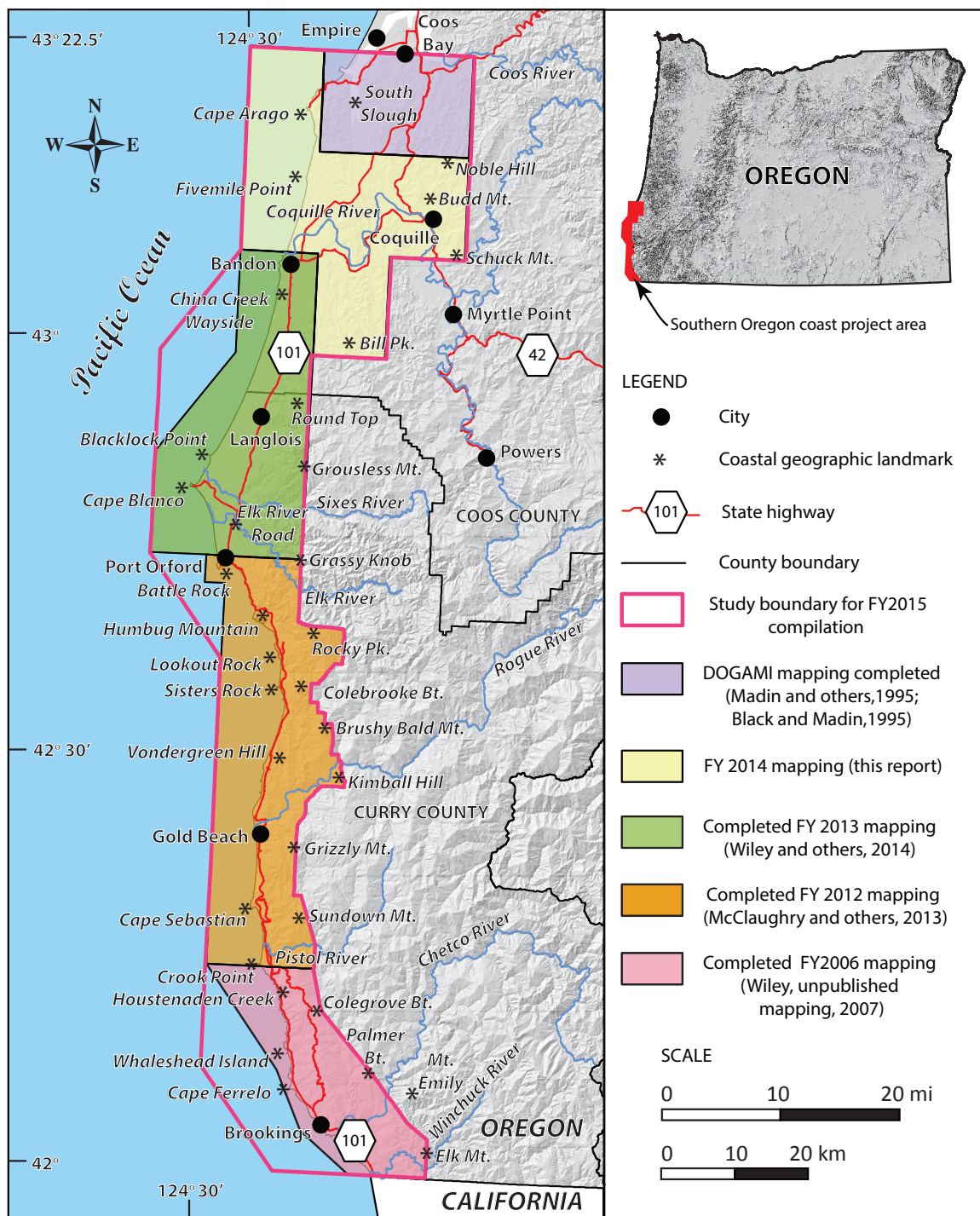


Figure 1. Location of the southern coast study area in Oregon (pink outline), including major cities, geographic locations, and highways discussed in the text. The tan polygon shows the Bandon-Coquille-Sunset Bay area mapped by the Oregon Department of Geology and Mineral Industries during FY2014 and discussed in this report; the pink polygon is the area mapped for FY2006 (T. J. Wiley, unpublished mapping, 2007); the orange polygon is the area mapped for FY2012 (McClaghry and others, 2013); the green polygon is the area mapped during FY2013 (Wiley and others, 2014); the purple polygon is an area mapped at the 1:24,000 scale by Madin and others (1995) and Black and Madin (1995).

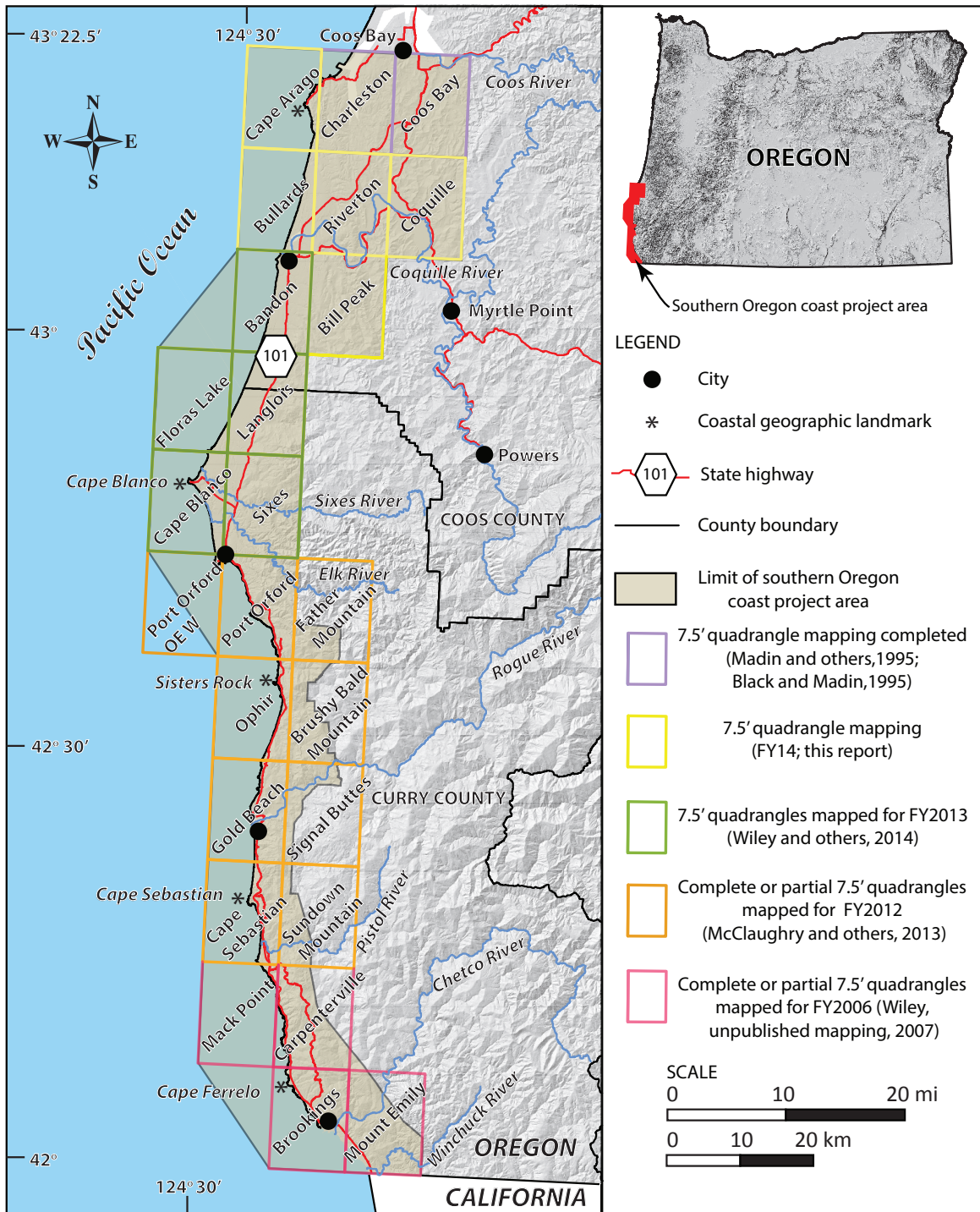


Figure 2. The current project area (yellow-outlined 7.5' quadrangles) encompasses five 7.5' quadrangles covering approximately 468 km² (181 mi²) along the southern Oregon coast. Shaded area is the entire southern Oregon coast mapping area. Pink-outlined quadrangles include geologic mapping completed during FY2006; orange-outlined quadrangles include geologic mapping completed during FY2012; green-outlined quadrangles include geologic mapping completed during FY2013; purple-outlined quadrangles were mapped at the 1:24,000 scale by Madin and others (1995) and Black and Madin (1995).

GEOGRAPHIC AND GEOLOGIC SETTING

The coastal region of central Coos County, Oregon, is typically rugged, with a 1- to 4-km-wide (0.6 to 2.5 mi), wave-cut coastal bench that transitions abruptly into deeply incised, upland topography of uplifted marine terraces that ramp onto the Oregon Coast Range to the east. Topographic relief is moderate, ranging from sea-level to numerous ridges and mountains including, from south to north, Bill Peak (460 m [1,510 ft]), Grigsby Rock (412 m [1,352 ft]), Lampa Mountain (240 m [787 ft]), Schuck Mountain (293 m [962 ft]), Budd Mountain (136 m [447 ft]), Noble Hill (261 m [855 ft]), and Arago Peak (225 m [736 ft]) (Figure 1; map plates [note that elevations shown on map plates are lidar derived]). The Coast Range is drained in the map area by a number of west-flowing streams. Major stream drainages include Bear Creek, the Coquille River, Cunningham Creek, Beaver Creek, Sevenmile Creek, Whiskey Run, Twomile Creek, Threemile Creek, and Fivemile Creek. The rugged coastal relief is accompanied by a wet maritime climate (precipitation is ~188 cm/year [74 in/year]) and dense vegetation. Due to steep topography and thick, impenetrable forests, good outcrops of unaltered rock are generally limited to sea stacks, coastal bluffs, stream bottoms, roadcuts, and areas of active logging.

Bedrock geology along the central Coos County coast is composed of two complexly folded and faulted tectonostratigraphic terranes, the Sixes River and Siletz terranes, and a less deformed clastic overlap sequence. The two terranes record a history of oceanic and continental margin sedimentation, magmatism, and terrane accretion from the Late Jurassic into the Eocene (Dott, 1971; Roure and Blanchett, 1983; Blake and others, 1985; Diller, 1896, 1901, 1903). These terranes are now situated inboard of the active Cascadia subduction zone, where oceanic crust is presently being obliquely subducted beneath the North American continental plate (Figure 3). Jurassic to Eocene aged sedimentary rocks and mélangé (Hsü, 1968; Silver and Beutner, 1980; Cowan, 1985; Festa and others, 2010, 2012; Raymond, 1984) of the Sixes River terrane are in fault contact with Paleogene volcanic and sedimentary rocks of the Siletz terrane. South and east of the study area these two terranes are faulted against terranes of the Klamath Mountains province along the Canyonville fault to the south and unnamed thrust faults to the east. South of the Siletz terrane, six discrete terranes underlie the coastal area of southwestern Oregon (Blake and others, 1985) (Figure 4), all of which are separated by major faults or fault zones. Several of these fault zones are low-angle thrusts, so that the terrane assemblage represents stacks of subhorizontal

nappes. In addition to the Siletz and Sixes River terranes of the study area, terranes assembled nearby include the Gold Beach, Pickett Peak, Western Klamath (Elk subterrane), Snow Camp, and Yolla Bolly terranes (Blake and others, 1985; Giaramita and Harper, 2006). The terranes that lie south of the Canyonville fault are unconformably overlain by less deformed Upper Cretaceous and younger sedimentary sequences that constrain the minimum ages for terrane amalgamation.

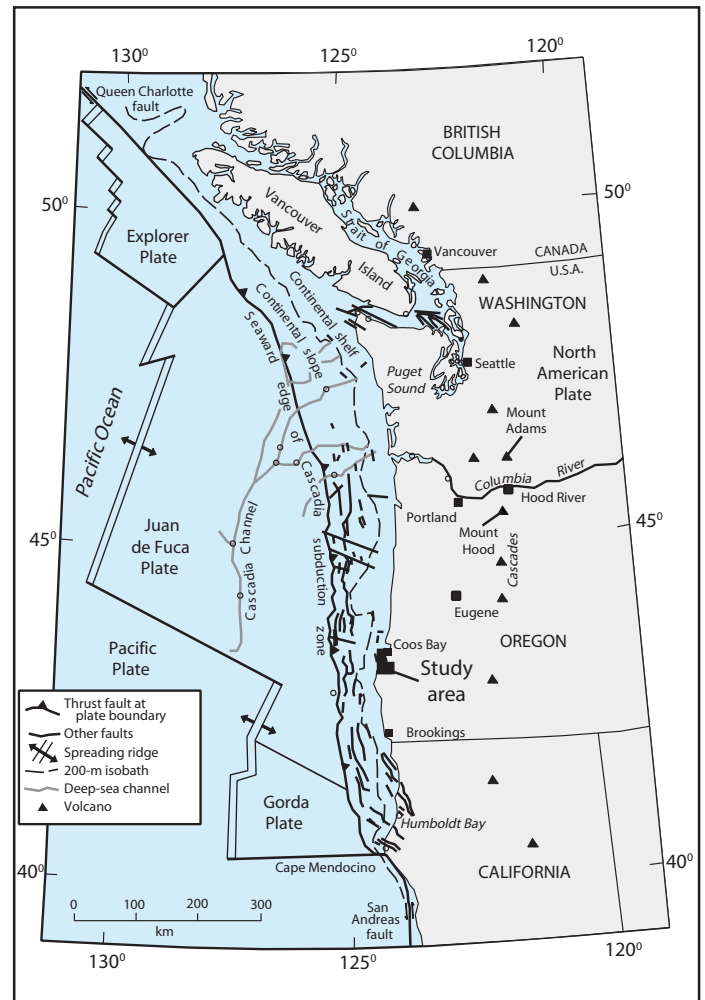


Figure 3. Tectonic setting of the United States Pacific Northwest region showing the Cascadia Subduction Zone and regional plate boundaries, selected Quaternary faults in the North American plate, and the location of the study area along the southern Oregon coast (modified from Nelson and others, 2004). The deformation front (barbed line) is defined by bathymetry where the abyssal plain meets the continental slope and is inferred to represent the surface projection of the Cascadia thrust fault. Triangles depict major Cascade Range volcanoes/

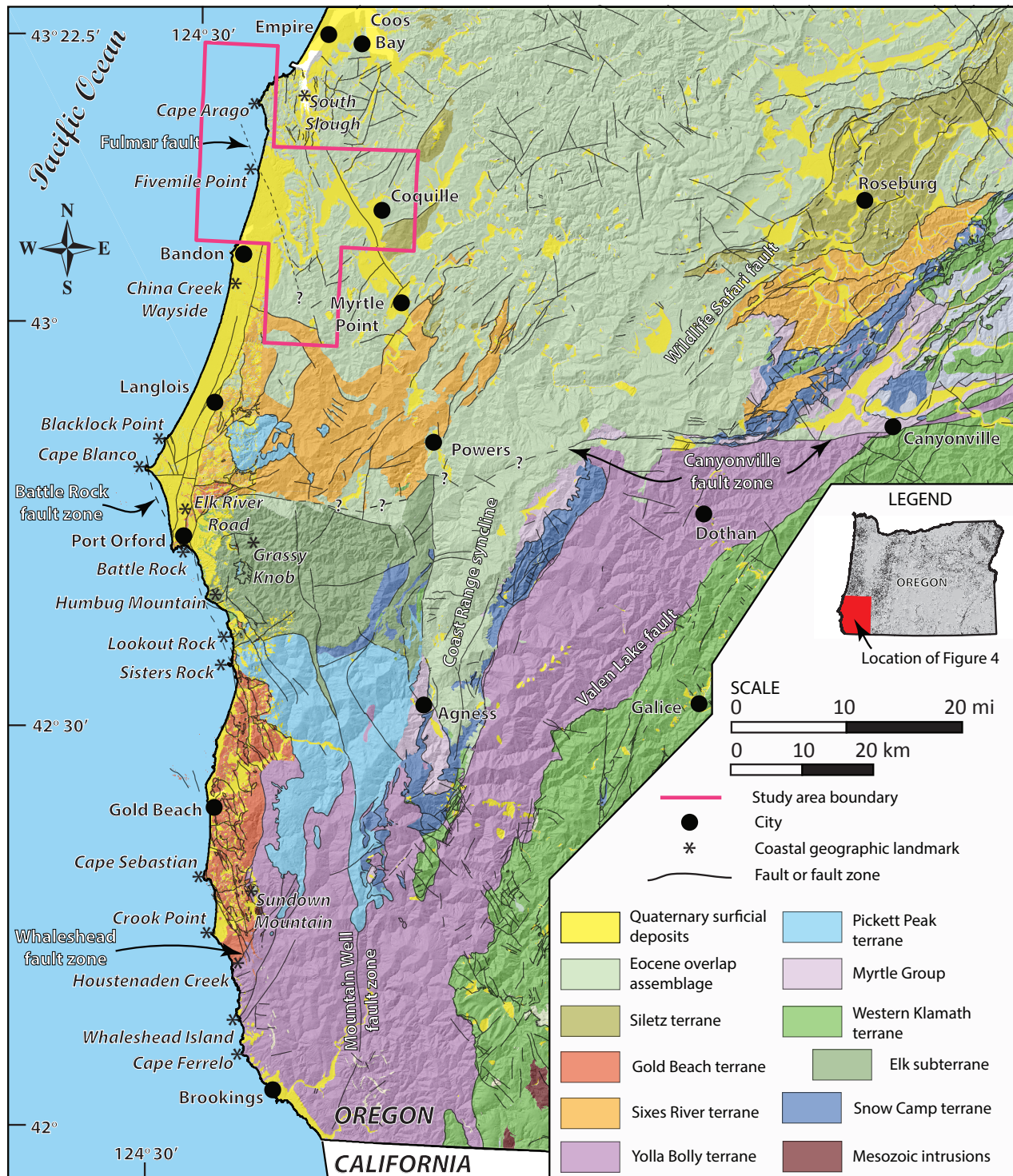


Figure 4. Tectonic sketch map showing tectonostratigraphic terranes of southwestern Oregon. Geology from Ma and others (2009) with terrane boundaries modified from Blake and others (1985). Magenta outline shows the study boundary of the geologic mapping discussed in this report.

Siletz terrane

The Siletz terrane consists of a thick accumulation of upper Paleocene and lower Eocene tholeiitic and alkalic submarine and subaerial basalt flows, diabase and gabbro intrusive rocks, submarine breccias, marine sedimentary rocks, and rare silicic flows exposed in anticlinal uplifts from southern Washington to Roseburg and Coquille, Oregon (Figure 4; Silberling and others, 1987; Howell and others, 1985; Wells and others, 2000, 2014). In Oregon, this terrane includes the Siletz River Volcanics, a sequence of rocks emplaced as seamounts built on oceanic crust (Snively and others, 1968). These rocks form part of a larger oceanic terrane, Siletzia, which was accreted to North America during the Eocene (Wells and others, 2014). North of the Canyonville fault, these rocks are overlain by lower Eocene sedimentary rocks and are thrust beneath the Sixes River terrane along the Wildlife Safari and related faults that may lie in the subsurface in the southeastern part of the Bill Peak quadrangle.

Sixes River terrane

The Sixes River terrane (Figure 4) includes sediment-matrix mélange and intensely sheared broken formation that includes Tertiary, Upper Cretaceous, Lower Cretaceous and Upper Jurassic strata. Mélange units within the Sixes River terrane are defined by numerous exotic tectonic blocks (knockers) including high-grade blueschist (Brown and Blake, 1987; Medaris, 1972), garnet-bearing schist, and eclogite (Coleman and Lanphere, 1971). Following Wiley and others (2014), the Sixes River terrane is divided into three adjacent subterrane that each contain blocks of exotic blueschist and garnet blueschist but have important tectonostratigraphic features that are not shared. The Fulmar subterrane is present within the map area. The Whitsett subterrane lies east of the Fulmar fault and extends east of Interstate 5 in Douglas County; it may be present beneath the southeastern corner of the Bill Peak quadrangle. The Cape Blanco subterrane is exposed south of the study area between Blacklock Point and Cape Blanco. Sedimentary rocks within the Sixes River terrane were previously mapped as part of the Otter Point Formation by Lent (1969), Beaulieu and Hughes (1976), and Brownfield and others (1982). Unlike the Otter Point Formation in the Gold Beach terrane (Aalto, 1968; Aalto and Dott, 1970; Dott, 1971; Goodfellow, 1987; Garey, 1987), the sedimentary sequences in the Sixes River terrane have a quartzofeldspathic composition (Lent, 1969).

Fulmar (central) subterrane. The Fulmar (central) subterrane of the Sixes River terrane includes a mudstone and fine-sandstone matrix mélange overlain by lower Eocene

sedimentary rock. The lower Eocene section includes turbidites that are part of the sandstone of Fivemile Point (**Tefm**), a mica-poor, arkosic wacke that differs from lower Eocene volcanoclastic sandstone recognized as part of the Whitsett subterrane and Siletz terrane to the east (Snively, 1987). The Fulmar subterrane is unconformably overlain by an Eocene sedimentary overlap sequence that includes the upper part of the Umpqua Group (**Teu**), Tyee Formation (**Tet**), beds at Sacchi Beach (**Tes**), and Coaledo Formation (**Tecl**, **Tecm**, **Tecu**). The boundary between the Fulmar subterrane on the east and the Cape Blanco subterrane on the west is considered to be the Blacklock Point fault zone, a significant shear zone that juxtaposes mélange of the Cape Blanco subterrane, serpentinite, and Upper Cretaceous sedimentary rocks at Blacklock Point.

Whitsett (eastern) subterrane (not present at the surface in the study area, may be present in the subsurface). The Whitsett (eastern) subterrane of the Sixes River terrane also includes a basal mudstone- and fine-sandstone-matrix mélange; but this mélange is unconformably overlain by Cretaceous(?) and lower Eocene sedimentary rocks. Mélange assigned to this subterrane crops out 10 km (6 mi) miles east of the Bill Peak quadrangle. It may be present in the subsurface in the extreme southeastern part of the study area but is not exposed at the surface. The Whitsett subterrane is distinguished from the Fulmar and Cape Blanco subterrane by the presence of possible Cretaceous sandstone that unconformably overlies the mélange and by the presence of the exotic Whitsett limestone lentils of Diller (1898). This group of far-traveled mid-Cretaceous age (Albian and/or Cenomanian, ca. 113 to 93.9 Ma) limestone blocks crops out south of Roseburg and probably originated in southern latitudes (Sliter, 1984). The Whitsett subterrane is separated from the Fulmar subterrane by the north-northwest-trending Fulmar fault zone. Snively and others (1980) recognized that the Fulmar fault separates stratigraphically different sequences in offshore areas northwest of Fivemile Point. The trace of the fault mapped here, or perhaps a parallel strand buried beneath the Eocene overlap sequence to the east, separates the Whitsett subterrane and the Siletz terrane to the east from the Fulmar subterrane.

Cape Blanco (western) subterrane (not present in the study area). The Cape Blanco (western) subterrane of the Sixes River terrane lies south of the map area. It consists of mudstone- and fine-sandstone-matrix mélange that enclose a suite of harder blocks of various lithologies including sandstone, conglomerate, chert, serpentinite, glaucophane schist, and garnet-bearing schist. These rocks differ from

the other two subterrane of the Sixes River terrane in that they contain relatively mica-poor middle Eocene turbidites at Cape Blanco (Bandy, 1944; Dott, 1962, 1965) that form part of the *mélange* matrix (Wiley and others, 2014). The mica-poor rocks at Cape Blanco contrast markedly with the micaceous beds at Sacchi Beach assigned to the sequence that overlaps the Siletz terrane, Fulmar subterrane, and Whitsett subterrane. The *mélange* in the Cape Blanco area is therefore much younger than fossil ages suggest for the *mélange* in the Fulmar and Whitsett subterrane to the east. The Cape Blanco subterrane is separated from the Gold Beach terrane by the northern extension of the Battle Rock–Whaleshead fault zone and from the Fulmar subterrane by the Blacklock Point fault or a similar fault buried beneath Miocene and younger sedimentary rocks farther east.

Paleogene overlap sequence

The Siletz and Sixes River terranes are unconformably overlain by an Eocene overlap sequence. These strata include the upper part of the Umpqua Group and the Tyee, Coaledo, and Bastendorff Formations (Baldwin, 1974; Molenaar, 1985). These strata are interpreted as nearshore, deltaic, shelf, and submarine fan deposits that accumulated in marginal basins above the terrane boundary. Sediment source areas were largely located in the uplifted Klamath Mountains and the continental interior (Figure 4). Paleogene overlap assemblages constrain the northward translation and age of docking of the Siletz and Sixes River terranes to this part of Oregon to ca. 50 Ma.

The overlap sequence alternates between sandstone- and mudstone-dominated strata at many scales. Regionally, these transitions can be understood in sequence stratigraphic terms and interpreted as resulting from repeated cycles of transgression and regression related to a combination of local tectonics and global sea level change. Similar interpretations have been made elsewhere for Paleogene rocks

in Oregon including McKeel (1984), Ryu and Niem (1999), and McClaughry and others (2010). The nature of Paleogene sedimentary rocks in southwestern Oregon suggests that sea level change played an important role in determining the distribution of clastic rock types. Comparison of the timing and magnitude of these sea level changes with global sea level data suggests that both global sea level change and local tectonics were important. Overall, the Paleogene overlap sequence in this area records at least six major sea level transgressions from deepwater turbidite sequences to shallow marine shelf sequences including 1) the Tenmile to Whitetail Ridge Formations, 2) Camas Valley Formation to the disconformity at the base of the Tyee Formation, 3) Tyee Mountain Member to Hubbard Creek Member to Baughman Member of the Tyee Formation, 4) beds at Sacchi Beach to the Lower Member of Coaledo Formation, 5) Middle to Upper Members of Coaledo Formation, and 6) Bastendorff Shale to Tunnel Point Sandstone.

Lower Pleistocene and Miocene rocks

Within the study area, the late Pleistocene Coquille Formation is set into *mélange* of the Fulmar subterrane of the Sixes River terrane north of Bandon where it lies beneath younger marine terrace deposits and buries the sandstone of Fivemile Point (**Tefm**) south of Whiskey Run (Baldwin, 1945).

Miocene rocks have not been recognized in the map area. They crop out nearby to the north (Allen and Baldwin, 1944; Madin and others, 1995) and to the south (Bandy, 1941; Orr and Zaitzeff, 1970; Orr and others, 1971; Fowler and others, 1971; Addicott, 1983; Emerson, 2007; Raymond and others, 2008; Wiley and others, 2014).

Surficial deposits

Upper Pleistocene and younger marine terrace, landslide, beach, dune, river, and fan deposits mantle older rocks throughout the study area.

PREVIOUS WORK

Table 1 shows a list of previous regional geologic investigations that were used to inform this study of the southern Oregon coast. Reports listed in Table 1 are organized in chronological order; those shown in bold are geologic maps that lie within the study area. The index map shown in Figure 5 summarizes the sources of mapping used for our geologic depiction and other sources consulted during the preparation of this report. Following Diller (1899, 1901), the geology of the coastal area between Bandon, Coquille, and Sunset Bay has been mapped by a number of workers, each focusing on parts of the area and at a variety of scales (Baldwin, 1966; Ehlen, 1967; Baldwin, 1969; Baldwin and others, 1973; Rooth, 1974; Beaulieu and Hughes, 1975; Newton and others, 1980; Walker and McLeod, 1991; Goldfinger and others, 1992; Madin and others, 1995; Black and Madin, 1995). Various other studies have examined more detailed aspects of the local and regional geology (Allen and Baldwin, 1944; Baldwin, 1965; Dott, 1966; Baldwin, 1974; Ryberg, 1978; Robertson, 1982; Dott and Bourgeois, 1982; Heller, 1983; Blake and others, 1985; Heller and others, 1987; Ryu and others, 1992; Prothero and Donohoo, 2001), distribution of coal resources (Diller, 1899; Allen and Baldwin, 1944; Toenges and others, 1948; Duncan, 1953), chromite (Griggs, 1945); oil and gas potential in the Coos basin (Rau, 1973; Newton and others, 1980; McKeel, 1984), and coastal landforms were examined by Lund (1973). The tectonics of Pleistocene coastal terraces has been discussed by Janda (1969, 1970), Kelsey (1990), Muhs and others (1990), McInelly and Kelsey (1990), and Kelsey and Bockheim (1994). Tsunami hazards on the southern Oregon coast have been discussed by Kelsey and others (1998, 2003, 2005); tsunami hazard maps have been produced by DOGAMI for the coast between Bandon and Coos Bay (DOGAMI, 2012a-f; Priest and Baptista, 1995a,b; Priest and others, 2002). A hazard inventory map of the Oregon coastal zone was prepared by Beaulieu and others (1974).

Table 1. Partial chronological listing of maps and reports on which this study builds.

| Author | Year | Subject | Scale |
|--------------------------------|-------------|---|---------------------|
| Diller | 1899 | The coos Bay coal field | |
| Diller | 1901 | Description of the Coos Bay quadrangle | |
| Allen & Baldwin | 1944 | Description and resources of the Coos Bay quadrangle | 1:96,500 |
| Baldwin | 1945 | Cenozoic stratigraphy, southern Oregon coast | |
| Griggs | 1945 | Chromite bearing sands | |
| Addicott | 1964 | Invertebrate fauna of southwestern Oregon | |
| Duncan | 1953 | Geology and coal deposits in part of the Coos Bay coal field | |
| Baldwin | 1965 | Geology of the south end of the Oregon Coast Range Tertiary Basin | |
| Dott | 1966 | Eocene deltaic sedimentation at Coos Bay | |
| Baldwin | 1966 | Revisions to the geology of the Coos Bay area | 1:15,840 |
| Ehlen | 1967 | Geology of state parks near Cape Arago | |
| Baldwin | 1969 | Geologic map of the Myrtle Point area | 1:48,000 |
| Janda | 1969 | Age of marine terraces near Cape Blanco | |
| Brownfield | 1972 | Geology of the Floras Creek drainage | 1:31,250 |
| Rau | 1973 | Preliminary identification of foraminifera, Coos County No. 1-7 well | |
| Baldwin & others | 1973 | Geology and mineral resources of Coos County | 1:62,500 |
| Rooth | 1974 | Biostratigraphy and paleoecology of the Coaledo and Bastendorff Fms. | |
| Baldwin | 1974 | Eocene stratigraphy of southwestern Oregon | |
| Beaulieu & others | 1974 | Geologic hazards inventory of the Oregon coastal zone | 1:250,000 |
| Beaulieu & Hughes | 1975 | Environmental geology of western Coos and Douglas Counties | 1:62,500 |
| Ryberg | 1978 | Lithofacies and depositional environments Coaledo Fm. | |
| Newton & others | 1980 | Prospects for oil and gas in the Coos Bay basin | |
| Brownfield & others | 1982 | Geologic map of the Langlois quadrangle | 1:62,500 |
| Robertson | 1982 | Subsurface stratigraphic correlations Eocene Coaledo Fm. | |
| Heller | 1983 | Sedimentary response to Eocene tectonic rotation in w. Oregon | |
| McKeel | 1984 | Biostratigraphy of exploratory wells, western Coos County | |
| Blake & others | 1985 | Tectonostratigraphic terranes in southwest Oregon | |
| Clarke & others | 1985 | Reconnaissance geology offshore Coos Bay basin | |
| Seiders & Blome | 1987 | Upper Cretaceous rocks in coastal southwest Oregon | |
| Heller & others | 1987 | Paleogeographic evolution of the United States Pacific Northwest | |
| Kelsey | 1990 | Deformation of coastal terraces near Cape Blanco | 1:728,952 |
| McInelly & Kelsey | 1990 | Deformation of coastal terraces near Bandon | 1:10,934,280 |
| Muhs & others | 1990 | Uplift rates for late Pleistocene marine terraces | |
| Walker & MacLeod | 1991 | Geologic map of Oregon | 1:500,000 |
| Goldfinger & others | 1992 | Neotectonic map of the Oregon continental margin | 1:392,832 |
| Madin & others | 1995 | Geologic map of the Charleston quadrangle | 1:24,000 |
| Black & Madin | 1995 | Geologic map of the Coos Bay quadrangle | 1:24,000 |
| Prothero & Donohoo | 2001 | Magnetic stratigraphy middle Eocene Coaledo Fm. | |
| Witter & others | 2003 | Cascadia earthquakes recorded in Coquille River estuary | |
| Kelsey & others | 2005 | Tsunami history of Bradley Lake | |
| Peterson & others | 2007 | Upland coastal dune sheets in Oregon | 1:295,200 |

Reports used to compile the southern Oregon coast geodatabase are shown in boldface. Author(s), date, abbreviated subject(s), and map scale (if appropriate) are shown; more complete references are listed at the end of this report.

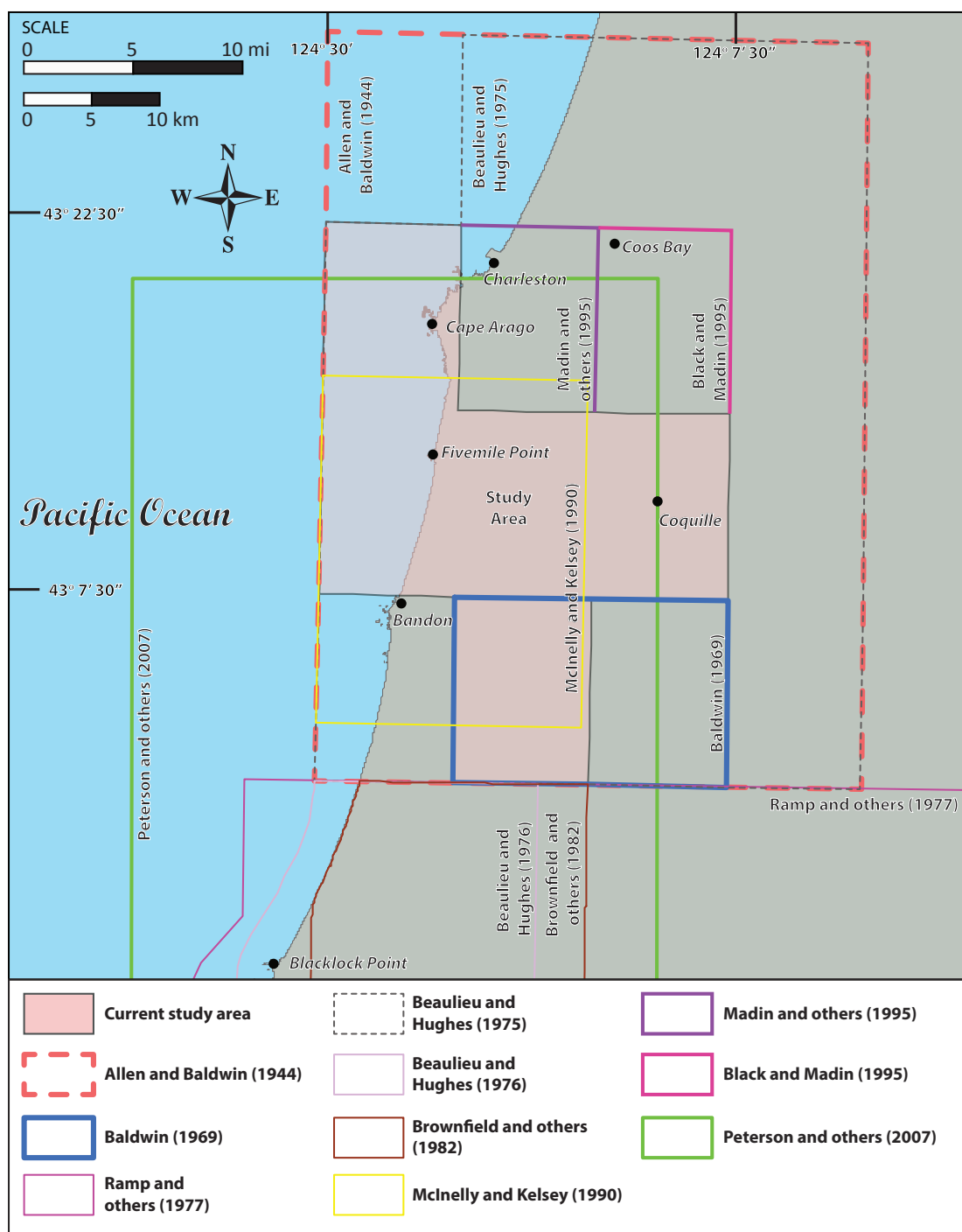


Figure 5. Sources of geologic mapping used during the preparation of this report.

METHODOLOGY

Geologic data were collected digitally using a GPS-enabled Apple™ iPad 2 loaded with iGIS™, a geographic information system software package compatible with Esri ArcGIS™. Digital mapping used tiled, hillshaded raster images, derived from high-resolution (8 pts/m²) lidar digital elevation models (DEMs) as base maps. Additional base map information was derived from standard 1:24,000-scale USGS digital raster images (DRGs) and digital orthophoto imagery (2013) obtained from Google Earth™. Fieldwork conducted during 2014 and 2015 consisted largely of data collection along major highways, roads, and accessible ocean shores. Where access was available, secondary roads across rangelands and timberlands provided more detailed information between otherwise widely spaced traverses. The distribution of 1,337 landslide deposits mapped in the area was determined remotely, using the protocol for inventory mapping of landslide deposits from lidar imagery (Burns and Madin, 2009). A small percentage (~5 percent) of remotely mapped landslide deposits were field checked for accuracy during the course of fieldwork. The shoreline boundary depicted on the geologic maps represents the land-water interface at the mean high water tidal datum as determined from lidar by the National Oceanic and Atmospheric Administration (NOAA). Current shoreline data for North America is available for download from the NOAA shoreline data explorer at <http://www.ngs.noaa.gov/CUSP/>.

New mapping was compiled with published and unpublished data, and converted into digital format using Esri ArcGIS ArcMAP® 10.1 GIS software. On-screen digitizing was performed on a Wacom® Cintiq® touch monitor using georeferenced 1-m lidar DEMs and 1:24,000-scale USGS digital raster images (DRGs) as base maps. Geologic interpretations were aided by GIS analyses based in part on 1-m lidar DEMs, USGS 10-m DEMs, and 2011 and 2014 National Agriculture Imagery Program (NAIP) digital orthophotos. The mapped distribution of surficial deposits is derived in part from soils maps and descriptions published by the Natural Resource Conservation Service (NRCS) of the U.S. Department of Agriculture (Haagen, 1989). Lidar DEMs were used to depict the distribution of both bedrock and surficial geologic units at a maximum scale of 1:8,000. The geologic time scale used is the 2015 (v2015/01) version of the International Stratigraphic Commission's International Stratigraphic Chart <http://www.stratigraphy.org/index.php/ics-chart-timescale> revised from Cohen and others (2013).

Mapping was supported by X-ray fluorescence (XRF) geochemical analyses of whole-rock samples, radiometric age determinations, thin-section petrography, and strike and dip measurements of inclined bedding (see map plates; Appendix). Whole-rock geochemical samples were prepared and analyzed by XRF at the Department of Geosciences, Franklin and Marshall College, Lancaster, Pennsylvania. Analytical procedures for the Franklin and Marshall X-ray laboratory were described by Boyd and Mertzman (1987) and Mertzman (2000) and are available online at <http://www.fandm.edu/earth-environment/laboratory-facilities/xrf-and-xrd-lab>. Major element determinations are normalized to a 100-percent total on a volatile-free basis and recalculated with total iron expressed as FeO*. Descriptive rock unit names for volcanic rocks are based in part on the online British Geological Survey classification schemes (Gillespie and Styles, 1999; Robertson, 1999; Hallsworth and Knox, 1999) and normalized major element analyses plotted on the total alkalis (Na₂O + K₂O) versus silica (SiO₂) diagram (TAS) of Le Bas and others (1986), Le Bas and Streckeisen (1991), and Le Maitre and others (1989, 2004). Four new ²⁰⁶Pb/²³⁸U radiometric age determinations, derived from detrital zircons in sandstones, were prepared and analyzed by Joshua Schwartz at California State University, Northridge, California. Chang and others (2006) described the sample preparation methods and data collection techniques employed for obtaining the zircon ages. Microsoft® Excel® spreadsheets tabulating geochemical analyses, isotopic ages, strike and dip measurements, and additional structural measurements are provided as part of this publication and are located in the Appendix.

In this report, volcanic rocks with fine-grained volcanic rocks (those with groundmass crystal or particle diameters less than 1 mm (0.04 in) (MacKenzie and others, 1997; Le Maitre and others, 2004) are described as having “coarse groundmass” if the average size is <1 mm (0.04 in) and they can be determined by using the naked eye (>~0.5 mm [0.02 in]); as having “medium groundmass” if crystals of average size cannot be determined by eye but can be distinguished by using a hand lens (>~0.05 mm [0.02 in]); as having “fine groundmass” if crystals or grains of average size can be determined only by using a microscope (or by hand lens recognition of phyllite-like sparkle or sheen in reflected light, indicating the presence of crystalline groundmass); or as having a “glassy groundmass” if the groundmass has (fresh), or originally had (altered), groundmass with the characteristics of glass (conchoidal fracture; sharp, trans-

parent edges; vitreous luster; etc.). Mixtures of crystalline and glassy groundmass are described as intersertal; ratios of glass to crystalline materials may be indicated by textural terms including holocrystalline, hypocrySTALLine, hyalophitic, and hyalopilitic. Microphenocrysts are defined as crystals larger than the overall groundmass and < 1 mm (0.04 in) across.

Intrusive igneous rocks are described as being coarse-grained if crystal diameters exceed 5 mm (0.2 in); as being medium-grained if the absolute range of crystal diameters falls between 1 and 5 mm (0.04 in and 0.2 in); and as being fine-grained if the absolute range of crystal diameters falls below 1 mm (0.04 in) (MacKenzie and others, 1997; Le Maitre and others, 2004).

The grain size of unconsolidated sediments and clastic sedimentary rocks is described following the Wentworth scale (Wentworth, 1922). Hand samples of unconsolidated sediments and clastic sedimentary rocks were compared in the field and/or in the laboratory to graphical representations (comparator) of the Wentworth Scale to determine average representative grain size in various parts of a respective sedimentary geologic unit. Colors given for hand-sample descriptions are from the Geological Society of America Rock-Color Chart Committee (1991).

Subsurface geology shown in the geologic cross sections incorporates lithologic interpretations from water well drill records available through the Oregon Water Resources Department (OWRD) GRID system (see map plates; Appendix). An attempt was made to locate water wells and other drill holes that have well logs archived by OWRD. Approximate locations were estimated by using a combination of sources, including Google Earth™, tax lot maps, street addresses, and aerial photographs. The accuracy of the locations ranges widely, from errors of ~ 0.7 mi (1.1 km) possible for wells located only by section and plotted at the section centroid to a few meters (tens of feet) for wells located by address or tax lot number on a city lot with bearing and distance from a corner. Very few wells were visited in the field. For each well, the OWRD GRID number of the well log is indicated in the database. This number can be combined with the first four letters of the county name (e.g., COOS 5473), to retrieve an image of the well log from the OWRD web site (http://apps.wrd.state.or.us/apps/gw/well_log/). A database of 1,300 located water well logs with interpreted subsurface geologic units is provided in the Appendix.

Geologic hazards including landslides (Burns and Watzig, 2014), subduction zone earthquakes (Goldfinger and others, 2012), and tsunamis (Witter and others, 2003, 2011) are treated in greater detail in other reports and data releases.

EXPLANATION OF MAP UNITS

The stack of tectonostratigraphic terranes that underlies the southern Oregon Coast Range is Upper Jurassic to Paleogene in age (Figures 4 and 6; see map plates). Widely separated stratigraphic units, which are often characterized by complex, discontinuous geometries, are grouped on the basis of apparent stratigraphic position, lithology, geochemical composition, and fossil assemblages. Unit names follow local stratigraphic nomenclature if available; where formal rock names are not appropriate, informal names are given on the basis of composition or a well-exposed section.

In areas close to the coast, bedrock geologic units are often capped by Quaternary surficial deposits. Quaternary surficial deposits are divided on the basis of apparent age into Anthropocene, Holocene, and Pleistocene units. Following the suggestions of Crutzen (2002) and Wiley and others (2011), we use the term Anthropocene for the time

period beginning with the first significant accumulations of American, Canadian, Californian, Russian, and European settlers' and ships' logs, journals, diaries, maps, charts, artifacts, roads, farms, diversions, or artificial fills and extending to the present day. In Oregon this corresponds to a date of 1792 when Robert Gray first crossed the Columbia River bar. Accordingly, Anthropocene deposits are those that 1) contain artifacts of industrial origin, or 2) modify the geology reliably described in any log, journal, or diary, or reliably depicted on any chart, sketch, or map, or 3) modify, cover, or can be shown to be associated with erosion of any road, fill, or dam, or 4) are known to postdate 1791, or 5) can otherwise be shown to postdate deposits meeting criteria 1 to 4. Figure 6. is a time-rock chart showing age ranges for Mesozoic and Cenozoic bedrock and surficial units.

OVERVIEW OF MAP UNITS ALONG THE SOUTHWEST OREGON COAST

W water

Note: Water is included as a unit here because it occurs as a unit in the geodatabase.

UPPER CENOZOIC SURFICIAL DEPOSITS

ANTHROPOCENE SURFICIAL DEPOSITS

Af modern fill and construction material (Anthropocene)
Aa alluvium (Anthropocene) – divided to show:
 Aac channel deposits (Anthropocene)
Als landslide deposits (Anthropocene)
Adf debris fan deposits (Anthropocene)
Aaf alluvial fan deposits (Anthropocene)
Abs beach deposits (Anthropocene)
Ads foredune deposits (Anthropocene)

ANTHROPOCENE AND HOLOCENE SURFICIAL DEPOSITS

AHcl coastal lacustrine deposits (Anthropocene(?) and Holocene)
AHcm coastal marsh deposits (Anthropocene(?) and Holocene)
AHdu unvegetated dune deposits (Anthropocene(?) to upper Pleistocene)
AHdp deflation plain sand (Anthropocene(?) and Holocene)

HOLOCENE SURFICIAL DEPOSITS

Ha alluvium (Holocene)
Haf alluvial fan deposits (Holocene)
Hdf debris fan deposits (Holocene)
Hls landslide deposits (Holocene)

QUATERNARY SURFICIAL DEPOSITS

Qa alluvium (Holocene(?) and upper Pleistocene(?))
Qls landslide deposits (Holocene(?) and upper Pleistocene(?))
Qds upland coastal dune deposits (Holocene(?) and upper Pleistocene(?))

Fluvial terrace deposits and strath terraces (upper Pleistocene) — divided to show:

Qft1 fluvial terrace sediments 1 (upper Pleistocene)
Qft2 fluvial terrace sediments 2 (upper Pleistocene)
Qft3 fluvial terrace sediments 3 (upper Pleistocene)
Qft4 fluvial terrace sediments 4 (upper Pleistocene)
Qft5 fluvial terrace sediments 5 (upper Pleistocene)

Coastal marine terrace deposits (Pleistocene) – divided to show:

Qmtw Whiskey Run terrace sediments (north of Floras Creek, upper Pleistocene, ~80 ka)
Qmtp Pioneer terrace sediments (upper Pleistocene, ~105 ka)
Qmtd Seven Devils terrace sediments (north of Floras Creek, upper to middle Pleistocene, ~125 ka)
Qmtm Metcalf terrace sediments (middle Pleistocene)
Qmta Arago Peak terrace sediments (middle to lower(?) Pleistocene)

Unconformity

LOWER PLEISTOCENE SEDIMENTARY ROCKS

Qgcq Coquille Formation (lower Pleistocene)

(continued on next page)

(MAP UNIT AND GEOLOGIC UNIT CORRELATION, continued)

Unconformity

LOWER CENOZOIC AND MESOZOIC ROCKS**PALEOGENE OVERLAP SEQUENCE**

Teb Bastendorff Shale (upper Eocene)

Coaledo Formation (middle Eocene) — divided to show:

Tecu Upper Member (middle Eocene)

Tecm Middle Member (middle Eocene)

TecI Lower Member (middle Eocene)

Tes beds at Sacchi Beach (middle Eocene)

Tet Tyee Mountain Member of the Tyee Formation (middle Eocene)

Teu Umpqua Group (lower Eocene)

Unconformity

SILETZ TERRANE

Tesr Siletz River Volcanics (Paleocene to lower Eocene)

Faulted terrane boundary

SIXES RIVER TERRANE

Fulmar subterrane

Tefm sandstone of Fivemile Point (lower Eocene)

Unconformity

KJs mélange of Sixes River (Upper(?) Cretaceous to Jurassic(?))

KJss sandstone

KJsv volcanic and meta-volcanic rock

KJsc chert

KJcg conglomerate

KJsm other metamorphic rock

KJsp serpentinite and meta-serpentinite

KJst siltstone

KJm marble

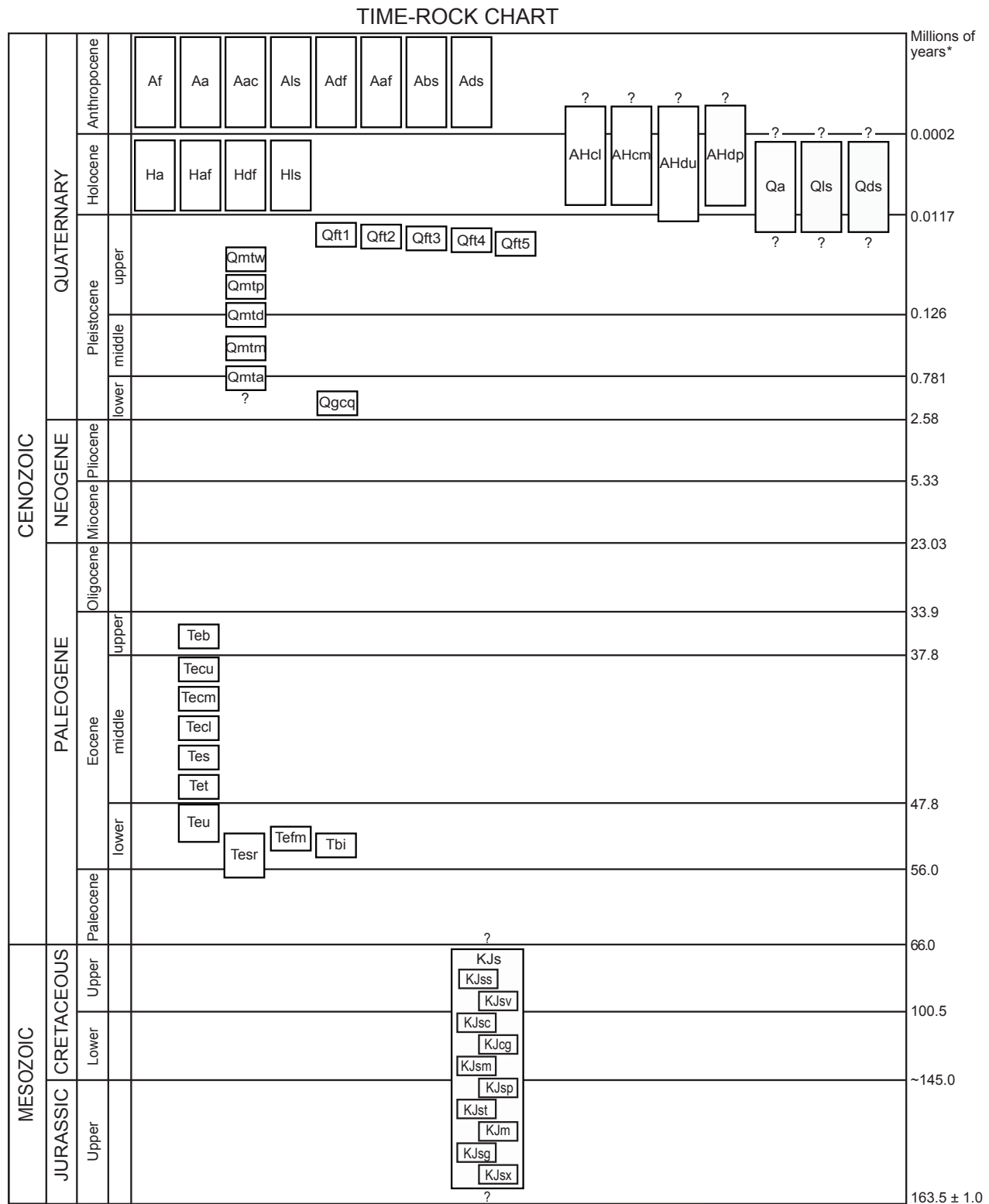
KJsg garnet schist

KJsx mélange blocks, undivided

Rocks that intrude the Fulmar subterrane of the Sixes River terrane

Tbi Intrusive rocks (lower Eocene)

Faulted terrane boundary



*International Chronostratigraphic Chart, International Stratigraphic Commission, 2015/V1, Time scale after Gradstein and others (2004), Ogg and others (2008), and Cohen and others (2013). <http://www.stratigraphy.org/index.php/ics-chart-timescale>

Figure 6. Time-rock chart showing the 51 geologic units in the Bandon, Coquille, and Sunset Bay areas along the southern Oregon coast identified by this study.

UPPER CENOZOIC SURFICIAL DEPOSITS

Mesozoic and Cenozoic rocks exposed along the southern Oregon coast are locally mantled by Quaternary surficial deposits (see map plates). Surficial units include alluvial-plain and fluvial terrace deposits, coastal marine terrace deposits, and valley-fringing landslide, alluvial fan, and debris fan deposits. Surficial units within the project area are delineated on the basis of geomorphology as interpreted from a combination of field observations, 1-m lidar DEMs, 2011 NAIP orthophotos, and USGS 7.5' topographic maps.

W water—Areas covered by ocean. (*Note: Water is included as a unit here because it occurs as a unit in the geodatabase.*)

ANTHROPOCENE SURFICIAL DEPOSITS

Af modern fill and construction material (Anthropocene)—Man-made deposits of poorly sorted and crudely layered mixed gravel, sand, clay, and other engineered fill (see map plates). These deposits may contain rounded to angular clasts ranging from small pebbles up to the largest size that can be moved with road building equipment. The orientation of clasts is typically less uniform than is found in naturally occurring imbricated or bedding-parallel gravel. Deposits mapped as modern fill and construction material include those that make up jetties, tiered cranberry fields (“bogs”), dams and levies, road embankments, causeways and culvert fills, and mined land (see map plates). Fill thickness may exceed 30 m (98 ft).

Aa alluvium (Anthropocene)—Unconsolidated gravel, sand, silt, and clay deposited along active stream channels and on adjoining floodplains (see map plates). Gravel deposited as imbricated, massive to cross-stratified accumulations on mid-channel islands and bars is the most common type of near-channel alluvium along major tributaries. Thickness of alluvial deposits is generally less than 5 to 7 m (16 to 23 ft); bedrock units may be variably exposed in the base of stream channels within areas mapped as unit **Aa**. Areas mapped as **Aa** are known to have been inundated by record floods during 1861, 1964, 1996 to 1997, and 2006 and include deposits containing man-made debris or artifacts, or deposits filling ar-

eas known to have been modified by man such as excavations, roadways, or gravel pits. Smaller floods of ten overtop natural levees (Figure 7). Locally divided to show:

Aac channel deposits (Anthropocene)—Sand, gravel, and silt deposited along channels of major streams and their larger tributaries. The unit includes in-channel deposits and adjacent natural levees, crevasse splay deposits, and other overbank facies that were likely deposited by currents. Channel deposits are mapped on the basis of subtle changes in slope and morphology recognized on 1-m lidar DEMs.

Als landslide deposits (Anthropocene)—Unconsolidated, chaotically mixed masses of rock, soil, and colluvium deposited by landslides (i.e., slumps, slides, debris flows, rock avalanches; see map plates). Recent landslide terrain is characterized by sloping hummocky surfaces, locally marked by closed depressions, springs and wet seeps, and scarps. Active or recently active landslides are marked by marginal levees and open ground fissures; tilted trees and bent trunks may be common on the surface. Landslide deposits are traceable uphill to headwall scarps or slip



Figure 7. The Coquille River Valley looking southwest of Highway 425 near Coquille, Oregon. The photograph shows high water on the floodplain following a winter storm event that overtopped natural levees (WGS84 geographic coordinates: 402350mE., 4780731mN; photo by T. J. Wiley, 2014).

surfaces. Toes to more recent deposits retain convex-up, fan-shaped morphologies. The unit locally includes rockfall, large talus piles, shallow-seated landslides of colluvium, rapidly emplaced debris flow deposits, and more deeply-seated bedrock slides. Individual landslide deposits generally cover less than 2.8 hectares (7 acres). Thickness of landslide deposits is highly varied; maximum thickness is several tens of meters. Landslide deposits are assigned an Anthropocene age on the basis of disturbed roads, historic records, and other cultural features. May be identified on 1-m lidar DEMs where old logging roads are buried or offset by recent landslide lobes.

Adf debris fan deposits (Anthropocene)—Unconsolidated deposits of gravel, sand, silt, and woody debris in fan-shaped accumulations preserved at the outlets of steep, intermittent upland drainages (see map plates). Debris fans typically accumulate through intermittent fluvial deposition and during high-discharge rainfall events when accumulations of soil, colluvium, or landslide deposits are remobilized and transported downslope as fast-moving sediment gravity flows (e.g., debris flows). The unit may locally include rapidly deposited talus as a result of rockfall in steep drainages. Debris fans are differentiated from alluvial fans on the basis of steeper gradients over their longitudinal profiles; gradients are greater than 6 percent and in some cases may exceed 25 percent (Alluvial Fan Process Group, n.d.). Individual or coalescing complexes of debris fan deposits generally cover less than 0.4 hectares (1 acre); local thickness of debris fan deposits is variable but is probably <10 m (32 ft). Debris fan deposits are considered to be Anthropocene in age on the basis of stratigraphic position near the mouths of active drainages and a relatively youthful-appearing deposit morphology.

Aaf alluvial fan deposits (Anthropocene)—Unconsolidated deposits of gravel, sand, silt, clay, and woody debris preserved in low fan-shaped accumulations that occur at the transition between low-gradient valley floodplains and steeper upland drainages (see map plates). Surfaces of alluvial fans are characterized by anastomosing, intermittent fluvial channels, formed where pools or obstructions such as log-jams or debris flow levees create flow diversions. Sediment accumulates on the fan surface through normal

fluvial deposition, avulsions, and lateral migration as streams emerge from upland settings and the gradient falls below the threshold for further sediment transport. Debris flows occurring during episodic high-discharge precipitation events are also an important mechanism for transport and deposition on the alluvial fan surface. Alluvial fans have gradients ranging from 1 to 6 percent over their longitudinal profile (Alluvial Fan Process Group, n.d.). They typically have a steep gradient at the apex, moderate gradient through the middle section, and low gradient near the toe. Individual fans generally cover less than 0.6 hectares (1.5 acres); local thickness of alluvial fan deposits is variable but is probably <15 m (50 ft). These deposits are considered to be Anthropocene in age on the basis of stratigraphic position near the mouths of active stream channels and relatively youthful-appearing deposit morphology.

Abs beach deposits (Anthropocene)—Unconsolidated, well-sorted sand, pebbly sand, shelly sand, sandy gravel, and open-framework gravel deposited in active ocean beaches (Plates 3 and 4). Locally, the unit may be gravel dominated, particularly on steep, narrow beaches. Pebbles and cobbles in open-framework gravel may be imbricated such that most tilt toward oncoming waves. Beach deposits are seasonally ephemeral features, where grain size distribution and thickness of the deposit, and amount of exposed underlying bedrock can vary greatly from high to low tide and from year to year as sand and gravel migrate on to, off of, or along the shore. Beach deposits may also be quickly eroded during major storms. The unit is assigned an Anthropocene age on the basis of the ephemeral nature of the deposit and common inclusion of man-made debris or artifacts.

Ads foredune deposits (Anthropocene)—Unconsolidated, well-sorted, fine- to medium-grained sand deposited by the wind in nearshore, back-beach settings that parallel the shoreline (Plates 3 and 4). The unit is typically characterized by unvegetated to moderately grass-covered surfaces on the seaward surface (stoss slopes), with lesser amounts of larger woody shrubs developed on landward slopes (lee slopes). The seaward side of the active foredune is commonly the depositional site of large amounts of driftwood. The thickness of the unit is typically < 8 m

(26 ft). The unit is assigned an Anthropocene age on the basis of stratigraphic position directly adjacent (landward) to the active beach (**Abs**) and inclusion of man-made debris or artifacts.

ANTHROPOCENE AND HOLOCENE SURFICIAL DEPOSITS

AHcl coastal lacustrine deposits (Anthropocene(?) and Holocene)—Interbedded laminated mud, massive, organic-rich mud, sandy mud, muddy debris, and sand deposited in coastal lakes. The coastal lakes are restricted to the broad plain situated between Fivemile Point on the north and the Coquille River on the south, where they are impounded behind Anthropocene/Holocene dune fields (Plate 3). Inlets and fringes of lakes are typically covered by marsh deposits (**AHcm**). Lacustrine environments, such as Bradley Lake south of Bandon (Wiley and others, 2014; south of map area) contain landward-thinning sand sheets recording periodic (~ every 390 years) marine incursions generated by local tsunamis and seismic shaking on the Cascadia subduction zone (Kelsey and others, 2005). Bradley Lake has been a catchment for tsunami deposits since its formation after ~7,300 yr B.P., and since that time has been inundated by at least 16 distinct tsunami disturbance events (Kelsey and others, 2005). The most recent tsunami-generated deposits in Bradley Lake record the A.D. 1700 Cascadia subduction zone earthquake. The unit is assigned an Anthropocene and Holocene age on the basis of impoundment behind Anthropocene and Holocene dune deposits (**Ads**, **AHdu**; Plate 3) and numerous ^{14}C ages obtained from nearby Bradley Lake (Kelsey and others, 2005).

AHcm coastal marsh deposits (Anthropocene(?) and Holocene)—Interbedded mud, massive, organic-rich mud, and peat deposited in marsh environments along the fringes of coastal lakes and within stream channels emptying into coastal lakes (Plate 3). Large areas mapped as coastal marsh deposits are also present along the lower reaches of the Coquille River. These areas are recognized on the basis of muted topography, saturated ground, abundant vegetation, and sinuous drainage. Areas of marsh are also known to occur within depressions on top of low-lying Quaternary coastal marine terrace deposits and along

the margins of stream drainages but have not been mapped separately here. The unit is assigned an Anthropocene and Holocene age on the basis of association with coastal lakes. Witter and others (2003) reported more than 4 m (13 ft) of buried peaty soils, incipient buried soils, peat-dominated facies, and clean (tsunami related) sand present in swamp and marsh areas near the mouth of Fahys Creek and assigned an age of 4,000 to $4,480 \pm 50$ ^{14}C yr B.P. to carbon recovered from depths of 2 to 3 m (6.6 to 9.8 ft) (Plate 3; Appendix).

AHdu unvegetated dune deposits (Anthropocene(?) to upper Pleistocene)—Unconsolidated, well-sorted, fine- to medium-grained sand deposited by the wind within narrow dunes paralleling the coastal margin between the Coquille River and Fivemile Point (Plate 3). Active dunes lack vegetative cover and include both oblique and parabolic dune forms, with wind-blown sand derived from both beaches (**Abs**) and deflation plains (**AHdp**; Beaulieu and Hughes, 1975; Peterson and others, 2007). Migration rates of dunes range from a few centimeters to several meters per year, depending on the source area (Beaulieu and Hughes, 1975). Dune thickness may locally be up to 25 m (80 ft). The unit is assigned an Anthropocene and Holocene age on the basis of a youthful-appearing morphology, lack of vegetation, and stratigraphic association with Holocene lakes (**AHcl**) and marshes (**AHcm**). Peterson and others (2007) reported ^{14}C ages from charcoal obtained from the dune base, 1.5 km (0.9 mi) southeast, ranging between 1,530 and 1,780 yr B.P. (Plate 3; Appendix; Sample BAND8); additional ^{14}C and thermoluminescence ages obtained within the unit from a nearby site (~150 m [492 ft] south) range between ca. 35.4 and 39.7 ka (Plate 3; Appendix; Samples BAND9, 9a, 9b). Deposition of these dunes corresponds with the decline in the rate of sea level rise during the middle part of the Holocene, when onshore wave transport delivered inner shelf sand to beaches. Subsequent eolian transport of surplus beach sand, during peak onshore wind velocities, led to the formation of upland Holocene dune sheets (Peterson and others, 2007).

AHdp deflation plain sand (Anthropocene(?) and Holocene)—Unconsolidated, well-sorted, fine- to medium-grained sand deposited by the wind within broad, low-lying areas paralleling the coastal mar-

gin between the Coquille River and Fivemile Point (Plate 3). Deflation plains are commonly situated immediately inland from the foredune (**Ads**) environment and lie adjacent to lacustrine and marsh areas (see map plates). Deflation plains are characterized by widespread fields of low transverse dunes or flat areas eroded to the level of the summer water table; water table rise during the winter produces lakes and marshes. Peat and silty clay may therefore underlie many areas mapped as deflation plain, due to the close association with lakes and marshes. Deflation plains may be sources of windblown sand for larger, nearby active dunes (**AHdu**). Deflation plain sand in the map area is assigned an Anthropocene or Holocene age on the basis of stratigraphic association with Holocene and younger dune sand (**AHdu**; Peterson and others, 2007) and lacustrine (**AHcl**) and marsh (**AHcm**) deposits (Kelsey and others, 2005). Beaulieu and Hughes (1975) indicated a maximum age of 5,000 years for deflation plains as they lie at or slightly above modern day sea level.

HOLOCENE SURFICIAL DEPOSITS

Ha alluvium (Holocene)—Unconsolidated, well- to poorly-sorted and stratified gravel, sand, silt, and clay deposited in active stream channels and on adjoining flood plains of major rivers and their tributaries (see map plates). These deposits commonly rest directly on bedrock and may locally include strath terraces. The thickness of the unit probably does not exceed 15 m (50 ft). Along small streams, unit **Ha** alluvial deposits may be incised by modern floodplains (**Aa**) that have been overtopped during historic flood events. Along large streams such as the Coquille River natural levees and related deposits adjacent to the channels are assigned to an Anthropocene near channel unit, **Aac**, while low ground in the floodplain that was likely deposited by pre-Anthropocene migration of older channels is assigned to **Ha**, even though a thin veneer of Anthropocene flood plain deposits is likely present as well. The unit is considered to be Holocene in age on the basis of stratigraphic position in and near active stream-channels and youthful-appearing deposit morphology. Witter and others (2003) reported more than 9 m (29.5 ft) of buried soils, estuarine mud, pebbly alluvium, and clean (tsunami related) sand present along the lower

reaches of Sevenmile Creek and assigned an age of 5,770 to $5,830 \pm 50$ ^{14}C yr B.P. to carbon recovered from depths of 7 to 8 m (23 to 26 ft) (Plate 3; Appendix). Conifer needles recovered from the upper part of the unit along the north bank of the Coquille River near Bullards have an age of 170 ± 50 ^{14}C yr B.P. (Witter and others, 2003; Plate 3; Appendix).

Haf alluvial fan deposits (Holocene)—Unconsolidated deposits of gravel, sand, silt, clay, and woody debris preserved in low fan-shaped accumulations that occur at the transition between low-gradient valley floodplains and steeper upland drainages (see map plates). Surfaces of alluvial fans are characterized by anastomosing, intermittent fluvial channels, formed where pools or obstructions such as log-jams or debris flow levees create flow diversions. Sediment accumulates on the fan surface through normal fluvial deposition, avulsions, and lateral migration as streams emerge from upland settings and the gradient falls below the threshold for further sediment transport. Debris flows occurring during episodic high-discharge precipitation events are also an important mechanism for transport and deposition on the alluvial fan surface. Alluvial fans have gradients ranging from 1 to 6 percent over their longitudinal profile (Alluvial Fan Process Group, n.d.). They typically have a steep gradient at the apex, moderate gradient through the middle section, and low gradient near the toe. Individual fans may cover areas up to 21 hectares (52 acres), but most deposits extend over areas less than 1.6 hectares (4 acres). The local thickness of alluvial fan deposits is variable but is probably <15 m (50 ft). These deposits are largely considered to be Holocene in age on the basis of stratigraphic position near the mouths of active stream-channels and relatively youthful-appearing deposit morphology.

Hdf debris fan deposits (Holocene)—Unconsolidated deposits of gravel, sand, silt, and woody debris in fan-shaped accumulations preserved at the outlets of steep, intermittent upland drainages (see map plates). Debris fans typically accumulate through intermittent fluvial deposition and during high-discharge rainfall events when accumulations of soil, colluvium, or landslide deposits are remobilized and transported downslope as fast moving sediment gravity flows (e.g., debris flows). The unit may locally include rapidly deposited talus as a result of rock-

fall in steep drainages. Debris fans are differentiated from alluvial fans on the basis of steeper gradients over their longitudinal profiles; gradients are greater than 6 percent and in some cases may exceed 25 percent (Alluvial Fan Process Group, n.d.). Individual or coalescing complexes of debris fan deposits generally cover less than 2 hectares (5 acres); local thickness of debris fan deposits is variable but is probably <10 m (32 ft). These deposits are largely considered to be Holocene in age on the basis of stratigraphic position near the mouths of active drainages and relatively youthful-appearing deposit morphology.

Hls landslide deposits (Holocene)—Unconsolidated, chaotically mixed masses of rock, soil, and colluvium deposited by landslides (i.e., slumps, slides, debris flows, rock avalanches; see map plates). Recent landslide terrain is characterized by sloping hummocky surfaces, locally marked by closed depressions, springs and wet seeps, and scarps. Active or recently active landslides are marked by marginal levees and open ground fissures; tilted trees and bent trunks may be common on the surface. Landslide deposits are traceable uphill to headwall scarps or slip surfaces. Toes to more recent deposits retain convex-up, fan-shaped morphologies. The unit locally includes rockfall, large talus piles, shallow-seated landslides of colluvium, rapidly emplaced debris flow deposits, and more deeply seated bedrock slides. Individual Holocene landslide deposits in the map area range in size from small deposits covering 0.04 hectares (0.1 acres) to larger composite features covering areas up to 200 hectares (495 acres) (see map plates). The greatest extent and number of mapped Holocene landslide complexes are located in upland areas of the Bill Peak 7.5' quadrangle (Plate 1) associated with the Sixes River Mélange (**KJs**), Umpqua Group (**Teu**), or the Lower and Middle Members of the Coaledo Formation (**Tecl**, **Tecm**). Many other smaller slides are prevalent along lower elevation drainages and along the edges of elevated coastal marine terrace deposits (e.g., **Qmtd**, **Qmtm**). Slides occurring within areas of mélange (**KJs**) often incorporate or flow around large mélange blocks which are here mapped as bedrock units; it is unclear in most cases if these are incorporated in the slide mass or if shallow seated slides are creeping around stable or deeply rooted blocks. The thickness of landslide deposits is highly varied; the maximum thickness is several tens of meters. Land-

slides are assigned a Holocene age where deposits appear relatively fresh, with well-defined hummocks and preservation of relatively small features such as levees and internal scarps. Holocene landslide deposits generally lack the deeply incised streams that typify landslide deposits assigned a Quaternary age (**Qls**). Some Anthropocene landslide deposits (**Als**) are probably included in the unit where more precise age indicators are poorly developed or lacking. In water well logs, landslide deposits are typically referred to as clay, boulders, rock, or rock and clay.

QUATERNARY SURFICIAL DEPOSITS

Qa alluvium (Holocene(?) and upper Pleistocene(?))—Unconsolidated, well to poorly sorted and stratified gravel, sand, silt, and clay deposited in active stream channels and on adjoining flood plains (Plates 2 and 3). These deposits are only locally recognized and mapped in the Riverton 7.5' quadrangle (Plate 3) where they reside adjacent to younger, incised drainages filled with Holocene alluvium (**Ha**). Thickness of the unit probably does not exceed 6 m (20 ft). The unit is considered to have a Quaternary age on the basis of stratigraphic position adjacent to active stream-channels that cut through Quaternary coastal marine terrace deposits.

Qls landslide deposits (Holocene(?) and upper Pleistocene(?))—Unconsolidated, chaotically mixed masses of rock and soil deposited by landslides (e.g., slumps, slides, debris flows, rock avalanches; see map plates). Deposits may consist of individual slide masses or may form large complexes resulting from multiple generations of landslide activity. Landslide terrain is characterized by sloping hummocky surfaces, locally marked by closed depressions, springs, and wet seeps, head scarps and internal scarps, open ground fissures, and tilted trees and bent trunks. Slides are often traceable uphill to headwall scarps or slip surfaces. In more deeply seated landslides, these head scarps commonly expose bedrock. Locally, Quaternary landslide deposits are deeply incised by drainages that contain remobilized rock and debris deposited by sediment-gravity flows. Quaternary landslide complexes in the map area range in size from small deposits covering 0.1 hectares (0.3 acres) to larger composite features covering areas up

to 316 hectares (781 acres). Slides occurring within areas of *mélange* (**KJs**) often incorporate or flow around large *mélange* blocks that are here mapped as bedrock units; it is unclear in most cases if these are incorporated in the slide mass or if shallow seated slides are creeping around stable or deeply rooted blocks. Thickness of landslide deposits is highly varied but may be more than several tens of meters in larger deposits. Large areas mapped as Quaternary landslide deposits typically include many discrete deposits of varying age that have not been differentiated here. Landslide deposits range in age from relatively stable Pleistocene features to recurrently active relatively recent (assigned to units **Als** and **Hls** where recognized). Most landslide deposits are assigned a Quaternary age on the basis of subdued geomorphic expression and incision by streams. Landslide deposits are typically referred to as clay, boulders, rock, or rock and clay in water well logs.

Qds upland coastal dune deposits (Holocene(?) and upper Pleistocene(?))—Unconsolidated, well-sorted, fine- to medium-grained sand deposited by the wind in upland coastal dune fields (see map plates). Dune fields are situated on top of coastal marine terraces and cover a large portion of the coast between Johnson Creek (Plate 1) and Agate Beach on the north (Plates 3 and 4). Peterson and others (2007) considered these dune fields to collectively form the ~58-km-long (36 mi) by ~7-km-wide (4.3 mi) Bandon dune sheet, the northern extent of which lies near Cape Arago. The maximum thickness of dune deposits is approximately 15 m (~50 ft). The unit is assigned a late Pleistocene age on the basis of stratigraphic position above late Pleistocene coastal marine terraces. Peterson and others (2007) reported calibrated radiocarbon ages (cal yr B.P.) for several sites within the Bandon dune sheet, with dates ranging between 900 and 36,200 cal yr B.P. Additional thermoluminescence ages for the Bandon dune sheet range between 38.1 and 111 ka (Peterson and others, 2007). Regional dune dating along the Oregon coast indicates that dune fields were emplaced thousands of years after the youngest (~80 ka) coastal marine terrace was abandoned (Beckstrand, 2001; Peterson and others, 2007).

Fluvial terrace deposits and strath terraces (upper Pleistocene)—Unconsolidated deposits of gravel and sand, with

subordinate amounts of silt and clay that form fluvial terraces above modern floodplains of major drainages in the map area (see map plates). The terraces are visible on 1-m lidar DEMs as planar to very gently sloping, equal-elevation surfaces (treads). Steeper descending slopes (risers) define the streamside edges of terraces. Terrace deposits may be more than 30 m (100 ft) thick but more typically form thin deposits covering strath terraces formed in discontinuously exposed bedrock. Fluvial terrace elevations locally overlap with but are significantly different from those recognized by Wiley and others (2014) between Port Orford and Bandon. Stacked fluvial terraces near Coquille may be structurally controlled.

Subdivided in the map area on the basis of tread elevation above modern stream level into the following units:

Qft1 fluvial terrace sediments 1 (upper Pleistocene)—Fluvial terrace deposits with tread elevations ranging from 4.6 to 7.5 m (15 to 25 ft) above modern stream elevation (see map plates). The unit is assigned a late Pleistocene age on the basis of stratigraphic position. Fluvial terrace sediments (**Qft1**) are inset into the ~105 ka Pioneer (**Qmtp**) and ~80 ka Whiskey Run (**Qmtw**) marine terrace sediments, so are therefore younger than those units (Plate 3).

Qft2 fluvial terrace sediments 2 (upper Pleistocene)—Fluvial terrace deposits with tread elevations ranging from 10 to 12.2 m (33 to 40 ft) above modern stream elevation (see map plates). The unit is assigned a late Pleistocene age on the basis of stratigraphic position. Fluvial terrace sediments (**Qft2**) are inset into the ~105 ka Pioneer (**Qmtp**) and ~80 ka Whiskey Run (**Qmtw**) marine terrace sediments, so are therefore younger than those units (Plate 3).

Qft3 fluvial terrace sediments 3 (upper Pleistocene)—Fluvial terrace deposits with tread elevations ranging from 12.2 to 18.3 m (40 to 60 ft) above modern stream elevation (see map plates). The unit is assigned a late Pleistocene age on the basis of stratigraphic position. Fluvial terrace sediments (**Qft3**) are inset into the ~105 ka Pioneer (**Qmtp**) and ~80 ka Whiskey Run (**Qmtw**) marine terrace sediments, so are therefore younger than those units (Plate 3).

Qft4 fluvial terrace sediments 4 (upper Pleistocene)—Fluvial terrace deposits with tread elevations ranging from 21.3 to 24.7 m (70 to 81 ft) above mod-

ern stream elevation (see map plates). The unit is assigned a late Pleistocene age on the basis of stratigraphic position. Fluvial terrace sediments (**Qft4**) are inset into the ~105 ka Pioneer (**Qmtp**) and ~80 ka Whiskey Run (**Qmtw**) marine terrace sediments, so are therefore younger than those units (Plate 3).

Qft5 fluvial terrace sediments 5 (upper Pleistocene)—Fluvial terrace deposits with tread elevations ranging from 27.4 to 34.7 m (90 to 114 ft) above modern stream elevation (see map plates). The unit is assigned a late Pleistocene age on the basis of stratigraphic position. Fluvial terrace sediments (**Qft5**) are inset into the ~105 ka Pioneer (**Qmtp**) and ~80 ka Whiskey Run (**Qmtw**) marine terrace sediments, so are therefore younger than those units (Plate 3).

Coastal marine terrace deposits (Pleistocene)—Weakly consolidated to locally clay-altered gravel and sand interpreted as nearshore, beach, dune, and stream facies deposited on wave-cut marine platforms during successive marine transgressions associated with Pleistocene interglacial periods. Relatively flat to shallowly dipping marine terraces unconformably overlie older bedrock units. Gravel facies typically contain well-rounded pebbles of exotic lithologies, including metamorphic and igneous rocks (volcanic and intrusive) and quartz; locally derived clast lithologies are less common. Within gravel facies, the transition from onshore to beach processes is often marked by a reversal of imbrication, with clasts in beach and marine environments indicating landward flow and clasts in fluvial and fan environments indicating seaward flow. Sand facies are typically pale yellowish orange (10YR 8/6), well sorted with an open-framework, medium- to coarse-grained, and have feldspathic mineral compositions containing subround grains of quartz, feldspar, mica, and lithics. Marine terraces may locally include unmapped areas of terrace-capping sand dunes. The current height of marine terraces above sea level can be highly variable due to late Quaternary deformation.

The distribution of marine terrace deposits has been determined from field observations, morphology interpreted from 1-m lidar DEMs, elevation, degrees of erosional dissection, and modification of previous mapping by Diller (1902; “Elk River Beds”), Allen and Baldwin (1944), Griggs (1945), Brownfield (1972), Beaulieu and Hughes (1975; 1976), Kelsey (1990), McNelly and Kelsey (1990), Muhs and others (1990), and Kelsey and others (1996). Unit names applied to coastal marine terraces follow the local stratigraphic nomenclature established by Griggs (1945), Janda (1969, 1970), Kelsey (1990), McNelly and Kelsey (1990), and Kelsey and others (1996). Table 2, modified after Kelsey and others (1996), graphically displays the ages and stratigraphic correlations of locally named coastal terrace units along the southern Oregon coast between the California border and Coos Bay. Mapped distribution of marine terraces is based on lidar signatures and may include areas of strath terrace, resulting in areas more extensive than actual terrace deposits.

Table 2. Correlation of marine terraces along the southern and central Oregon coast (after Kelsey and others [1996]).

| South-Central Oregon | | | | Southern Oregon* | | | |
|---|------------|--|------------|---|------------|--|------------|
| Cape Arago (Muhs and others, 1990; McInelly and Kelsey, 1990) | | Cape Blanco Kelsey, 1990; Muhs and others, 1990) | | Brookings (Kelsey and Bockheim, 1994) | | Brookings* (T. J. Wiley, unpublished mapping 2007) | |
| Terrace | ~ Age (ka) | Terrace | ~ Age (ka) | Terrace | ~ Age (ka) | Terrace | ~ Age (ka) |
| Whiskey Run | 80 | Cape Blanco | 80 | Harris Beach | 80 | Qtc1 | 80 |
| Pioneer | 105 | Pioneer | 105 | Brookings | 105 | Qtc2 | 105 |
| Seven Devils | 125 | Silver Butte | 125 | Gowman | 125 | Qtc3, Qtc4, Qtc5 | 125 |
| Metcalf | ≥200 | Indian Creek | ≥200 | Aqua Vista | ≥200 | Qtc4, Qtc5, Qtc6 | ≥200 |
| | | | | Cornett | nd | Qtc6, Qtc7 | nd |
| Arago Peak | nd | | | Homestead | nd | Qtc8, Qtc9 | nd |
| | | Poverty Ridge | nd | Alder Ridge | nd | Qtc10 | nd |

*Age assignments for southern Oregon marine terraces near Brookings reported by T. J. Wiley are from Kelsey and Bockheim (1994). nd = no data.

Qmtw Whiskey Run terrace sediments (upper Pleistocene, ~80 ka)—Undissected to slightly dissected terrace sediments exposed between Bandon on the south and Gregory Point on the north (Plates 3 and 4). Outside the map area, the terrace platform extends farther south to Floras Creek (Wiley and others, 2014; ~23 km [14.3 mi] south of Bandon). Whiskey Run terrace sediments exposed between Bandon and Fivemile Point cap a broad platform up to 5 km (3.1 mi) in width, extending from coastal exposures to a backedge situated along Sevenmile Creek (Plate 3). Between Cape Arago and Gregory Point, in the northwest corner of the map area, terrace sediments are more aerially restricted, with platforms < 0.5 km (0.3 mi) in width, overlying and inset into deeply incised bedrock headlands. The Whiskey Run terrace surface attains a maximum backedge elevation of 48 m (157.5 ft) at Cape Arago (Plate 4) and gradually descends in elevation to the south; north of the Coquille River, the terrace surface lies near sea level. South of the Coquille River, the terrace is again emergent with backedge elevations ranging from ~30 m (99 ft) at Bandon to near sea level at Floras Creek (Wiley and others, 2014). Average thickness of the terrace cover sediment ranges from ~3 to 20 m (9.8 to 65.6 ft).

The unit was informally named the Whiskey Run terrace by Griggs (1945) for terrace sediments at the Pioneer mine type section, located in the drainage of Cut Creek, 9 km (5.6 mi) northeast of Bandon (Plate

3). Muhs and others (1990) and Kelsey (1990) assigned Whiskey Run sediments a late Pleistocene age on the basis of uranium series analysis of fossil corals collected at Coquille Point in Bandon, which yielded an age of 83 ± 5 ka. The Whiskey Run terrace is correlative to terrace 1 (Harris Beach) mapped by Kelsey and Bockheim (1994) and unit Qtc1 mapped by T. J. Wiley (unpublished mapping, 2007) in the Cape Ferello-Brookings area, and is approximately coeval with to Cape Blanco terrace sediments mapped by Kelsey (1990) and Wiley and others (2014) (Table 2).

Qmtp Pioneer terrace sediments (upper Pleistocene, ~105 ka)—Slightly dissected terrace sediments exposed between Bandon on the south and Cape Arago on the north (Plates 1, 3, and 4). The terrace extends farther north at least to Coos Head (4 km [2.5 mi] northeast of Cape Arago; Madin and others, 1995) and farther south, past Gold Beach (80 km [50 mi] south of Bandon; McClaghry and others, 2013; Wiley and others, 2014). Pioneer terrace sediments exposed between Bandon and Threemile Creek cap a broad platform up to 3 km (1.9 mi) in width extending from coastal exposures to a backedge situated along Sevenmile Creek (Plate 3). North of Threemile Creek, terrace sediments are more aerially restricted, with a platform ranging between 0.1 and 0.4 km (0.06 and 0.2 mi) in width, overlying and inset into deeply incised bedrock headlands. Backedge elevations for

the terrace range from ~17 m (57 ft) at Port Orford (Wiley and others, 2014; south of map area) to ~61 m (200 ft) east of Bandon (Plates 1 and 3). Northern exposures of the terrace, near Mussel Creek, have backedge elevations of ~41 m (135 ft), while isolated terrace remnants residing northeast of Cape Arago have backedge elevations up to 66 m (217 ft) (Plate 4). Average thickness of the terrace cover sediment ranges from ~16 to 23 m (52.5 to 75.5 ft).

The unit was informally named the Pioneer terrace by Griggs (1945) for terrace sediments at the Pioneer mine type section, located in the headwaters of Cut Creek, 9 km (5.6 mi) northeast of Bandon (Plate 3). Kelsey (1990) and Muhs and others (1990) assigned the sediments a late Pleistocene age on the basis of the extent of epimerization of amino acids in *Saxidomus* shells and correlation with an interstadial high stand of the sea around 105 ka (Oxygen isotope stage 5c). The Pioneer terrace is correlative to terrace 2 (Brookings) mapped by Kelsey and Bockheim (1994) and unit Qtc2 mapped by T. J. Wiley (unpublished mapping, 2007) in the Cape Ferello-Brookings area, and to the Pioneer terrace mapped south of the study area by Kelsey (1990), McClaughry and others (2013), and Wiley and others (2014) (Table 2).

Qmtd Seven Devils terrace sediments (upper to middle Pleistocene, ~125 ka)—Moderately to deeply dissected terrace sediments forming an extensive platform above deeply dissected bedrock ridges between Floras Creek (Wiley and others, 2014; south and west of map area) on the south and Sunset Bay on the north (Plates 1, 3, and 4). The width of the preserved terrace ranges from ~1.3 km (0.8 mi) east of Bandon to ~2.6 km (1.6 mi) between Twomile and Threemile Creeks (Plate 3). North of Threemile Creek, terrace sediments are more aerially restricted, with a platform ranging between 0.1 and 0.4 km (0.06 and 0.2 mi) in width, overlying and inset into deeply incised bedrock headlands. Backedge elevations for the terrace range from ~57 m (187 ft) at Floras Creek on the south, climbing to ~105 m (346 ft) east of Bandon, ~117 m (385 ft) in the headwaters of Threemile Creek, and ~125 m (410 ft) east of Cape Arago on the north (Plates 3 and 4). Average thickness of the terrace cover sediment ranges from ~3 to 18 m (9.8 to 59 ft).

The unit was informally named the Seven Devils terrace by Griggs (1945) for terrace sediments at the Seven Devils mine type section, located in the

headwaters of Threemile Creek (Plate 3). McNelly and Kelsey (1990) suggested a late Pleistocene age of ~125 ka for the Seven Devils terrace, equivalent to the last interglacial period. The Seven Devils terrace is correlative to terrace 3 (Gowman terrace) mapped by Kelsey and Bockheim (1994) and units Qtc3, Qtc4, Qtc5 mapped by T. J. Wiley (unpublished mapping, 2007) in the Pistol River-Cape Ferello-Brookings area, and is coeval with the Silver Butte terrace (Qmtd) mapped by Kelsey (1990) and Wiley and others (2014) (Table 2; Plate 1).

Qmtm Metcalf terrace sediments (middle Pleistocene)—Moderately to deeply dissected terrace sediments forming an extensive platform above deeply dissected bedrock ridges between Johnson Creek on the south and Coos Bay on the north (Plates 1, 3, and 4; Madin and others, 1995). The width of the preserved terrace ranges from ~0.7 km (0.4 mi) south-east of Bandon (Plate 1) to ~4 km (2.5 mi) north of Beaver Hill (Plate 3). North of the map area, Metcalf terrace sediments form a broad but structurally warped platform up to 10 km (6 mi) in width, extending across South Slough and west to Cape Arago State Park (Plate 4). Backedge elevations for the terrace range from ~207 m (680 ft) east of Bandon (Plate 1) descending to ~127 m (415 ft) at Beaver Hill (Plate 3), and ~152 m (500 ft) east of Cape Arago (Plate 4). Average thickness of the terrace cover sediment ranges from ~3 to 16 m (9.8 to 52.5 ft). Madin and others (1995) reported greater thicknesses for the Metcalf terrace east of South Slough (≥ 28 m [92 ft]) and ~48 m (157 ft) logged from a borehole at upper Pony Creek Reservoir (13 km [8 mi] northeast of Cape Arago).

The unit was originally mapped as part of the "Higher terraces" by Griggs (1945, plate 2) and was informally named the Metcalf terrace by McNelly and Kelsey (1990). McNelly and Kelsey (1990) speculatively suggested a late Pleistocene age of ≥ 200 ka for the Metcalf terrace, predating the last interglacial period (Kelsey, 1990). The Metcalf terrace is correlative to terrace 4 (Aqua Vista) mapped by Kelsey and Bockheim (1994) and units Qtc4, Qtc5, and Qtc6 mapped by T. J. Wiley (unpublished mapping, 2007) in the Cape Ferello-Brookings area, and to the Indian Creek terrace mapped south of the study area by Kelsey (1990), McClaughry and others (2013), and Wiley and others (2014) (Table 2).

Qmta Arago Peak terrace sediments (middle to lower(?) Pleistocene)—Deeply dissected terrace sediments forming a narrow, discontinuous platform capping ridges southeast of Cape Arago (Plate 4) and west of South Slough (Madin and others, 1995). Bedrock platform elevations for the Arago Peak terrace range from ~203 to 213 m (667 to 700 ft) (Plate 4). Average thickness of the terrace cover sediment ranges from ~13 to 17 m (42.6 to 55.8 ft).

The unit was originally mapped as part of the ‘Higher terraces’ by Griggs (1945, Plate 2) and informally named the Arago Peak terrace by McNelly and Kelsey (1990). Platform elevation of the Arago Peak terrace is similar to that of the Poverty Ridge terrace capping deeply dissected ridges near Port Orford (Kelsey, 1990, McClaughry and others, 2013; Wiley and others, 2014; south of map area), but the absolute age and regional correlation of the Arago Peak terrace has not yet been definitively established.

Unconformity

LOWER PLEISTOCENE SEDIMENTARY ROCKS

Qgcq Coquille Formation (lower Pleistocene)—Very poorly exposed, partly cemented gravel (conglomerate), sand, and pebbly sand, with lesser amounts of clay, mud, peat, and wood (Plate 3). The formation was originally named and described by Baldwin (1945), who measured a then well-exposed 28.3 m-thick (93 ft) type section, in the coastal bluff between Whiskey Run and Cut Creek, north of the Coquille River (Plate 3). The type section is now largely covered with slumped material and/or is overgrown with vegetation. As described by Baldwin (1945), the measured type section consists of 7.3 m (24 ft) of locally cemented gravel, ~18 m (59 ft) of coarse to fine,

locally cross-bedded and occasionally pebbly sand with local pebble lenses and woody material, and ~3 m (10 ft) of thin-bedded sandy clay. Beds containing woody material, occurring as stumps, logs, and peat, account for about 1 m (3.3 ft) of the measured section. Baldwin (1945) reported that the exposed thickness of the formation is likely greater than 61 m (200 ft); additional material has likely been stripped from the upper part of the formation and also may be hidden below sea level. Beds in the type section were interpreted to be gently deformed, with dips ranging from horizontal up to 25 degrees (Baldwin, 1945). A photograph included by Baldwin (1945) displays the Coquille Formation resting unconformably beneath terrace deposits of the Whiskey Run Terrace (**Qmtw**); Baldwin (1945) also described an unconformity at the mouth of Whiskey Run (Plate 3), where the formation overlies the sandstone of Fivemile Point (**Tefm**).

Gravel and pebbly sandstone that Wiley and others (2014) mapped as part of Quaternary terrace deposits in the bluffs surrounding the harbor at Bandon may be correlative, at least in part, with the Coquille Formation. Additionally, a small outcrop of partly cemented pebbly sand exposed inland, near the northwestern edge of the Riverton 7.5' quadrangle (NAD83 UTM Zone 10 coordinates 393607E., 4789175N.), with beds oriented N14°W, 17°NE, may be correlative to the Coquille Formation. Baldwin (1945) interpreted the Coquille Formation to fill a bedrock channel cut and filled during the oldest of three late Pleistocene episodes of channel cut and fill by the Coquille River. Reported dips and the degree of folding suggested by photographs in Baldwin (1945) show these rocks to be far more deformed than nearby upper Pleistocene marine terrace deposits. We tentatively assign them a lower Pleistocene (>780 ka) age.

Unconformity

**LOWER CENOZOIC AND
MESOZOIC ROCKS**
PALEOGENE OVERLAP SEQUENCE

Teb Bastendorff Shale (upper Eocene)—Laminated siltstone, mudstone, and minor fine-grained sandstone exposed between Riverton and Overland, west of Coquille (Plates 2 and 3). While sandstone in the unit is rare, several, meter-thick, resistant sandstone beds are present at the type section at Bastendorff Beach (Charleston 7.5' quadrangle; Figure 2). The rock is typically medium to dark gray (N5 to N3) where fresh, and weathers to a light yellowish brown (10YR 6/2), light brown (5YR 6/4), or yellowish brown (10YR 5/4). Allen and Baldwin (1944) reported a thickness of 885 m (2,905 ft) at Bastendorff Beach, while Madin and others (1995) reported that the thickness may be greater locally. Only the lower part of the formation is present in the study area.

Allen and Baldwin (1944) noted that the formation conformably overlies the Upper Member of the Coaledo Formation (**Tecu**) in most places, with the possibility of a local disconformity in the Coquille area (Plates 2 and 3). Further north, at the type section near Coos Bay (Figure 2), the formation is conformably overlain by the upper Eocene Tunnel Point Sandstone. Along South Slough, immediately north of the study area, the formation is unconformably overlain by the Miocene Empire Formation (Figure 1).

The Bastendorff Shale is assigned an upper Eocene age on the basis stratigraphic position and microfossil assemblages. The formation was originally assigned an Oligocene age (Dall, 1909), which was revised to partly to wholly Eocene (Allen and Baldwin, 1944) and then to upper Eocene (Rooth, 1974; Warren and Newell, 1981; Armentrout and others, 1983; McKeel, 1984). Water depths in which the lower part of the formation was deposited were estimated on the basis of benthic foraminiferal assemblages by Rooth (1974) and Tipton (1975) and range from bathyal to abyssal.

Coaledo Formation (middle Eocene)—Sandstone, siltstone, and mudstone with minor pebbly sandstone, conglomerate, tuff, and coal, originally described by

Diller (1899). Turner (1938) divided the formation into three members including: 1) a Lower Member (**Tec1**) composed of coal-bearing sandstone; 2) a Middle Member (**Tecm**) composed primarily of siltstone, mudstone, and minor fine sandstone; and 3) an Upper Member (**Tecu**) composed of coal-bearing sandstone. Allen and Baldwin (1944) reported measured sections for the Coaledo Formation along the coast between Bastendorff Beach and Cape Arago (Plate 4). Duncan (1953) reported measured sections encountered in drill holes in the Riverton (Plate 3) and Coos Bay 7.5' quadrangles. Toenges and others (1948) reported coal characteristics and reserves. Depth of weathering within the formation varies greatly, with deeper weathered zones (paleosols?) common where the unconformity beneath older Quaternary terrace deposits is exposed at the modern surface. The formation is overlain, perhaps with local unconformity (Allen and Baldwin, 1944), by the Bastendorff Shale (**Teb**) and conformably underlain by the beds at Sacchi Beach (**Tes**). The formation's age, thickness, stratigraphic position, depositional environment, and composition suggest a correlation to marine facies of the Spencer Formation in the Willamette Valley (McCloughry and others, 2010). Strikingly similar sandstone facies with abundant molds and casts of small, 1 to 2 cm (0.4 to 0.8 in), clams occur at the base of the Spencer Formation southwest of Philomath (Wiley, 2008). Prothero and Donohoo (2001) assigned these rocks to Chrons C18r to C20r (40.0 to 44.0 Ma, middle Eocene) of the geomagnetic polarity time scale (GMPT).

Divided to show:

Tecu Upper Member (middle Eocene)—Feldspathic micaceous sandstone with pebbly sandstone, siltstone, mudstone, coal, carbonaceous shale, and conglomerate widely exposed across the central and eastern part of the map area (Plates 1, 2, and 3). Sandstone ranges from fine to coarse grained with sedimentary structures including planar bedding, ripple cross-laminations, low-angle cross-bedding, hummocky or swaley cross-bedding, trough cross-bedding, and tabular cross-bedding. Abundant shelly material occurs in thin, well-defined layers or scattered throughout the rock (bioturbated); locally, shells are concentrated to form patches of

coquina. In exposures where weathering has leached out original shell material, molds and casts of the shells can often still be recognized in the weathered rock. Mudstone rip-up clasts are present in many of the coarse sandstone, pebbly sandstone, and conglomerate beds. Thin sequences of siltstone, mudstone, coal, and carbonaceous shale occur locally, typically as fine-grained zones in coarsening upward sequences. Soft-sediment deformation has distorted some beds and groups of beds. Thickness of the Upper Member is reported to be ~400 m (~1,312 ft) as determined in the section exposed between Bastendorff and Lighthouse Beaches near the mouth of Coos Bay and ~850 m (~2,770 ft) near Riverton (Allen and Baldwin, 1944; Figure 1).

Coal beds within the Upper Member were described in detail by Allen and Baldwin (1944), Duncan (1953), and Toenges and others (1948). Chan and Dott (1986) reported repeated coarsening- and shallowing-upward sequences recording transitions from shelf to deltaic environments. It is not clear if these are due to fluctuations in sea level, local base level (tectonics), or migration of active delta lobes. The Upper Member conformably overlies deep-water facies that make up the Middle Member (**Tecm**), indicating a marine regression and shallowing trend.

Tecm Middle Member (middle Eocene)—Mudstone, shale, siltstone, and fine-grained sandstone with minor medium-grained sandstone exposed across the central and eastern part of the map area, extending from Grigsby Rock on the south to Sunset Bay on the north (see map plates). Fresh rocks in the unit are typically dark gray (N3) to greenish gray (5GY 6/1) and weather to variable shades of white (N9) to dark gray (N3) to pale or dark yellowish orange (10YR, 8/6; 10YR 6/6). Micaceous mudstone, shale, and massive to laminated siltstone are typically thin bedded; a few thick beds are present, some of which appear to be bioturbated. Micaceous sandstone is massive (bioturbated), plane laminated, or cross-bedded. Bioturbated sandstone locally contains varying amounts of fossils or fossil fragments.

Sandstone-siltstone-mudstone graded beds are present locally; many of these display the characteristic sedimentary structures of Bouma sequences (turbidites). At Lighthouse Beach the Middle Member of the Coaledo Formation is ~890 m thick (~2,925 ft) and ~640 m thick (~2,100 ft) near Lampa Creek (Plate 1) (Allen and Baldwin, 1944).

The member has been interpreted as pro-delta-shelf with less common shelf to slope deposits (Dott, 1966; Chan and Dott, 1986). These relatively deep water deposits overlie shallow water deposits of the Lower Member (**Tec1**), indicating deepening and marine transgression.

Tec1 Lower Member (middle Eocene)—Sandstone, pebbly sandstone, siltstone, mudstone, coal, and minor conglomerate exposed across the central and eastern part of the map area, extending from Grigsby Rock on the south to Sunset Bay on the north. Fresh rocks in the unit are typically very light gray (N8) to yellowish gray (5Y 7/2) and weather to variable shades of white (N9) to pale or dark yellowish orange (10YR, 8/6; 10YR 6/6). Sandstone is typically micaceous, with the most common framework grains composed of lithic fragments or feldspar ranging in size from fine to coarse sand. Sedimentary structures include common plane lamination, hummocky and/or swaley cross-bedding, trough cross-bedding, and ripple cross-lamination. Soft sediment deformation or dewatering has locally deformed some sedimentary structures and created others including flame structures and slumped bedding. In fresh exposures shelly material may be abundant, with shell types including delicate to robust pelecypods (often aligned parallel to bedding), *Turritellid* and other gastropods, and locally abundant *Dentalium* sp. In exposures where weathering has leached shell material from the beds, molds and casts of the shells can often still be recognized in the weathered rock. At Sunset Bay, the uppermost sandstone bed in the Lower Member is locally pebbly or contains thin lenses of conglomerate; its upper surface preserves a set of parallel meter-wavelength

dune features. Thickness of the Lower Member is about 540 m (1,775 ft) near Sunset Bay (Plate 4) and is at least 579 m (1,900 ft) along highway 42S, west of Lampa Creek (Plate 1) (Allen and Baldwin, 1944).

Sedimentary structures suggest deposition in water depths shallower than wave base (~50 m [164 ft]) in inner shelf, deltaic, and nearshore environments indicating a marine regression following deposition of the beds at Sacchi Beach (**Tes**).

Tes beds at Sacchi Beach (middle Eocene)—Typically well-bedded, moderately to strongly indurated, micaceous siltstone, mudstone, and fine sandstone with a few thin beds of medium sandstone, coal, or carbonaceous shale. Exposed in the northwest part of the map area between the Coquille River on the south and Cape Arago on the north (Plates 3 and 4). A few thin beds at Cape Arago consist of pebbly sandstone and shale breccia, containing angular to sub-round mudstone rip-up clasts ranging from 5 cm (2 in) up to 5 m (16.5 ft) across, in a sandstone matrix. The formation is characterized by a vertical sequence progressing from structureless to laminated mudstones near the base that becomes increasingly sandstone-dominated up section. These rocks are typically very poorly exposed except for outcrops at Cape Arago (Rooth, 1974), coastal bluffs above Merchants Beach and Agate Beach, and more recent roadcuts farther inland. Good outcrops at the type section at Sacchi Beach are now rarely exposed (see Rooth [1974] for a detailed description of this stratigraphic section), being limited to bluff-forming outcrops at the southern end of the beach. Fresh mudstone, siltstone, and fine-grained sandstone in the unit are typically medium gray (N5) to dark gray (N3) and weather to variable shades of white (N9) to pale or dark yellowish orange (10YR, 8/6; 10YR 6/6). Fresh sandstone beds are white (N9) to very light gray (N8) and weather to shades of grayish orange pink (5YR 7/2). Individual siltstone and fine-grained sandstone beds typically range from 1 cm (0.4 in) up to 25 cm (10 in) thick, while more massive medium-grained sandstone beds range from 10 cm (4 in) to several meters thick (tens of feet). Sedimentary structures include graded bedding, plane laminations, ripple cross-laminations, coal rip-up clasts, occasional scoured lower surfaces, flute and groove casts, and sole marks. Large channel

features are common within the unit in North and South Coves at Cape Arago (Plate 4). Soft-sediment deformation or dewatering within sandstone beds has locally deformed some sedimentary structures and created others including flame structures, dish and pillar structures, convolute bedding and laminations, and slumped bedding. The contact with thick-bedded, cross-bedded carbonaceous sandstones of the overlying Lower Member of the Coaledo Formation (**Tecl**) may be in part gradational (Rooth, 1974). Baldwin and others (1973) reported a thickness of ~550 m (1,804 ft) at Sacchi Beach in the northeastern part of the Bullards quadrangle.

The informally named beds at Sacchi Beach (Baldwin, 1965) were referred to as the Sacchi Beach beds by Stewart (1956, 1957). Regional stratigraphic correlation of the beds at Sacchi Beach has been controversial, with the unit being assigned to six different formations by a number of workers. Original work by Diller (1901) assigned these strata to the Eocene Pulaski and Neogene Empire formations. Subsequent workers assigned these rocks to a number of formations including the Umpqua Formation (Allen and Baldwin, 1944), Arago Formation (Weaver, 1945), Elkton Formation (Bird, 1967; Rooth, 1974), Sacchi Beach Member of the Tyee Formation (Baldwin, 1964), and Elkton Siltstone Member of the Tyee Formation (Baldwin and others, 1973). The formation is assigned a middle Eocene (Ulatisian) age on the basis of foraminifera (Stewart, 1957; Baldwin and others, 1973). P. D. Snively, Jr. (U.S. Geological Survey, personal communication to I. P. Madin, 1995) reported CP14a stage coccoliths from roadcut exposures, indicating a middle to upper Eocene age for the formation (Bukry and Snively, 1988), significantly younger than the CP12a age of the Elkton Formation (Ryu and others, 1992). The CP14a stage is now considered middle Eocene (Cohen and others, 2013). This assigned age is consistent with interpretations that place the beds at Sacchi Beach stratigraphically above the CP12 age (Wells and others, 2014) Tyee Formation (**Tet**)—although a contact between the Tyee Formation and the beds at Sacchi Beach has not been observed. Instead, there appears to be a disconformity where the shallow water deposits of the Lower Member of the Coaledo Formation rest on the Tyee Formation near the boundary between the Rivoton and Bill Peak 7.5' quadrangles (Plate 1).

The beds at Sacchi Beach form a sequence that progressively shallows upward from neritic (91 to 183 m [300 to 600 ft]) to middle or inner neritic (<91 m [300 ft]) water depths (Rooth, 1974). Lithology and sedimentary structures in the unit indicate deposition of the lower mudstone-dominated part of the formation during prolonged accumulation of very fine mud in quiet water, while middle and upper parts indicate deposition as turbidites (Rooth, 1974).

Tet Tyee Mountain Member of the Tyee Formation (middle Eocene)—Arkosic and abundantly micaceous sandstone and less common mudstone exposed between Bear Creek and Lampa Creek in the southern part of the map area (Plate 1). Fresh rocks in the unit are typically very pale orange (10YR 8/2) to pale yellowish brown (10YR 6/2). Sandstone ranges from fine to coarse grained and may locally contain woody debris. Pebbly sandstone, conglomerate, coal, and mega-fossils are generally absent. Bed thickness ranges from thin bedded to massive or amalgamated. Graded beds with sedimentary structures characteristic of Bouma sequences (Bouma, 1962) are common. Cross-bedding was not recognized except as convolute laminations in the Bouma Tc layers of turbidites. The Tyee Formation has a maximum thickness of 470 m (1,540 ft) in the Bill Peak 7.5' quadrangle (Plate 1).

Where outcrops are too small to distinguish turbidite sequences, particularly in amalgamated sandstone or thick mudstone sequences, the formation may be difficult to distinguish from the overlying Coaledo Formation. Locally present, well-developed convolute laminations in multiple beds can be used to distinguish strata of the Tyee Mountain Member from similarly micaceous beds of the Lower Member of the Coaledo Formation (**Tecl**). Additionally, in many cases, the Lower Member of the Coaledo Formation (**Tecl**) typically contains fossil pelecypods and gastropods or their casts and molds. The Tyee Mountain Member is distinguished from older lithic sandstone turbidites of the Umpqua and Roseburg Formations by its typically arkosic composition and the notable abundance of muscovite and biotite.

The Tyee Formation is assigned a middle Eocene age on the basis of ages reported elsewhere in the Coast Range and on correlations between adjacent formations, global sea level curves, and nearby oil wells. The Tyee Formation is divided into several

members in its type area; these include from bottom to top, the Tyee Mountain Member, a basal turbidite unit; the Hubbard Creek Member, thought to represent slope sandstone and siltstone; and the Baughman Member, interpreted as a beach and nearshore deposit (Wells and others, 2000). Rocks in the study area are interpreted as turbidites and are assigned to the Tyee Mountain Member.

Teu Umpqua Group (lower Eocene)—Sandstone and mudstone with less common intervals of pebbly sandstone and conglomerate exposed in the southern and eastern parts of the map area (Plates 1, 2, and 3). Fresh mudstone in the unit is typically moderate brown (5YR 3/4) to olive gray (5Y 3/2), while sandstone is pale brown (5YR 5/2) to pale yellowish brown (10YR 6/2). Sedimentary rocks of the Umpqua Group are generally not micaceous. Sandstone and mudstone are typically interlayered in medium- to thin-bedded turbidites but locally include thick-bedded to massive sandstone or mudstone intervals. The thickness of the unit in the map area is unknown, but Molenaar (1985) estimated the thickness to be as much as 3,000 m (10,000 ft) outside the map area.

Molenaar (1985) demonstrated that the upper part of the Umpqua Group is generally conformable with the overlying Tyee Formation. The lower part of the Umpqua Group is locally separated from the upper part of the Umpqua Group by an angular unconformity that may be quite well developed. In the western part of the study area rocks assigned to the Umpqua Group are conformable beneath Coaledo and Tyee Formations and are considered to represent the upper part of the group. In the eastern part of the study area, more deformed sedimentary rocks assigned to the Umpqua Group rest on Siletz River Volcanics and likely represent the lower part of the group. Working in the Remote 7.5' quadrangle, 25 km (15 mi) east of the study area, Black (1994) mapped similar relationships and placed this unconformity above the Ten-mile Formation and below the Whitetail Ridge and Camas Valley Formations. Farther east of the study area the Umpqua Group laps across contacts between Western Klamath, Yolla Bolly, and Sixes River terranes. Formations in the upper part of the group are deposited across the Canyonville fault in the vicinity of the Coast Range syncline 48 km (30 mi) east of the study area.

The unit is assigned an early Eocene age on the basis of coccolith ages and stratigraphic position interfingering with the upper part of the Siletz River volcanics (CP10 Zone; Bukry and Snavely, 1988; Wells and others, 2000, 2014). Sedimentary structures and lithology indicate deep marine to nonmarine depositional setting (Heller and Ryberg, 1983; Ryberg, 1984; Niem and Niem, 1990; Wells and others, 2000).

Unconformity

SILETZ TERRANE

Tesr Siletz River Volcanics (Paleocene and lower Eocene)—Basaltic lava flows including pillow lava, pillow breccia, breccia, columnar-jointed flows, and thin interbeds of sedimentary rocks exposed in the southeastern part of the Coquille 7.5' quadrangle (Plate 2). Typical hand samples of the basalt are dark gray (N3) to black (N1), aphyric to plagioclase and/or augite (ophitic) phyric, with a fine to medium grained, crystalline to glassy groundmass. Locally, the rock may be amygdaloidal and may contain disseminated sulfide minerals. Sedimentary interbeds of the Roseburg Member (upper Paleocene to lower Eocene; Wells and others, 2000) of the Siletz River Volcanics are present locally but not mapped separately. Thickness of the unit in the map area is unknown but may be up to a few hundred meters (~1,000 feet). Estimates of total thickness of the volcanic pile, conducted on the basis of geophysics outside the map area near latitude 44°N, range from roughly 12,000 m (40,000 ft; Figure 10 of Fleming and Tréhu, 1999) to 15,000 m (50,000 ft; Figure 6 of Snavely, 1987).

The unit is assigned a Paleocene and early Eocene age on the basis of eruptive ages for the Siletz terrane ranging from 56 to 49 Ma (Wells and others, 2014). Duncan (1982) reported four nearby basalt localities have Paleocene whole-rock, K-Ar radiometric dates (of uncertain quality) of 60.0 ± 1.7 Ma (4.3 km [2.7 mi] outside the study area in the McKinley 7.5' quadrangle), 61.7 ± 3.6 Ma (1.63 km [1.0 mi] east of the study area in the McKinley 7.5' quadrangle), 59.2 ± 2.8 Ma (9.4 km [5.8 mi] north-northeast of the study area in the Allegany 7.5' quadrangle), and 61.5 ± 1.6 Ma (12.0 km [7.5 mi] south-southeast of the study area in the Bridge 7.5' quadrangle). Lava flows in the study area were emplaced in submarine environments. The marine origin, rock chemistry, and basaltic provenance of coeval sediment suggest that these rocks are ocean island, plateau, or mid-ocean ridge basalts (MORBs).

Faulted terrane boundary

SIXES RIVER TERRANE

Fulmar subterrane—Arkosic sandstone and sandstone- and/or mudstone-matrix mélange. Distinguished from other subterrane of the Sixes River terrane by the presence of lower Eocene arkosic sandstone of Fivemile Point (**Tefm**) (Snavely and others, 1980, as cited by Snavely, 1987). Equivalent, in part, to the Fulmar terrane of Snavely and others (1982) and Howell and others (1985).

Tefm sandstone of Fivemile Point (lower Eocene)— Well-bedded sandstone with minor grit, black mudstone, pebbly sandstone, conglomerate, and shale exposed along the western edge of the map area between Bill Peak on the south and Fivemile Point on the north (Plates 1 and 3). The unit is also recognized in offshore wells including the Pan American Coos Bay No. 1 Well, located west of Coos Bay, and the Union Oil Company's Fulmar No. 1 Well, located west of Florence (Snively and others, 1982). These rocks are best exposed at the type section at Fivemile Point on the coast (Figure 8; Plate 3) and more recent roadcuts farther inland. Fresh rocks in the unit are typically very light gray (N8) to medium gray (N5). Sandstone is typically a poorly to moderately sorted, very fine- to coarse-grained arkosic wacke, with very minor amounts of mica. Black, green, white, and red chert grains are common. Geochemical analysis (XRF) of a sandstone sample at Fivemile Point indicate an arkosic wacke composition, with major element concentrations of 71.54 weight percent SiO_2 , 13.27 weight percent Al_2O_3 , 5.11 weight percent FeO^* , and

1.42 weight percent K_2O and trace element concentrations of 109 ppm Zr, 5.1 ppm Nb, 23 ppm Y, 17 ppm La, and 29 ppm Ce (Table 3; Plate 3; Appendix, sample 14 SCJ 14). Conglomerate and sandstone beds exposed in many outcrops contain distinctive, fine-grained, cream-colored sedimentary clasts (?) or recycled concretions (?) (Figure 9). Individual sandstone beds typically range from 3 cm (1.2 in) up to 1 m (3.3 ft) thick and may contain multiple fining upward cycles. Sedimentary structures include graded bedding, plane laminations, occasional scoured lower surfaces, and ellipsoidal concretions that parallel bedding. Sections of steeply dipping beds are broadly warped, suggesting that at least two folding events have deformed the unit (Figure 8). The greatest measurable thickness of the formation is at Fivemile Point, where more than 420 m (1,378 ft) is exposed at the point and just offshore (Figure 8a). Snively and others (1982) recorded 2,225 m (7,300 ft) of Penutian sandstone in the Union Oil Co. Fulmar No. 1 well, which they correlate to the sandstone of Fivemile Point.

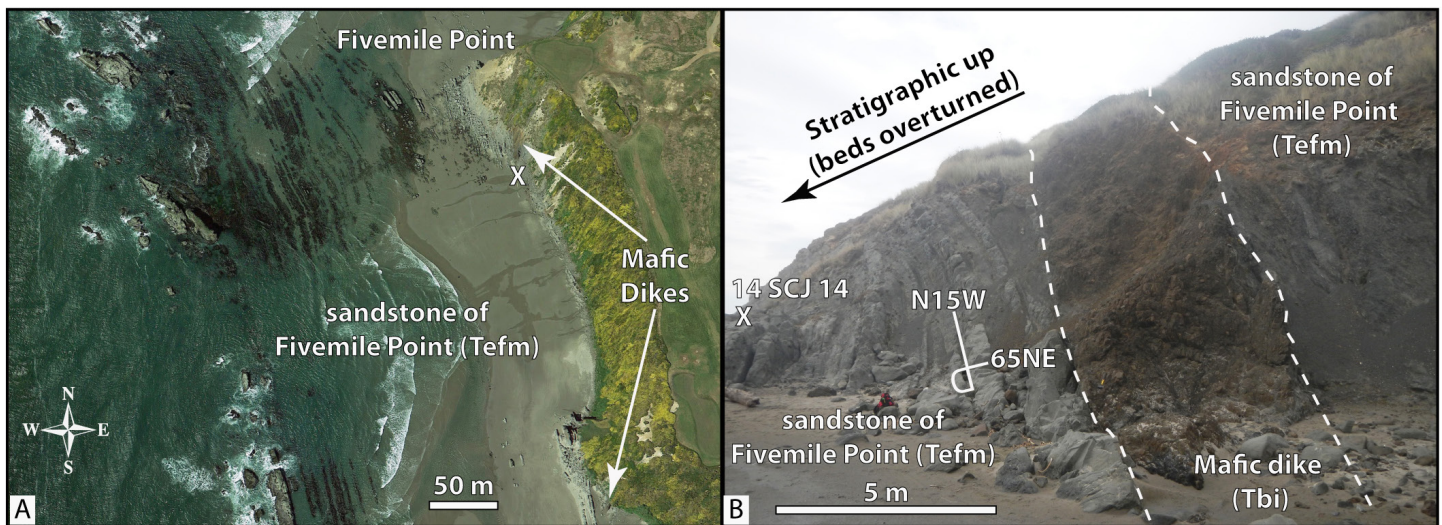


Figure 8. (a) Sandstone of Fivemile Point (Tefm). (a) Google Earth™ image showing steeply dipping, overturned sandstone and mudstone turbidite beds in the vicinity of Fivemile Point in the Bullards 7.5' quadrangle (Plate 3). The sandstone is intruded by a series of bedding parallel mafic dikes (Tbi) whose locations are indicated by white arrows. White X shows the location of the photograph in B. Scale bar in bottom-center part of the image is 50 m (164 ft) wide. (b) Steeply east-dipping, overturned sandstone and mudstone turbidite beds forming Fivemile Point (WGS84 geographic coordinates: 386546mE., 4786133mN.). Brown-weathering, bedding-parallel mafic dike is shown by white dashed lines. The site marked by X and labeled 14 SCJ 14 is the location of a $^{206}\text{Pb}/^{238}\text{U}$ detrital zircon age sample. Scale bar in bottom-left part of the image is 5 m (16.4 ft) wide. View in the photograph is looking north.

Table 3. Representative X-ray fluorescence analyses for rocks in the Bandon, Coquille, and Sunset Bay areas.

| Sample No. | 79 SCJ 13 | 80 SCJ 13 | SR13-LV | SR13-UQ | 71MWJ07 | 2W039 | B-24-9/14 | 14 SCJ 14 |
|--|---------------------|---------------------|------------------------|------------------------|------------------------|------------------------|---------------------|---------------------|
| Map No. | B1 | B2 | na | na | na | na | BP1 | B3 |
| Quadrangle | Bullards | Bullards | Myrtle Point | Roseburg West | Corvallis | Roseburg East | Bill Peak | Bullards |
| Terrane Group | Sixes River terrane | Sixes River terrane | Siletz terrane | Siletz terrane | Siletz terrane | Siletz terrane | Sixes River terrane | Sixes River terrane |
| Formation | nd | nd | Siletz River Volcanics | Siletz River Volcanics | Siletz River Volcanics | Siletz River Volcanics | Fulmar subterrane | Fulmar subterrane |
| Map Unit | Tbi | Tbi | na | na | na | na | KJss | Tefm |
| UTM N (NAD 83) | 4785818 | 4786155 | 4774684 | 4781843 | 4933056 | 4785487 | 4763292 | 4786199 |
| UTM E (NAD83) | 386626 | 386543 | 406666 | 463969 | 457650 | 477732 | 392968 | 386499 |
| <i>Oxides, weight percent</i> | | | | | | | | |
| SiO ₂ | 48.42 | 44.82 | 48.87 | 49.70 | 48.34 | 48.35 | 69.59 | 71.54 |
| Al ₂ O ₃ | 15.13 | 14.65 | 14.72 | 14.14 | 15.91 | 14.43 | 12.18 | 13.27 |
| TiO ₂ | 1.95 | 2.13 | 1.77 | 1.94 | 1.59 | 1.88 | 0.64 | 0.59 |
| FeO* | 11.99 | 12.76 | 11.56 | 12.36 | 11.49 | 11.26 | 5.94 | 5.11 |
| MnO | 0.18 | 0.51 | 0.19 | 0.20 | 0.18 | 0.55 | 0.11 | 0.09 |
| CaO | 10.87 | 14.66 | 12.66 | 11.82 | 12.94 | 12.51 | 3.23 | 1.81 |
| MgO | 7.95 | 7.11 | 7.52 | 6.87 | 7.19 | 7.52 | 3.93 | 2.85 |
| K ₂ O | 0.20 | 0.17 | 0.18 | 0.22 | 0.15 | 0.52 | 1.92 | 1.42 |
| Na ₂ O | 3.11 | 2.95 | 2.36 | 2.57 | 2.04 | 2.48 | 2.29 | 3.21 |
| P ₂ O ₅ | 0.21 | 0.22 | 0.17 | 0.18 | 0.17 | 0.50 | 0.17 | 0.12 |
| LOI | 3.69 | 7.87 | 3.54 | 4.51 | 4.72 | nd | 3.43 | 2.61 |
| <i>Trace elements, parts per million</i> | | | | | | | | |
| Ni | 85 | 82 | 100 | 90 | 112 | nd | 76 | 88 |
| Cr | 139 | 93 | 300 | 160 | 313 | nd | 167 | 183 |
| Sc | 33 | 42 | 45 | 43 | 40 | nd | 13 | 14 |
| V | 323 | 416 | 367 | 386 | 330 | nd | 135 | 123 |
| Ba | 62 | 81 | 49 | 48 | 15 | nd | 487 | 429 |
| Rb | 4.7 | 3.8 | 2 | 2 | <0.5 | nd | 55.2 | 40.2 |
| Sr | 210 | 225 | 192 | 190 | 183 | nd | 135 | 160 |
| Zr | 115 | 110 | 103 | 106 | 92 | nd | 125 | 109 |
| Y | 34 | 36 | 24.8 | 26.1 | 25.1 | nd | 23 | 23 |
| Nb | 10.3 | 8.4 | 7.9 | 9 | 6.5 | nd | 8.6 | 5.1 |
| Ga | 18.7 | 18.8 | 21 | 20 | 16.8 | nd | 14.9 | 15 |
| Cu | 89 | 79 | 180 | 180 | 140 | nd | 39 | 39 |
| Zn | 73 | 106 | 90 | 110 | 85 | nd | 92 | 81 |
| Pb | <1 | <1 | <5 | <5 | 2 | nd | <1 | 2 |
| La | 10 | 10 | 8.26 | 8.28 | 9 | nd | 22 | 17 |
| Ce | 26 | 25 | 21.4 | 20.6 | 17 | nd | 38 | 29 |
| Th | 2.1 | 2.7 | 0.71 | 0.66 | 1.6 | nd | 16.7 | 7.2 |
| U | <0.5 | 0.5 | 0.23 | 0.2 | nd | nd | <0.5 | 0.5 |
| Co | 50 | 47 | 50 | 48 | 46 | nd | 23 | 19 |

Major element determinations have been normalized to a 100-percent total on a volatile-free basis and recalculated with total iron expressed as FeO*; nd = no data. Samples analyzed at Franklin and Marshall University. Sample 71 MWJ 07 from McClaughry and others (2010); sample 2W039 from Wells and others (2000); samples SR13-LV and SR13-UQ from Lawrence (2014) originally reported with iron as Fe₂O₃; values shown here have been converted to FeO* and renormalized.



Figure 9. Distinctive light-colored clasts in quarry blocks of sandstone of Fivemile Point (**Tefm**) (WGS84 geographic coordinates: 389690mE., 4771684mN.). Hand lens for scale is 2 cm (0.8 in) wide.

The sandstone of Fivemile Point is distinguished from coeval strata of the Umpqua Group (**Teu**), which crop out farther east, by its arkosic wacke composition (Snively and others, 1980). Fine-grained sedimentary rocks, poorly exposed at inland localities, closely resemble fine-grained facies of the Umpqua Group (**Teu**), Tyee Mountain Member of the Tyee Formation (**Tet**), Middle Member of the Coaledo Formation (**Tecm**), and the beds at Sacchi Beach (**Tes**). These fine-grained rocks have been assigned to the sandstone of Fivemile Point on the basis of their proximity to known outcrops of Fivemile Point sandstone and the presence of small amounts of mica (largely absent in coeval rocks of the Umpqua Group to the east, and common to abundant in the younger beds at Sacchi Beach and Coaledo Formation). Bedding patterns indicate that an angular unconformity separates the sandstone of Fivemile Point from younger beds at Sacchi Beach in the northern part of the Riverton 7.5' quadrangle (Plate 3). A fault or unconfor-

mity separates the sandstone of Fivemile Point from an east-dipping section of Umpqua Group and Tyee Formation in the Bills Peak 7.5' quadrangle (Plate 1) and the southern part of the Riverton 7.5' quadrangle (Plate 3).

The sandstone of Fivemile Point is assigned an early Eocene age on the basis of microfossils collected at Fivemile Point and in offshore wells (David Bukry, as cited by Miles, 1981; Snively and others, 1982; Snively, 1987). Rau (as cited by Snively and others, 1982) assigned foraminifera collected from this unit an early Eocene age (Penutian Stage) and suggested deposition occurred in middle to lower bathyal depths. Bukry (as cited by Snively and others, 1982) assigned coccoliths an early Eocene age. Three isotopic ages obtained from $^{206}\text{Pb}/^{238}\text{U}$ analysis of detrital zircons from sandstone samples in this unit indicate a maximum depositional age ranging between the Early Eocene (Ypresian) and Late Cretaceous (Turonian/Coniacian). A sandstone sample from the Fivemile Point type section yielded 97 detrital zircons with peak age populations at 92, 99, 108, 120, 158, 201, 320, and 1,365 Ma (Plate 3; Appendix, sample 14 SCJ 14). The 10 youngest zircons analyzed from sample 14 SCJ 14 range from 87.5 ± 2.5 Ma to 99.1 ± 2.5 Ma, with the youngest coherent peak population of seven grains defining a maximum depositional age of ca. 92 Ma (Late Cretaceous [Turonian/Coniacian]) for this sample. A second sandstone sample from the exposures along Bill Creek yielded 105 detrital zircons with peak age populations at 54, 98, 112, 152, 195, 268, and 329 Ma (Plate 1; Appendix, sample 212-12-1). The 10 youngest zircons analyzed from sample 212-12-1 range from 52.3 ± 1.2 Ma to 96.8 ± 2.5 Ma, with the youngest coherent peak population of four grains defining a maximum depositional age of ca. 54 Ma (Early Eocene [Ypresian]) for this sample. A third sandstone sample from the exposures near Parkersburg along the Coquille River yielded 95 detrital zircons with peak age populations at 89, 95, 118, 152, 171, and 191 Ma (Plate 3; Appendix, sample 115-15-1). The 10 youngest zircons analyzed from sample 115-15-1 range from 67.7 ± 1.4 Ma to 91.3 ± 1.8 Ma, with the youngest coherent peak population of 10 grains defining a maximum depositional age of ca. 89 Ma (Late Cretaceous [Turonian/Coniacian]) for this sample.

Mafic dikes (**Tbi**), with chemical compositions similar to that of the Siletz River Volcanics (Table 3),

intrude the sandstone at Fivemile Point. This stratigraphic relationship suggests that the Sixes River terrane may have amalgamated with the Siletz terrane before mafic volcanism in the Siletz terrane stopped completely.

Unconformity

KJs mélange of Sixes River (Upper(?) Cretaceous to Jurassic(?))—Mudstone- and/or sandstone-matrix mélange with infolded sections of mudstone and/or sandstone turbidites and other blocks of various lithologies. A Late (?) Cretaceous to Jurassic age has been determined on the basis of ages of included blocks (Blake and others, 1985) and on calcareous nannofossils reported by Miles (1981) from the Floras Creek drainage (south of the study area). Outside the study area, along the coast, south of Bandon, the Fulmar subterrane contains abundant blocks of glaucophane schist (Wiley and others, 2014). Locally divided to show the lithologies of blocks including:

KJss sandstone—Medium- to coarse-grained sandstone, grit, and pebbly sandstone. Sandstone in this unit, sampled from the quarry atop Bill Peak is very light gray (N8) to medium gray (N5), poorly to moderately sorted, very fine- to coarse-grained arkosic wacke, with very minor amounts of mica. Black, green, white, and red chert grains are common. The sandstone is typically calcite cemented with calcite veins and patches. Complementary geochemical data (XRF) for a sandstone sample at Bill Peak indicate an arkosic wacke composition, with major element concentrations of 69.59 weight percent SiO₂, 12.18 weight percent Al₂O₃, 1.92 weight percent K₂O, and 5.94 weight percent FeO* and trace element concentrations of 125 ppm Zr, 23 ppm Y, 8.6 ppm Nb, 22 ppm La, and 38 ppm Ce (Table 3; Plate 1; Appendix, sample B-24-9/14). Isotopic ages obtained from ²⁰⁶Pb/²³⁸U analysis of detrital zircons from a sandstone sample from the Bill Peak quarry yielded 86 detrital zircons with peak age populations at 119, 140, and 161 Ma (Plate 1; Appendix, sample B-24-9/14). The 10 youngest zircons analyzed from sample B-24-9/14 range from 114.3 ± 2.9 Ma

to 117.9 ± 2.6 Ma, with the youngest coherent peak population of 36 grains defining a maximum depositional age of ca. 119 Ma (Early Cretaceous [Aptian]) for this sample.

KJsv volcanic and meta-volcanic rock—Mafic volcanic rock, with some blocks metamorphosed to greenschist facies. Samples obtained from flow and intrusive blocks in this unit have spilitic (Le Maitre and others, 2004) chemical compositions with 50.6 to 51.22 weight percent SiO₂, 6.53 to 7.53 weight percent MgO, and 4.49 to 4.64 weight percent Na₂O (Wiley and others, 2014).

KJsc chert—Grayish green (10GY 5/2), grayish blue green (5BG 5/2), brown (5YR 2/2), black (N1), medium gray (N5), and red (5R 4/6) chert. Blocks include those that are manganeseiferous, contain radiolaria, or are banded. The unit includes blocks of chert-pebble to chert-cobble conglomerate with a chert matrix. Chert blocks are assigned an Early Cretaceous and Late Jurassic age on the basis of ages reported from the Sixes River terrane by Blake and others (1985).

KJcg conglomerate—Pebble and cobble conglomerate. Blocks may contain distinctive clasts of limestone, serpentine, or blueschist that indicate provenance related to the mélange.

KJsm other metamorphic rock—Grayish green (10GY 5/2), fine-grained meta-volcanic rocks, fine-grained sandstone, and siltstone containing actinolite, chlorite, and/or epidote suggesting metamorphism to greenschist facies.

KJsp serpentinite and meta-serpentinite—Dusky blue green (5BG 3/2) serpentinite and meta-serpentinite and serpentinitized ultramafic rocks.

KJst siltstone—Silicified siltstone.

KJm marble—White (N9), coarsely crystalline marble.

KJsg garnet schist—garnet-bearing schist.

KJsx mélange blocks, undivided—Mélangé blocks recognized on the basis of topographic expression using 1-m lidar DEMs, but not sampled or visited in the field.

ROCKS THAT INTRUDE THE FULMAR SUBTERRANE OF THE SIXES RIVER TERRANE

Tbi Intrusive rocks (lower Eocene)—Aphyric to microporphyritic basaltic dikes exposed at Fivemile Point in the western part of the map area (Plate 3). Dikes exposed at Fivemile Point and in sea stacks just to the south intrude the sandstone of Fivemile Point (**Tefm**) along bedding planes (N 15° W, 60° NE).

Typical hand samples are black (N1) to dark gray (N3), and aphyric to microporphyritic, containing sparse subhedral plagioclase microphenocrysts <1 mm (0.04 in) across distributed within a fine-grained groundmass. Samples obtained from the dikes at

Fivemile Point have a tholeiitic basaltic chemical composition of MORB affinity with 44.82 to 48.42 weight percent SiO₂, 14.65 to 15.13 weight percent Al₂O₃, 1.95 to 2.13 weight percent TiO₂, 11.99 to 12.76 weight percent FeO*, 7.11 to 7.95 weight percent MgO, and 0.17 to 0.20 weight percent K₂O (Table 3; Appendix, samples 79 SCJ 13 and 80 SCJ 13). The basalt has characteristically low incompatible trace element concentrations for large-ion lithophile elements (LILE) with 62 to 81 ppm Ba, 3.8 to 4.7 ppm Rb, and 210 to 225 ppm Sr, and low concentrations of the light rare earth elements (LREE) with 10 ppm La and 25 to 26 ppm Ce. The unit is assigned a lower Eocene age on the basis of stratigraphic relationship, intruding the lower Eocene sandstone of Fivemile Point and upper limit of age range of chemically similar Siletz River Volcanics.

Faulted terrane boundary

STRUCTURAL GEOLOGY

Geologic structure along the southern Oregon coast is defined by the mapped distribution of geologic units, faults, topographic lineaments (as observed in 1-m lidar DEMs), folds, and bedding attitudes (Appendix). Primary structural features (e.g., slickensides or fault breccia) are common in *mélange* matrix and less common in other lithologies. Fault zones are best exposed along sea cliffs, stream banks, roadcuts, and rock pits. Along most faults the relative amount of offset is not well constrained, as few stratigraphic piercing points have been recognized and lithologies on opposite sides of fault zones are often indistinguishable. Only locally along the coast and in coal mines is the relative amount of offset well constrained by offset geologic units.

The complex geologic structure of this part of the southern Oregon coast records Jurassic and younger development, amalgamation, accretion, and subsequent deformation and displacement of tectonostratigraphic terranes that now form the Cascadia margin of southern Oregon (Figure 4). No simple regional pattern of structure can easily be portrayed for the southern Oregon coast, but individual domains and phases of deformation can be discerned from careful mapping of bedrock and surficial geology. Each of the tectonostratigraphic terranes that underlie the study area displays: 1) its own structural history prior to amalgamation, 2) structural regimes related to amalgamation and/or accretion, and 3) post-accretionary structural modifications that are shared and recorded by the younger overlap sequence. As with most terrane models, the one described here (adapted from Blake and others, 1985; Wiley and others, 2014) assumes separate early histories for regions with distinct stratigraphy. However, we recognize that some of these rock packages may have originated as adjacent provinces in complex tectonic settings.

Two bedrock terranes underlie the map area: the Sixes River terrane and the Siletz terrane. The Sixes River terrane has been divided into three subterrane (Wiley and others, 2014), two of which crop out in or near the map area. The Fulmar subterrane crops out west of the Fulmar fault, and the Whitsett subterrane is suspected to be present at depth east of the Fulmar fault (see map plates). The Siletz terrane also lies east of the Fulmar fault and is thrust beneath the Whitsett subterrane to the south.

Sixes River terrane

The Sixes River terrane includes an extensive mudstone- and fine sandstone-matrix *mélange* (**KJs**) that contains distinctive blocks of blue greenschist, blueschist, and garnet-

bearing schist as well as many other lithologies. The blocks include lithologies that represent diverse environments including subduction zone depths of more than 15 km (9.3 mi) (blueschist), spreading centers, and volcanic arc(s). Wiley and others (2014) tentatively divided the Sixes River terrane into three subterrane thought to be juxtaposed along north-northwest-trending faults. The close relationship between these three subterrane is indicated by the presence of blueschist and garnet-bearing schist blocks in each, a lithologic combination that is relatively rare in southern Oregon. Rocks of the Whitsett (eastern) subterrane crop out 15 km (9.3 mi) east-southeast of Coquille (Plate 2) and are likely present at depth beneath the southeastern part of the map area. The Whitsett subterrane includes *mélange* overlain by Cretaceous (?) sandstone and conglomerate and lower Eocene volcanic sandstone. Exotic blocks enclosed in *mélange* of the Whitsett subterrane include the Whitsett Limestone lentils of Diller (1898), exposed a few miles south of Roseburg, that were originally deposited at low or southern latitudes (Sliter, 1984). West of the Fulmar fault, *mélange* (**KJs**) of the Fulmar subterrane (Plates 1 and 3) includes Cretaceous and Jurassic age blocks and is unconformably overlain by deformed arkosic turbidites of the lower Eocene sandstone of Fivemile Point (**Tefm**) (Snively and others, 1980; Snively, 1987). Rocks of the western or Cape Blanco subterrane lie outside the map area to the south and include younger, nonmicaceous, middle Eocene sandstone that appears to be incorporated in the *mélange* matrix. The distribution of radiometric and fossil ages in the *mélange* and the overlap sequences, as well as the similarity of the exotic lithologies across the terrane, suggests that Sixes River subterrane reflect westward-younging *mélange* formation in otherwise similar settings.

During or shortly after the late stages of *mélange* formation, the lower Eocene sandstone of Fivemile Point (**Tefm**) was deposited on, incorporated into, or faulted against the Fulmar subterrane. Snively and others (1980) recognized this unit where it was sampled by oil and gas wells offshore to the north and noted that strata at Fivemile Point were similar. Outcrops farther inland are widely separated, and lateral continuity is uncertain. At Fivemile Point, dips in the sandstone range from steep to overturned (Plate 3; Figure 8b). At Bill Peak, massive steeply dipping sandstone that is chemically indistinguishable from the sandstone of Fivemile Point (sampled at Fivemile Point itself) juts from the *mélange*, not unlike an exotic block. Other sandstone, pebbly sandstone, grit, and pebble conglomerate occur-

rences in the *mélange* in that area appear to be similar. The sandstone of Fivemile Point (**Tefm**) has not been recognized in the other two subterrane.

The Fulmar and Whitsett subterrane, as well as the Siletz terrane to the north and east and several terranes south of the Canyonville fault, are overlapped by micaceous sandstone including the Tyee (**Tet**) and Coaledo Formations (**Tecl**, **Tecm**, **Tecu**) and the beds of Sacchi Beach (**Tes**). These three formations are as old, or older than, fossils recovered from *mélange* in the Cape Blanco (western) subterrane of the Sixes River terrane. This suggests that non-micaceous sandstone deposition and *mélange* formation was occurring in the Cape Blanco subterrane to the south and west while the Whitsett and Fulmar subterrane were being buried by micaceous sandstone farther north and east.

South of the study area the Picket Peak terrane forms a regionally extensive structural nappe that includes ultramafic rocks (serpentinite) and the Colebrooke Schist (Coleman, 1972; Blake and others, 1985; Cashman and Cashman, 1989; Katrib, 2006). These rocks overlie *mélange* assigned to the Cape Blanco and Fulmar subterrane of the Sixes River terrane (Blake and others, 1985; Wiley and others, 2014) as well as several terranes that are present south of the Canyonville fault. The thrust fault that places the Colebrooke Schist over these terranes postdates their juxtaposition along the western extension of the Canyonville fault zone (Figure 4).

Mélange with blueschist, garnet-bearing schist, and limestone blocks is not present immediately south of the Canyonville fault. However, limestone blocks that originated south of the equator occur in a similar blueschist bearing *mélange* near Laytonville, California (Tarduno and others, 1990), suggesting that terranes related to the Sixes River terrane may be present much farther to the south.

Siletz terrane

The Siletz terrane (Silberling and others, 1987) or Siletzia (Howell and others, 1985) consists of a sequence of oceanic basalt, less common diabase, minor gabbro and related intrusive rocks, and interlayered and overlying sedimentary rocks. It forms the basement for much of western Oregon and Washington north of the Canyonville fault. Ages for the oceanic basalt range from late Paleocene to early Eocene (Sloan and others, 2003; Wells and others, 2014). Sedimentary rocks that overlie the basalt, as well as most of those that are interlayered with the basaltic lava, are lower Eocene in age. The oceanic basalt sequence in the study area was originally mapped by Diller (1901), was later considered part of the Roseburg Volcanics (Baldwin,

1974), and has more recently been assigned to the Siletz River Volcanics (**Tesr**) with the name Roseburg Member applied to associated sedimentary rocks (Wells and others, 2000). Exposures of the volcanic sequence lie on the eastern and western margins of the Oregon Coast Range north of the Wildlife Safari fault, the terrane boundary between the Siletz and Sixes River terranes (Figure 4). The axis of the Oregon Coast Range is largely underlain by younger Paleogene sedimentary rocks of the Tyee Basin that lie atop the Siletz River Volcanics. To the south these sedimentary rocks lap across the Siletz terrane and adjacent Mesozoic terranes. The presence of this upper lower Eocene overlap sequence indicates a late early Eocene age for juxtaposition of the Siletz terrane and older Mesozoic terranes nearby.

Within the study area, a sequence of basaltic pillow lava, lava flows, volcanic breccia, and minor interlayered sedimentary rock crops out in the southeastern part of the Coquille quadrangle (Plate 2). Geochemistry of the lava is reported by Lawrence (2014). This is overlain on the east by a sequence of mudstone and fine sandstone dominated turbidites. The volcanic rocks appear to be truncated to the south beneath alluvium that fills the Coquille River Valley. On the west side of the volcanic exposures, rocks older than the Coaledo Formation are absent, suggesting that this contact is also faulted. Although not labeled as a fold on the map, the overall nature of the exposures suggests a faulted anticline with Siletz River Volcanics at its core. Such a relationship is similar to that shown by Allen and Baldwin (1944), who drew the Norway anticline in thin bedded turbidites truncated by volcanic outcrops in the Myrtle Point quadrangle.

Terrane bounding faults

South of the study area the Sixes River terrane is faulted against several terranes along the Canyonville fault (Figure 4). An early phase of motion on this fault produced right lateral offset of the Yolla Bolly terrane prior to deposition of lower Eocene strata that lap across the fault and after formation of the mid-Cretaceous (Albian to Cenomanian, 123 to 93.9 Ma; Sliter, 1984) Whitsett Limestone Lenticles (blocks) of Diller (1898) in the Whitsett subterrane of the Sixes River terrane. Poorly dated Upper Cretaceous or lower Paleogene sandstone, pebbly sandstone, and conglomerate crop out north of the Canyonville fault near Winston (Wells and others, 2000) and east of Tenmile (Wiley and Black, 1994), where they lie on or are intercalated in Whitsett subterrane *mélange*. A late phase of motion on the Canyonville fault cuts the Cape Blanco subterrane of the Sixes River terrane which contains lower middle Eocene fossils.

The northern extension of the Battle Rock–Whaleshead fault zone is inferred to truncate the Sixes River terrane and the extreme western end of the Canyonville fault south of the map area between Garrison Lake and Cape Blanco (Figure 4; Wiley and others, 2014).

The Colebrooke Schist of the Pickett Peak terrane structurally overlies the Sixes River terrane north of the Canyonville fault and structurally overlies the Gold Beach and Yolla Bolly terranes south of the Canyonville fault. It is not clear if the low-angle fault that separates them is extensional or compressional. Unlike the terranes below this fault, the Pickett Peak terrane does not appear to be appreciably offset across the Canyonville fault. Although this may be due to the low-angle orientation of the fault contact beneath the schist, emplacement of the schist postdates much of the movement along the Canyonville fault.

The Wildlife Safari and related faults east of the study area separate the Whitsett subterrane of the Sixes River terrane on the south from the Siletz terrane on the north. The fault is interpreted as a thrust that places the Siletz terrane beneath the Sixes River terrane (Wells and others, 2000). The eastern and northern limits of the Siletz terrane lie far outside the study area.

The Sixes River terrane appears to be thrust beneath the Snow Camp terrane (Coast Range ophiolite) along a northeast-trending fault (and Fenster) between Canyonville and Roseburg (Blake and others, 1985). The Snow Camp terrane and its bounding faults separate the Sixes River terrane from the Yolla Bolly terrane (Dothan Formation) throughout the region.

Younger (post-amalgamation) deformation

High-angle faults

Rocks within the map area are offset by a number of Eocene and younger high-angle, north-northwest- and east-northeast-trending fault zones that crosscut older features. High-angle faults include those with strike-slip, oblique strike-slip, reverse, and normal displacement. A number of these structures in the study area are mapped as generic faults with an unknown sense of slip as few stratigraphic piercing points are preserved (see map plates). Many of the major high-angle fault and shear zones, including the Fulmar fault and Sunset Bay fault zone, are inferred to have an important strike-slip component on the basis of the intensity of shearing over wide areas, attitudes of many small-scale folds and slickensides, relatively straight boundaries, and heterogeneous structural mixing of rock types. A similar dextral (right-lateral) slip component is indicated on sev-

eral coastal fault zones south of the map area (Howard and Dott, 1961; Kaiser, 1962; Bourgeois and Dott, 1985; Kelsey, 1990; McClaughry and others, 2013) including the Battle Rock–Whaleshead, Brush Creek, Pistol River, and East Boundary faults (Howard and Dott, 1961). North-trending, high-angle fault zones that parallel the coast may be present in the project area beneath the terrace deposits or lie offshore.

Onshore, many of the high-angle fault zones are located along valleys or correspond, in part, to the mapped distribution of large landslide deposits, debris-flow gullies, or fault-line ridges. Along the coast and farther offshore, high-angle fault zones and shear zones are recognized by linear trains of sea stacks. In places the marine terraces appear to be offset. While some of these offsets may be former sea cliffs cut at the backs of terraces, others coincide with lineaments in bedrock valleys that are not likely associated with terrace formation and are probably young faults.

Several major, named examples of high-angle fault zones, including the Sunset Bay fault zone and Seven Devils fault zone in the northern part of the map area and the Fulmar fault extending between Fivemile Point and Bill Peak, cut across the project area. These fault zones represent major structural zones along the coast and are discussed further in the following sections.

Fulmar fault

The Fulmar fault (Plates 1 and 3) is a north-northeast-trending high-angle strike-slip fault that was first identified offshore by Snively and others (1980) and subsequently depicted as a terrane boundary between the Fulmar terrane (our Fulmar subterrane of the Sixes River terrane) to the west and Siletzia to the east (Howell and others, 1985; Snively, 1987). The existence of the Fulmar fault was inferred from litho-stratigraphic contrasts between lower Eocene rocks recovered from offshore oil and gas wells. Wells drilled to the west contain lower Eocene arkosic wackes, while those drilled to the east contained lower Eocene volcanic wackes and volcanic rocks (Snively and others, 1982). Snively and others (1980) recognized onshore equivalents of the strata in the eastern wells in the Siletz terrane (lower part of the Umpqua Group [Teu] and Roseburg Member of Siletz River Volcanics [Tcsr]) and onshore equivalents of the strata in the western wells at Fivemile Point. We interpret the fault that separates outcrops of the sandstone of Fivemile Point (Tefm) on the beach north of Fivemile Point from the beds at Sacchi Beach (Tes) to be a strand of the Fulmar fault. This interpretation predicts that oceanic basalts of the Siletz terrane underlie most of the lower to middle Eocene overlap

sequence (upper part of Umpqua Group [Teu], Tyee Formation [Tet], Coaledo Formation (Tecl, Tecm, Tecu), and beds at Sacchi Beach [Tes]), east of Fivemile Point (Plates 1, 2, and 3). Gravity, seismic, and magnetic anomalies cross the coastline near this location and continue inland to the south-southeast. The easternmost anomalies have been interpreted as representing a steeply west-dipping truncation of dense, relatively strongly magnetized oceanic basalt of the Siletz River Volcanics (Fleming and Tréhu, 1999). Inland, the fault is interpreted to have several strands with the main strand lying along the course of the Coquille River and trending south-southeast into the Bill Peak 7.5' quadrangle (Plates 1 and 3). Wiley and others (2014) interpreted the Fulmar fault to be the boundary between the Fulmar and Whitsett subterrane of the Sixes River terrane. Snavely (1987) inferred a right-lateral strike-slip sense of motion based on correlation of the sandstone of Fivemile Point with arkosic wackes of similar age in California. Right lateral offset on the Fulmar fault would be consistent with the Siletz terrane being thrust beneath the Sixes River terrane east of the Fulmar fault. Several younger cross faults cut the Fulmar fault in the map area (Plates 1 and 3).

Seven Devils fault zone

The Seven Devils fault zone includes several strands of N50°W-trending, northeast-dipping high-angle reverse faults that cut both bedrock and surficial geologic units at the south end of Sacchi Beach (Plate 4). Major strands in the fault zone may extend inland to the Seven Devils mine area (4 km [2.5 mi] southeast), where Griggs (1945) identified a northwest-trending fault offsetting Seven Devils terrace sediments (Qmtd). McInelly and Kelsey (1990) suggested that offset in the Seven Devils fault zone occurred along bedding-plane flexural-slip faults on the basis of inferred coplanarity of fault strands and bedding plane orientation, and a reverse sense of offset. Northeast-dipping strands in the Seven Devils fault zone are oriented approximately parallel to the local strike of bedding, but bedrock units (Tes, Tecl) in the vicinity of the fault zone dip 30° to 79° to the southwest. The observed non-coplanar relationship between fault planes and bedding at Sacchi Beach indicates that fault slip is not along bedding planes but crosscuts it. Latest movement in the fault zone occurred following deposition of the Seven Devils terrace sediments (Qmtd; ca. 125 ka) and prior to cutting of the Pioneer terrace sediments (Qmtp; ca. 105 ka), which are not offset by the fault zone (McInelly and Kelsey, 1990).

Sunset Bay fault zone

Wavecut benches between Cape Arago and Sunset Bay, in the Cape Arago 7.5' quadrangle, reveal a complex system of closely spaced, N60° to N80°W-trending, strike-slip faults (e.g., Sunset Bay fault zone) that run transverse to locally, steeply eastward-dipping strata (Plate 4). Separate strands along the fault zone are identified on the coast by the offset of geologic contacts, offset of key marker beds within the Lower Member of the Coaledo Formation, the common presence of drag folds, pervasive shearing in some bedrock outcrops, lines of boulders in small trenches eroded along fault zones, and larger topographic lineaments recognized in a variety of imagery (1-m lidar DEMs, 2011 NAIP digital orthophotos, Google Earth™). The continuation of fault strands inland, where exposure is poor, is less clear. Individual fault strands and numerous associated splays have accommodated lateral offset ranging from several meters (tens of feet) to ≥ 140 m (≥ 460 ft) of offset of the contact between the Lower and Middle Members of the Coaledo Formation (Tecl, Tecm) across Sunset Bay (Plate 4). Some component of oblique slip along some of the west-northwest-trending fault strands between Cape Arago and Sunset Bay is indicated by the orientation of drag folds and by previous workers who indicated vertical movement on a number of these faults (Allen and Baldwin, 1944; Ehlen, 1967; Rooth, 1974).

Thrust faults

A suite of thrust faults has been mapped that generally parallel and locally coincide with the axes of large folds (Plates 2 and 3). These faults are rarely seen in the field; they have been mapped on the basis of variations in measured bedding and apparent unit thickness.

Folding

At least four phases of folding have affected the area since the Siletz and Sixes River terranes amalgamated during the late early (?) or early middle Eocene. The most complex and presumably oldest folds affect the lower part of the Umpqua Group (Teu) and possibly the sandstone of Fivemile Point (Tefm). Molenaar (1985) presented evidence from the Roseburg area that rocks of the Umpqua Group are tightly folded and disrupted in some areas and only broadly folded in others. Two mechanisms can result in this type of structure. The first is deformation only in wide but restricted zones that likely reflect differential movement of large bedrock blocks. The second relates to the tendency of fine-grained, thin-bedded facies such as mudstone and thin-bedded turbidites to deform at shorter wavelengths

than coarse-grained facies like thick bedded sandstone. Bedding measurements suggest that in the study area a significant angular unconformity separates the older tightly folded rocks from younger, more broadly folded strata in the overlap sequence. However, in one area, relatively young micaceous beds at Sacchi Beach (**Tes**) are tightly folded and vertical to overturned (Figure 10).

The second phase of folding involved the formation of large north-trending folds and accompanying faults. The overall football-shaped outline of the Coos Bay basin and coal field is that of a north-trending doubly-plunging synclinorium. It parallels a large faulted anticlinal structure to the east that is cored by volcanic rocks, some of which are depicted in the eastern part of the Coquille quadrangle (Plate 2). Regionally, these structures parallel the axis of the Oregon Coast Range, the north-trending axis of the Tyee basin, and the strike of the east-dipping homocline that forms the Willamette Valley and the western Cascade Range. The largest mapped fold of this group in the study area is the east-tilted homocline or faulted syncline whose axis lies about 1.6 km (1 mi) west of Coquille, southward to the vicinity of Riverton, and then well into the Bill Peak quadrangle (Plates 1, 2, and 3). The western, eastward-dipping limb of this structure extends to the vicinity of U.S. Highway 101 and is obvious in the Bill Peak quadrangle but



Figure 10. Recumbent fold in beds at Sacchi Beach (**Tes**) (WGS84 geographic coordinates: 390700mE., 4785600mN.). White dashed line shows bedding fabric in thinly bedded siltstone. Hammer for scale is ~ 30 cm (12 in) long.

disrupted north of the Coquille River. A second notable fold in this group is the north-plunging South Slough syncline that crops out north of the study area (Madin and others, 1995).

The third phase of folding is reflected in local folding and faulting of broadly folded Paleogene sedimentary rocks and by the absence of Oligo-Miocene sedimentary rocks (Tunnel Point Sandstone, sandstone of Floras Lake, Empire Formation, diatomite of China Creek) in the study area. It reflects a change from east-west directed folding to north-south directed folding. Like earlier folding, it seems likely that this phase was long-lived and complex, possibly involving multiple episodes and coeval faulting. A few of the larger named structures parallel the football-shaped outline of the basin. In the study area these include the north-northeast trending Coquille basin and Pulaski arch (Plates 1, 2, and 3). Many structures are left-stepping. Younger (?) structures have axes with trends that range from northeast-southwest to east-west, to southeast-northwest. The presence of Miocene strata north and south of the study area suggests a broad, east-west-trending post-Miocene uplift or fold. The unconformity at the base of the Miocene section in the Charleston 7.5' quadrangle (Madin and others, 1995) helps date and define this deformation. Left-stepping en echelon folds in the Bill Peak 7.5' quadrangle (Plate 1) deform one of the older north-trending folds. An east-west-trending syncline involving strata that elsewhere lap across the terrane boundary (upper part of the Umpqua Group [**Teu**] and Tyee Formation [**Tet**]) is folded into underlying *mélange* of the Sixes River terrane in the southwest corner of the Bill Peak 7.5' quadrangle (Plate 1). In the Coquille 7.5' quadrangle, north-northeast- to northeast-trending folds are more common north and east of Highway 42 (Plate 2). The double plunge of pre-Miocene structures toward the center of the Coos Bay basin nearly mirrors the post-Miocene unconformity that reflects removal of most of the Bastendorff Shale (**Teb**), Tunnel Point Sandstone, and younger Miocene formations between South Slough and Bandon (Figure 1). A similar transition from east-west directed folding to north-south directed folding was recognized in the Dothan Formation in the Brookings area to the south (T. J. Wiley, unpublished mapping, 2007).

The youngest folds recognized are involved in tilting of the circa 80 ka Whiskey Run terrace. Such post-80 ka tilting may be an ongoing process. The older, ~105 ka, Pioneer terrace has been folded about a southeast- to south-trending anticlinal axis between Cape Arago and Rocky Point on the Coquille River (Plates 3 and 4). McNelly and Kelsey (1990) recognized this fold and named it the Pioneer

Anticline. The axis of the anticline is largely parallel to the strike of the tilt of the Whiskey Run terrace and so may reflect an earlier phase of the same event. This fold may be broad enough that the tilted Whiskey Run terrace forms its western limb. The northern end of the Pioneer Anticline parallels, and may coincide with, the southern end of the Cape Arago anticline of Allen and Baldwin (1944) (Plate 4). Well-developed fluvial terrace sets on both sides of the Coquille River at Coquille suggest the presence of a young, north-northeast-trending fault or fold (Plate 2).

Elevated marine platforms

Elevated marine platforms and terrace deposits, preserved along the southern Oregon coast, record non-uniform and spatially variable Quaternary uplift of the coastal mountains. South of the study area, near Cape Blanco, uplift rates on the Pioneer Terrace (**Qmtp**) over the past 80 ky were estimated by Kelsey (1990) to range between 0.7 and

1.5 mm/yr (0.7 and 1.5 m/ky). Uplift rates along the Cape Blanco anticline are estimated to be higher for the last 2 ky, with rates approaching 6 to 10 mm/yr (6 to 10 m/ky; Kelsey, 1990). In contrast to the Cape Blanco area, Kelsey (1990) suggested that subsidence is occurring within 10 km (6 mi) north of Cape Blanco. Terrace deposits as young as the Pioneer Terrace (**Qmtp**) have been gently folded to form the Pioneer anticline between Cape Arago and Rocky Point on the Coquille River (Plates 3 and 4).

Pliocene and early Pleistocene deformation rates along the southern Oregon coast were probably similar to the late Pleistocene rates described above. Approximately 10 km (6 mi) south of the Oregon-California border, near California's High Divide, the upper Miocene and lower Pliocene Wimer Formation crops out at an elevation of about 720 m (2,360 ft), while its western equivalent, the St. George Formation, crops out near sea level along the coast near Crescent City.

ACKNOWLEDGMENTS

This report is a product of geologic mapping along the southern Oregon coast that was partially funded by the STATEMAP component of the U.S. Geological Survey (USGS) National Cooperative Geologic Mapping program under assistance award G14AC00165 during 2014 and 2015. Funding for geologic mapping was also provided by the State of Oregon. XRF geochemical analyses were prepared and analyzed by Dr. Stanley Mertzman, Franklin and Marshall College, Pennsylvania. New $^{206}\text{Pb}/^{238}\text{U}$ radiometric age determinations were prepared and analyzed by Dr.

Joshua Schwartz at California State University, Northridge, California. The authors acknowledge a number of area landowners who provided local knowledge and graciously allowed access to private holdings within the study area. The Oregon Civil Air Patrol provided an airplane that allowed DOGAMI to photograph the study area as an exercise designed to simulate a post-disaster aerial survey. Technical review was provided by Mark Ferns (Eastern Oregon University). Cartography for the map plates was provided by John Bauer, DOGAMI.

REFERENCES

- Aalto, K. R., 1968, The sedimentology of the Late Jurassic (Portlandian) Otter Point Formation of southwestern Oregon: Madison, Wisc., University of Wisconsin, M.S. thesis, 60 p.
- Aalto, K. R., and Dott, R. H., Jr., 1970, Late Mesozoic conglomeratic flysch in southwestern Oregon, and the problem of transport of coarse gravel in deep water: Geological Association of Canada Special Paper 7, p. 53–65.
- Addicott, W. O., 1964, A late Pleistocene invertebrate fauna from southwestern Oregon: *Journal of Paleontology*, v. 38, p. 650–661.
- Addicott, W. O., 1983, Biostratigraphy of the marine Neogene sequence at Cape Blanco, southwestern Oregon: U.S. Geological Survey Professional Paper 774-G, 19 p. <http://pubs.usgs.gov/pp/0774g/report.pdf>
- Allen, J. A., and Baldwin, E. M., 1944, Geology and coal resources of the Coos Bay quadrangle, Oregon: Oregon Department of Geology and Mineral Industries Bulletin 27, 157 p., 3 pl., scale 1:96,500. <http://www.oregongeology.org/pubs/B/B-027.pdf>
- Alluvial Fan Process Group, n.d. http://www.fs.fed.us/r10/tongass/forest_facts/ct_rev/Alluvial%20Fan%20Process%20Group_final.pdf
- Armentrout, J. M., Hull, D. A., Beaulieu, J. D., and Rau, W. W., 1983, Correlation of Cenozoic stratigraphic units of western Oregon and Washington: Oregon Department of Geology and Mineral Industries Oil and Gas Investigation 7, 90 p. <http://www.oregongeology.org/pubs/ogi/OGI-07.pdf>
- Baldwin, E. M., 1945, Some revisions of the late Cenozoic stratigraphy of the southern Oregon coast: *Journal of Geology*, v. 53, no. 1, p. 35–46.
- Baldwin, E. M., 1964, *Geology of Oregon* (2nd ed.): Eugene, Ore., University of Oregon, 165 p.
- Baldwin, E. M., 1965, Geology of the south end of the Oregon Coast Range Tertiary Basin: *Northwest Science*, v. 39, no. 3, p. 93–103.
- Baldwin, E. M., 1966, Some revisions of the geology of the Coos Bay area, Oregon: *Ore Bin*, v. 28, no. 11, p. 189–203. <http://www.oregongeology.org/pubs/og/OB-v28n11.pdf>
- Baldwin, E. M., 1969, Geologic map of the Myrtle Point area, Coos County, Oregon: U.S. Geological Survey Mineral Investigations Map MF-302. <http://pubs.er.usgs.gov/publication/mf302>
- Baldwin, E. M., 1974, Eocene stratigraphy of southwestern Oregon: Oregon Department of Geology and Mineral Industries Bulletin 83, 40 p., 1 pl., scale 1:250,000. <http://www.oregongeology.org/pubs/B/B-083.pdf>
- Baldwin, E. M., Beaulieu, J. D., Ramp, L., Gray, J., Newton, V. C., Jr., and Mason, R. S., 1973, Geology and mineral resources of Coos County, Oregon: Oregon Department of Geology and Mineral Industries Bulletin 80, 82 p., 4 pl., scale 1:62,500. <http://www.oregongeology.org/pubs/B/B-080.pdf>
- Bandy, O. L., 1941, Invertebrate paleontology of Cape Blanco: Corvallis, Ore., Oregon State University M.S. thesis, 138 p.
- Bandy, O. L., 1944, Eocene foraminifera from Cape Blanco, Oregon: *Journal of Paleontology*, v. 18, p. 366–377.
- Beaulieu, J. D., and Hughes, P. W., 1975, Environmental geology of western Coos and Douglas Counties, Oregon: Oregon Department of Geology and Mineral Industries Bulletin 87, 148 p., 16 pl., scale 1:62,500. <http://www.oregongeology.org/pubs/B/B-087.pdf>
- Beaulieu, J. D., and Hughes, P. W., 1976, Land-use geology of western Curry County, Oregon: Oregon Department of Geology and Mineral Industries Bulletin 90, 148 p., 16 pl., scale 1:62,500. <http://www.oregongeology.org/pubs/B/B-090.pdf>
- Beaulieu, J. D., Hughes, P. W., and Mathiot, R. K., 1974, Geologic hazards inventory of the Oregon coastal zone: Oregon Department of Geology and Mineral Industries Miscellaneous Paper 17, 94 p., 2 pl., scale 1:250,000. <http://www.oregongeology.org/pubs/mp/MP-17.pdf>
- Beckstrand, D. L., 2001, Origin of the Coos Bay and Florence dune sheets, south central coast, Oregon: Portland, Oregon, Portland State University, M.S. thesis, 192 p.
- Bird, K. J., 1967, Biostratigraphy of the Tyee Formation (Eocene), southwest Oregon: Madison, University of Wisconsin Ph.D. dissertation, 209 p.
- Black, G. L., 1994, Geologic map of the Remote quadrangle, Coos County, Oregon: Oregon Department of Geology and Mineral Industries Geological Map Series GMS-84, scale 1:24,000. <http://www.oregongeology.org/pubs/gms/GMS-084.pdf>
- Black, G. L., and Madin, I. P., 1995, Geologic map of the Coos Bay quadrangle, Coos County, Oregon: Oregon Department of Geology and Mineral Industries Geological Map Series GMS-97, scale 1:24,000. <http://www.oregongeology.org/pubs/gms/GMS-097.pdf>

- Blake, M. C., Jr., Engebretson, D. C., Jayko, A. S., and Jones, D. L., 1985, Tectonostratigraphic terranes in southwest Oregon, *in* Howell, D. G., ed., Tectonostratigraphic terranes of the circum-Pacific region: Circum-Pacific Council for Energy and Mineral Resources Earth Science Series, no. 1, p. 147–157.
- Bouma, A. H., 1962, Sedimentology of some flysch deposits: A graphic approach to facies interpretation: Amsterdam, Elsevier, 168 p.
- Bourgeois, J., and Dott, R. H., Jr., 1985, Stratigraphy and sedimentology of Upper Cretaceous rocks in coastal southwest Oregon: Evidence for wrench-fault tectonics in a postulated accretionary terrane: Geological Society of America Bulletin, v. 96, p. 1007–1019.
- Boyd, F. R., and Mertzman, S. A., 1987, Composition of structure of the Kaapvaal lithosphere, southern Africa: *in* Mysen, B. O., ed., Magmatic Processes—Physicochemical Principles, The Geochemical Society, Special Publication #1, p. 13–24.
- Brown, E. H., and Blake, M. C., Jr., 1987, Correlation of Early Cretaceous blueschists in Washington, Oregon, and northern California: Tectonics, v. 6, p. 795–806.
- Brownfield, M. E., 1972, Geology of the Floras Creek drainage, Langlois quadrangle, Oregon: Eugene, Oregon, University of Oregon, M.S. thesis, 92 p.
- Brownfield, M. E., Phillips, R. L., and Lent, R. L., 1982, Geologic map of the Langlois quadrangle, Oregon: Oregon Department of Geology and Mineral Industries Open-File Report O-82-3, scale 1:62,500. <http://www.oregon-geology.org/pubs/ofr/O-82-03.pdf>
- Bukry, D., and Snively, P. D., Jr., 1988, Coccolith zonation for Paleogene strata in the Oregon Coast Range, *in* Fawcett, M. V., and Squires, R. L., eds., Paleogene stratigraphy, West Coast of North America: Society for Sedimentary Geology (SEPM), Pacific Section, Publication 58, p. 251–263.
- Burns, W. J., and Madin, I. P., 2009, Protocol for inventory mapping of landslide deposits from light detection and ranging (lidar) imagery: Oregon Department of Geology and Mineral Industries Special Paper 42, 30 p. <http://www.oregongeology.org/pubs/sp/SP-42.zip>
- Burns, W. J., and Watzig, R. J., 2014, Statewide Landslide Information Database for Oregon (SLIDO), release 3.0: Oregon Department of Geology and Mineral Industries, geodatabase. <http://www.oregongeology.org/sub/slido/data.htm>
- Cashman, S. M., and Cashman, P. H., 1989, The Redwood Creek Schist—A key to the deformational history of the Northern California Coast Ranges, *in* Aalto, K. R., Harper, G. D., Carver, G. A., Cashman, S. M., Miller, W. C., III, and Kelsey, H. M., Geologic evolution of the northernmost Coast Ranges and western Klamath Mountains, California: Galice, Oregon, to Eureka, California, July 20–28, 1989: American Geophysical Union, Washington, D.C., 53 p.
- Chan, M. A., and Dott, R. H., Jr., 1986, Depositional facies and progradational sequences in Eocene wave-dominated deltaic complexes, southwestern Oregon: AAPG Bulletin, v. 70, no. 4, p. 415–429.
- Chang, Z., Vervoort, J. D., McClelland, W. C., and Knaack, C., 2006, U-Pb dating of zircon by LA-ICP-MS: Geochemistry, Geophysics, Geosystems, v. 7, no. 5, p. 1–14.
- Clarke, S. H., Jr., Field, M. E., and Hirozawa, C. A., 1985, Reconnaissance geology and geologic hazards of the offshore Coos Bay basin, Oregon: U.S. Geological Survey Bulletin 1645, 52 p. <http://pubs.usgs.gov/bul/1645/report.pdf>
- Cohen, K. M., Finney, S. C., Gibbard, P. L., and Fan, J.-X., 2013 (updated 2015), The ICS International Chronostratigraphic Chart: Episodes 36, p. 199–204.
- Coleman, R. G., 1972, The Colebrook Schist of southwestern Oregon and its relation to the tectonic evolution of the region: U.S. Geological Survey Bulletin 1339, 61 p. <http://pubs.er.usgs.gov/publication/b1339>
- Coleman, R. G., and Lanphere, M. A., 1971, Distribution and age of high-grade blueschists, associated eclogites, and amphibolites from Oregon and California: Geological Society of America Bulletin, v. 82, p. 2397–2412.
- Cowan, D. S., 1985, Structural styles in Mesozoic and Cenozoic mélanges in the western Cordillera of North America: Geological Society of America Bulletin, v. 96, p. 451–462.
- Crutzen, P. J., 2002, The “Anthropocene”: Journal of Physics IV, France, v. 12, p. 1–5.
- Dall, W. H., 1909, Contributions to the Tertiary paleontology of the Pacific Coast; I, The Miocene of Astoria and Coos Bay, Oregon: U.S. Geological Survey Professional Paper 59, 278 p. <https://pubs.er.usgs.gov/publication/pp59>
- Diller, J. S., 1896, A geological reconnaissance in northwestern Oregon: U.S. Geological Survey 17th annual report, part 1, p. 458–462 and 475. <https://pubs.er.usgs.gov/publication/ar17>

- Diller, J. S., 1898, Roseburg folio, Oregon: U.S. Geological Survey Geologic Atlas of the United States Folio 49, 4 pl., 4 p. <https://pubs.er.usgs.gov/publication/gf49>
- Diller, J. S., 1899, The Coos Bay coal field, Oregon: U.S. Geological Survey Annual Report 19, pt. 3, p. 309–370. https://pubs.er.usgs.gov/publication/ar19_3
- Diller, J. S., 1901, Coos Bay folio, Oregon: U.S. Geological Survey Geologic Atlas of the United States Folio 73, 4 pl., 5 p. <https://pubs.er.usgs.gov/publication/gf73>
- Diller, J. S., 1902, Topographic development of the Klamath Mountains: U.S. Geological Survey Bulletin 196, 69 p. <https://pubs.er.usgs.gov/publication/b196>
- Diller, J. S., 1903, Port Orford folio, Oregon: U.S. Geological Survey Geologic Atlas of the United States Folio 89, 4 pl., 6 p. <https://pubs.er.usgs.gov/publication/gf89>
- DOGAMI, 2012a, Tsunami inundation maps for Charleston–Cape Arago, Coos County, Oregon: Oregon Department of Geology and Mineral Industries, TIM-Coos-08, scale 1:10,000. <http://www.oregongeology.org/pubs/tim/p-TIM-Coos-08.htm>
- DOGAMI, 2012b, Tsunami inundation maps for Bullards Beach, Coos County, Oregon: Oregon Department of Geology and Mineral Industries, TIM-Coos-12, scale 1:10,000. <http://www.oregongeology.org/pubs/tim/p-TIM-Coos-12.htm>
- DOGAMI, 2012c, Tsunami inundation maps for Leneve, Coos County, Oregon: Oregon Department of Geology and Mineral Industries, TIM-Coos-13, scale 1:10,000. <http://www.oregongeology.org/pubs/tim/p-TIM-Coos-13.htm>
- DOGAMI, 2012d, Tsunami inundation maps for Coquille, Coos County, Oregon: Oregon Department of Geology and Mineral Industries, TIM-Coos-14, scale 1:10,000. <http://www.oregongeology.org/pubs/tim/p-TIM-Coos-14.htm>
- DOGAMI, 2012e, Tsunami inundation maps for Coquille River, Coos County, Oregon: Oregon Department of Geology and Mineral Industries, TIM-Coos-15, scale 1:10,000. <http://www.oregongeology.org/pubs/tim/p-TIM-Coos-15.htm>
- DOGAMI, 2012f, Tsunami inundation maps for Bandon, Coos County, Oregon: Oregon Department of Geology and Mineral Industries, TIM-Coos-16, scale 1:10,000. <http://www.oregongeology.org/pubs/tim/p-TIM-Coos-16.htm>
- Dott, R. H., Jr., 1962, Geology of the Cape Blanco area, southwest Oregon: The Ore Bin, v. 24, no. 8, p. 121–133. <http://www.oregongeology.org/pubs/og/OBv24n08.pdf>
- Dott, R. H., Jr., 1965, Mesozoic-Cenozoic tectonic history of the southwestern Oregon coast in relation to Cordilleran Orogenesis: Journal of Geophysical Research, v. 70, no. 18, p. 4687–4706.
- Dott, R. H., Jr., 1966, Eocene deltaic sedimentation at Coos Bay, Oregon, Journal of Geology, v. 74, no. 4, p. 373–420.
- Dott, R. H., Jr., 1971, Geology of the southwestern Oregon coast west of the 124th meridian: Oregon Department of Geology and Mineral Industries Bulletin 69, 63 p., 2 pl., scale 1:250,000 and 1:62,500. <http://www.oregongeology.org/pubs/B/B-069.pdf>
- Dott, R. H., Jr., and Bourgeois, J., 1982, Hummocky stratification: significance of its variable bedding sequences: Geological Society of America Bulletin, v. 93, p. 663–680.
- Duncan, D. C., 1953, Geology and coal deposits in part of the Coos Bay coal field, Oregon: U.S. Geological Survey Bulletin 982-B, 72 p., 4 pl. <https://pubs.er.usgs.gov/publication/b982B>
- Duncan, R. A., 1982, A captured island chain in the Coast Range of Oregon and Washington: Journal of Geophysical Research, v. 87, no. B13, p. 10,827–10,837.
- Ehlen, J., 1967, Geology of the state parks near Cape Arago, Coos County, Oregon: Oregon Department of Geology and Mineral Industries Bulletin, Ore Bin, v. 29, no. 4, p. 63–83. <http://www.oregongeology.org/pubs/og/OB-v29n04.pdf>
- Emerson, L. F., 2007, Miocene coastal vegetation preserved by volcanic eruption at Cape Blanco, Oregon: Geological Society of America Abstracts with Programs, v. 39, no. 6, p. 401.
- Festa, A., Pini, G. A., Dilek, Y., and Codegone, G., 2010, Mélanges and mélange-forming processes: a historical overview and new concepts: International Geology Review, v. 52, nos. 10–12, p. 1010–1105.
- Festa, A., Dilek, Y., Pini, G. A., Codegone, G., and Ogata, K., 2012, Mechanisms and processes of stratal disruption and mixing in the development of mélanges and broken formations: Redefining and classifying mélanges: Tectonophysics, v. 568–569, p. 7–24.
- Fiebelkorn, R. B., Walker, G. W., MacLeod, N. S., McKee, E. H., and Smith, J. G., 1983, Index to K/Ar age determinations for the state of Oregon: Isochron/West, no. 37, p. 3–60.

- Fleming, S. W., and Tréhu, A. M., 1999, Crustal structure beneath the central Oregon convergent margin from potential field modeling: Evidence for a buried basement ridge in local contact with a seaward-dipping backstop, *Journal of Geophysical Research*, v. 104, p. 20,431–20,447.
- Fowler, G. A., Orr, W. N., and Kulm, L. D., 1971, An upper Miocene diatomaceous rock unit on the Oregon Continental Shelf: *The Journal of Geology*, v. 79, no. 5, p. 603–608.
- Garey, C. L., 1987, Radiolaria from the Otter Point Complex (Oregon) and the volcano-pelagic strata above the Coast-Range Ophiolite (California): University of Texas, M.S. thesis, 157 p.
- Geological Society of America Rock-Color Chart Committee, 1991, Rock Color Chart, 7th Printing.
- Giaramita, M. J., and Harper, G. D., 2006, Geochemistry of ophiolitic rocks associated with the western part of the Elk outlier of the Western Klamath terrane, southwestern Oregon, *in* Snoke, A. W., and Barnes, C. G., eds., *Geological studies in the Klamath Mountains Province, California and Oregon: A volume in honor of William P. Irwin*: Geological Society of America Special Paper 410, p. 152–176.
- Gillespie, M. R., and Styles, M. T., 1999, BGS rock classification scheme, v. 1, Classification of igneous rocks: British Geological Survey Research Report (2nd ed.) RR99-06, 52 p.
- Goldfinger, C., Kulm, L. D., Yeats, R. S., Mitchell, C., Weldon, R., Jr., Peterson, C., Darienzo, M., Grant, W., and Priest, G. R., 1992, Neotectonic map of the Oregon continental margin and adjacent abyssal plain: Oregon Department of Geology and Mineral Industries Open-File Report O-92-4, scale 1:392,832, 17 p. <http://www.oregongeology.org/pubs/ofr/O-92-04.pdf>
- Goldfinger, C., Nelson, C. H., Morey, A. E., Johnson, J. E., Patton, J. R., Karabanov, E., Gutiérrez-Pastor, J., Eriksson, A. T., Gràcia, E., Dunhill, G., Enkin, R. J., Dallimore, A., and Vallier, T., 2012, Turbidite event history—Methods and implications for Holocene paleoseismicity of the Cascadia subduction zone: U.S. Geological Survey Professional Paper 1661–F, 170 p. <https://pubs.er.usgs.gov/publication/pp1661F>
- Goodfellow, R. W., 1987, Petrography and provenance of sandstones from the Otter Point Formation, southwestern Oregon: Eugene, Oreg., University of Oregon M.S. thesis, 158 p.
- Gradstein, F. M., Ogg, J. G., and Smith, A. G., eds., 2004, *A geologic time scale 2004*: Cambridge, U.K., Cambridge University Press, 589 p.
- Griggs, A. B., 1945, Chromite-bearing sands of the southern part of the coast of Oregon: U.S. Geological Survey Bulletin 945-E, 150 p. <https://pubs.er.usgs.gov/publication/b945E>
- Haagen, J. T., 1989, Soil survey of Coos County, Oregon: Natural Resources Conservation Service Soil Conservation Survey 011, 175 p. http://www.nrcs.usda.gov/Internet/FSE_MANUSCRIPTS/oregon/OR011/0/or011_text.pdf
- Hallsworth, C. R., and Knox, R. W. O'B., 1999, BGS rock classification scheme, v. 3, Classification of sediments and sedimentary rocks: British Geological Survey Research Report 99-03, 44 p.
- Heller, P. L., 1983, Sedimentary response to Eocene tectonic rotation in western Oregon: Tuscon, Ariz., University of Arizona, Ph.D. dissertation, 321 p.
- Heller, P. L., and Ryberg, P. T., 1983, Sedimentary record of subduction to forearc transition in the rotated Eocene basin of western Oregon: *Geology*, v. 11, no. 7, p. 380–383.
- Heller, P. L., Tabor, R. W., and Suzcek, C. A., 1987, Paleogeographic evolution of the United States Pacific Northwest during Paleogene time: *Canadian Journal of Earth Science*, v. 24, p. 1652–1667.
- Howard, J. K., and Dott, R. H., Jr., 1961, Geology of Cape Sebastian State Park and its regional relationships: *The Ore Bin*, v. 23, no. 8, p. 75–81.
- Howell, D. G., Jones, D. L., and Schermer, E. R., 1985, Tectonostratigraphic terranes of the Circum-Pacific Region, *in* Howell, D. G., ed., *Tectonostratigraphic terranes of the circum-Pacific region*: Circum-Pacific Council for Energy and Mineral Resources Earth Science Series No. 1, p. 3–30.
- Hsü, K. J., 1968, Principles of mélanges and their bearing on the Franciscan-Knoxville paradox: *Geological Society of America Bulletin*, 79, p. 1063–1074.
- Janda, R. J., 1969, Age and correlation of marine terraces near Cape Blanco, Oregon: *Geological Society of America Abstracts with programs* v. 3, p. 29–30.
- Janda, R. J., 1970, Field guide to Pleistocene sediments and landforms and soil development in the Cape Arago-Cape Blanco area of Coos and Curry Counties, southern coastal Oregon: *Friends of the Pleistocene unpublished guidebook*.

- Kaiser, W. R., 1962, The late Mesozoic geology of the Pearce Peak Diorite—southwest Oregon: Madison, Wisconsin, University of Wisconsin, M.S. thesis, 75 p.
- Katrib, J., 2006, Source of meta-igneous blocks and structure of the Colebrooke Schist in the Snowcamp Peak area, Pickett Peak terrane, southwestern Oregon: Albany, New York, University of Albany, State University of New York, M.S. thesis, 111 p.
- Kelsey, H. M., 1990, Late Quaternary deformation of marine terraces on the Cascadia Subduction Zone near Cape Blanco, Oregon: *Tectonics*, v. 9, no. 5, p. 983–1014.
- Kelsey, H. M., and Bockheim, J. G., 1994, Coastal landscape evolution as a function of eustasy and surface uplift rate, Cascadia margin, southern Oregon: *Geological Society of America Bulletin*, v. 106, p. 824–839.
- Kelsey, H. M., Nelson, A. R., Hemphill-Haley, E., Witter, R. C., 2005, Tsunami history of an Oregon coastal lake reveals a 4600 yr record of great earthquakes on the Cascadia subduction zone: *Geological Society of America Bulletin*, v. 117, p. 1009–1032.
- Kelsey, H. M., Ticknor, R. L., Bockheim, J. G., and Mitchell, E., 1996, Quaternary upper plate deformation in coastal Oregon: *Geological Society of America Bulletin*, v. 108, p. 843–860.
- Kelsey, H. M., Witter, R. C., Hemphill-Haley, E., Witter, R. C., 1998, Response of a small Oregon estuary to coseismic subsidence and post-seismic uplift in the past 300 years: *Geology*, v. 26, p. 231–234.
- Kelsey, H. M., Witter, R. C., Hemphill-Haley, E., 2003, Plate-boundary earthquakes and tsunamis of the past 5500 yr, Sixes River estuary, southern Oregon: *Geological Society of America Bulletin*, v. 114, p. 298–314.
- Lawrence, R. L., 2014, Geochemistry of the early Eocene Coast Range volcanic province, Pacific northwestern United States, and evidence for plume-ridge interaction: Northfield, Minn., Carleton College, Senior Integrative Exercise, 57 p.
- Le Bas, M. J., Le Maitre, R. W., Streckeisen, A., and Zanettin, B., 1986, A chemical classification of volcanic rocks based on the total alkali-silica diagram: *Journal of Petrology*, v. 27, part 3, p. 745–750.
- Le Bas, M. J., and Streckeisen, A. L., 1991, The IUGS systematics of igneous rocks: *Journal of the Geological Society*, v. 148, p. 825–833.
- Le Maitre, R. W., Bateman, P., Dudek, A., Keller, J., Lemeyre, J., Le Bas, M. J., Sabine, P. A., Schmid, R., Sorenson, H., Streckeisen, A., Wooley, A. R., and Zanettin, B., 1989, A classification of igneous rocks and glossary of terms: Oxford, Blackwell, 193 p.
- Le Maitre, R. W. (ed.), Streckeisen, A., Zanettin, B., Le Bas, M. J., Bonin, B., Bateman, P., Bellieni, G., Dudek, A., Efremova, S., Keller, J., Lameyre, J., Sabine, P. A., Schmid, R., Sørensen, H., and Wooley, A. R., 2004, *Igneous Rocks: A classification and glossary of terms: Recommendations of the International Union of Geological Sciences, Subcommission on the Systematics of Igneous Rocks*, Cambridge University Press, United Kingdom, 236 p.
- Lent, R. L., 1969, Geology of the southern half of the Langlois quadrangle, Oregon: Eugene, Oregon, University of Oregon Ph.D. dissertation, 189 p.
- Lund, E. H., 1973, Landforms along the coast of southern Coos County, Oregon: *The Ore Bin*, v. 35, no. 12, p. 189–210.
- Ma, L., Madin, I. P., Olson, K. V., Watzig, R. J., Wells, R. E., and Priest, G. R., compilers, 2009, Oregon geologic data compilation [OGDC], release 5 (statewide): Oregon Department of Geology and Mineral Industries Digital Data Series OGDC-5, CD-ROM. [Superseded by OGDC-6: <http://www.oregongeology.org/pubs/dds/p-OGDC-6.htm>]
- MacKenzie, W. S., Donaldson, C. H., and Guilford, C., 1997, *Atlas of igneous rocks and their textures* (7th ed.): Addison Wesley Longman Limited, 148 p.
- Madin, I. P., McNelly, G. W., and Kelsey, H. M., 1995, Geologic map of the Charleston quadrangle, Coos County, Oregon: Oregon Department of Geology and Mineral Industries Geological Map Series GMS-94, scale 1:24,000. <http://www.oregongeology.org/pubs/gms/GMS-094.pdf>
- McCloughry, J. D., Ma, L., Jones, C. D., Mickelson, K. A., and Wiley, T. J., 2013, Geologic map of the southwestern Oregon coast between Crook Point and Port Orford, Curry County, Oregon: Oregon Department of Geology and Mineral Industries Open-File Report O-13-21, 3 pl., 1:24,000, database files, 55 p. <http://www.oregongeology.org/pubs/ofr/p-O-13-21.htm>
- McCloughry, J. D., Wiley, T. J., Ferns, M. L., and Madin, I. P., 2010, Geologic map of the southern Willamette Valley, Benton, Lane, Linn, Marion, and Polk Counties, Oregon: Oregon Department of Geology and Mineral Industries Open-File Report O-10-03, 1 pl., 1:63,360, database files, 116 p. <http://www.oregongeology.org/pubs/ofr/p-O-10-03.htm>

- McInelly, G. W., and Kelsey, H. M., 1990, Late Quaternary tectonic deformation in the Cape Arago-Bandon region of coastal Oregon as deduced from wave-cut platforms: *Journal of Geophysical Research*, v. 95, no. B5, p. 6699–6713.
- McKeel, D. R., 1984, Biostratigraphy of exploratory wells in western Coos, Douglas, and Lane Counties, Oregon: Oregon Department of Geology and Mineral Industries Oil and Gas Investigation 11, 19 p., 1 pl. <http://www.oregongeology.org/pubs/ogi/OGI-11.pdf>
- Medaris, L. G., 1972, High-pressure peridotites in southwestern Oregon: *Geological Society of America Bulletin*, v.83, p. 41–58.
- Mertzman, S. A., 2000, K-Ar results from the southern Oregon – northern California Cascade Range: *Oregon Geology*, v. 62, no. 4, p. 99–122. <http://www.oregongeology.org/pubs/og/OGv62n04.pdf>
- Miles, G. A., 1981, Planktonic foraminifers of the lower Tertiary Roseburg, Lookingglass, and Flournoy Formations (Umpqua Group), southwest Oregon, in *Armstrong, J. M., ed., Pacific Northwest Cenozoic biostratigraphy: Geological Society of America Special Paper 184*, p. 85–104.
- Molenaar, C. M., 1985, Depositional relations of Umpqua and Tyee Formations (Eocene), southwestern Oregon: *AAPG Bulletin*, v. 69, p. 1217–1229.
- Muhs, D. R., Kelsey, H. M., Miller, G. H., Kennedy, G. L., Whelan, J. F., and McInelly, G. W., 1990, Age estimates and uplift rates for late Pleistocene marine terraces: southern Oregon portion of the Cascadia Forearc: *Journal of Geophysical Research*, v. 95, p. 6685–6698.
- Nelson, A. R., Aspuith, A. C., and Grant, W. C., 2004, Great earthquakes and tsunamis of the past 2000 years at the Salmon River estuary, central Oregon coast, USA: *Geological Society of America*, v. 94, p. 1276–1292.
- Newton, V. C., Jr., Kulm, L. D., Couch, R. W., Braman, D., Pitts, G. S., Van Atta, R. O., and McKeel, D. R., 1980, Prospects for oil and gas in the Coos Bay basin, western Coos, Douglas, and Lane Counties, Oregon: Oregon Department of Geology and Mineral Industries Oil and Gas Investigation 6, 74 p. <http://www.oregongeology.org/pubs/ogi/OGI-06.pdf>
- Niem, A. R., and Niem, W. A., 1990, Geology and oil, gas, and coal resources, southern Tyee basin, southern Coast Range, Oregon: Oregon Department of Geology and Mineral Industries, Open-File Report O-89-3, 11 tables, 3 pl., 44 p. <http://www.oregongeology.org/pubs/ofr/O-89-03.zip>
- Ogg, J. G., Ogg, G., and Gradstein, F. M., 2008, *The concise geologic time scale*: New York, Cambridge University Press, 177 p.
- Orr, W. N., Ehlen, J., and Zaitzeff, J. B., 1971, A late Tertiary diatom flora from Oregon: *Proceedings of the California Academy of Sciences*, Fourth Series, v. 37, no. 16, p. 489–500.
- Orr, W. N., and Zaitzeff, J. B., 1970, Miocene silicoflagellates from southeast Oregon: *Northwest Science*, v. 44, no. 1, p. 12–15.
- Peterson, C. D., Stock, E., Price, D. M., Hart, R., Reckendorf, F., Erlandson, J. M., and Hostetler, S. W., 2007, Ages, distributions, and origins of upland coastal dune sheets in Oregon, USA: *Geomorphology*, v. 91, p. 80–102.
- Priest, G. R., Allen, J. C., Meyers III., E. P., and Baptista, A. M., 2002, Tsunami hazard map of the Coos Bay area, Coos County, Oregon: Oregon Department of Geology and Mineral Industries Interpretive Map Series IMS-21, 20 p., scale 1:24,000. <http://www.oregongeology.org/pubs/ims/IMS-021.zip>
- Priest, G. R., and Baptista, A. M., 1995a, Tsunami hazard map of Bandon quadrangle, Coos county, Oregon Department of Geology and Mineral Industries Open-File Report O-95-51, scale 1:24,000. <http://www.oregongeology.org/pubs/ofr/O-95-51.pdf>
- Priest, G. R., and Baptista, A. M., 1995b, Tsunami hazard map of Bill Peak quadrangle, Curry County, Oregon Department of Geology and Mineral Industries Open-File Report O-95-52, scale 1:24,000. <http://www.oregongeology.org/pubs/ofr/O-95-52.pdf>
- Prothero, D. R., and Donohoo, L. L., 2001, Magnetic stratigraphy and tectonic rotation of the middle Eocene Coaledo Formation, southwestern Oregon: *Geophysical Journal International*, v. 145, p. 223–232.
- Ramp, L., Schlicker, H. G., and Gray, J. J., 1977, Geology, mineral resources, and rock material of Curry County, Oregon: Oregon Department of Geology and Mineral Industries Bulletin 93, 79 p. <http://www.oregongeology.org/pubs/B/B-093.pdf>
- Rau, W. W., 1973, Preliminary identifications of foraminifera from E. M. Warren Coos County No. 1-7 well, Oregon: Oregon Department of Geology and Mineral Industries Oil and Gas Investigation 4, 2 p., 2 pl. <http://www.oregongeology.org/pubs/ogi/OGI-04.pdf>
- Raymond, K. R., Prothero, D., Emerson, L., and Retallack, G., 2008, Magnetogstratigraphy of the lower Miocene sandstone of Floras Lake and the Cape Blanco flora, Oregon: *Geologic Society of America Abstracts with Programs*, v. 40, no. 6, p. 477.

- Raymond, L. A., 1984, Classification of mélanges, *in* Raymond, L. A., ed., Mélanges: Their nature, origin and significance: Geological Society of America Special Paper 198, p. 7–20.
- Ricker, T. R., and Niewendorp, C. A., 2013, Radiometric age information layer for Oregon, release 1: Oregon Department of Geology and Mineral Industries RAILO-1, GIS files. <http://www.oregongeology.org/pubs/dds/p-RAILO-1.htm>
- Robertson, R. D., 1982, Subsurface stratigraphic correlations of the Eocene Coaledo Formation, Coos Bay basin, Oregon: Oregon Geology, v. 44, no. 7, p. 75–82. <http://www.oregongeology.org/pubs/og/OGv44n07.pdf>
- Robertson, S., 1999, BGS rock classification scheme, v. 2, Classification of metamorphic rocks: British Geological Survey Research Report 99-02, 24 p.
- Rooth, G. H., 1974, Biostratigraphy and paleocology of the Coaledo and Bastendorff Formations, southwestern Oregon: Corvallis, Oregon State University Ph.D. dissertation, 270 p.
- Roure, F., and Blanchet, R., 1983, A geological transect between the Klamath Mountains and the Pacific Ocean (southwestern Oregon): a model for paleosubductions: Tectonophysics, v. 91, p. 53–72.
- Ryberg, P. T., 1978, Lithofacies and depositional environment of the Coaledo Formation, Coos County, Oregon: Eugene, University of Oregon M.S. thesis, 159 p.
- Ryberg, P. T., 1984, Sedimentation, structure, and tectonics of the Umpqua Group (Paleocene to early Eocene), southwestern Oregon: Tucson, Arizona, University of Arizona, Ph.D. dissertation, 280 p.
- Ryu, I., and Niem, A. R., 1999, Tectonic influences on sequence architecture at a convergent margin, southern Eocene Tyee basin, Oregon Coast Range: Journal of Sedimentary Research, v. 69, no. 2, p. 384–393.
- Ryu, I., Niem, A. R., and Niem, W. A., 1992, Schematic fence diagram of the southern Tyee Basin, Oregon Coast Range, showing stratigraphic relationships of exploration wells to surface measured sections: Oregon Department of Geology and Mineral Industries Oil and Gas Investigation 18, 28 p., 1 pl. <http://www.oregongeology.org/pubs/ogi/OGI-18.pdf>
- Seiders, V. M., and Blome, C. D., 1987, Stratigraphy and sedimentology of Upper Cretaceous rocks in coastal southwest Oregon: Evidence for wrench-fault tectonics in a postulated accretionary terrane: Alternative interpretation and reply: Geological Society of America Bulletin, v. 98, p. 739–744.
- Silberling, N. J., Jones, D. L., Blake, M. C., Jr., and Howell, D. G., 1987, Lithotectonic terrane map of the western continuous United States: U.S. Geological Survey Miscellaneous Field Studies Map MF-1874-C, 1:2,500,000, 20 p. <https://pubs.er.usgs.gov/publication/mf1874C>
- Silver, E. A., and Beutner, E. C., 1980, Mélanges: Geology, v. 8, p. 32–34.
- Sliter, W. V., 1984, Cretaceous low-latitude pelagic limestone from the Franciscan complex, California, and the Sixes River terrane, Oregon: Geological Society of America Abstracts with Programs, v. 16, no. 5, p. 333.
- Sloan, Jan, Henry, C. D., Hopkins, M., Ludington, S. D., (eds.), and Zartman, R. E., Bush, C. A., and Abston, C. C., (compilers), 2003, National Geochronological Database (<http://mrddata.usgs.gov/geochron/>): U.S. Geological Survey Open-File Report 03-236. https://pubs.er.usgs.gov/publication/ofr03326_rev
- Snively, P. D., Jr., 1987, Tertiary geologic framework, neotectonics, and petroleum potential of the Oregon-Washington continental margin, *in* Scholl, D. S., Grantz, A., and Vedder, J. G., eds., Geology and resource potential of the continental margin of western North American and adjacent ocean basins; Beaufort Sea to Baja California: Circum-Pacific Council for Energy and Mineral Resources Earth Science Series, v. 6, p. 305–335.
- Snively, P. D., Jr., MacLeod, N. S., and Wagner, H. C., 1968, Tholeiitic and alkali basalts of the Eocene Siletz River Volcanics, Oregon Coast Range: American Journal of Science, v. 266, p. 454–481.
- Snively, P. D., Jr., Wagner, H. C., and Lander, D. L., 1980, Geological cross section of the central Oregon continental margin: Geological Society of America Map and Chart Series MC-28J, scale 1:250,000.
- Snively, P. D., Jr., Wagner, H. C., and Rau, W. W., 1982, Sections showing biostratigraphy and correlation of Tertiary rocks penetrated in wells drilled on the southern Oregon continental margin: U.S. Geological Survey Miscellaneous Field Studies Map MF-1482, 1 Sheet, 1:20,000. <https://pubs.er.usgs.gov/publication/mf1482>
- Stewart, R. E., 1956, Stratigraphic Implications of some Cenozoic foraminifera from western Oregon: Oregon Department of Geology and Mineral Industries, Ore.-Bin, v. 18, no. 7, p. 57–63. <http://www.oregongeology.org/pubs/og/OBv18n07.pdf>
- Stewart, R. E., 1957, Stratigraphic implications of some Cenozoic foraminifera from western Oregon: The Ore Bin, v. 19, no. 2, p. 11–15. <http://www.oregongeology.org/pubs/og/OBv19n02.pdf>

- Tarduno, J. A., McWilliams, M., and Sleep, N., 1990, Fast instantaneous oceanic plate velocities recorded by the Laytonville limestone: paleomagnetic analysis and kinematic implications: *Journal of Geophysical Research*, v. 95, no. B10, p. 15,503–15,527.
- Tipton, A. 1975, Foraminiferal biostratigraphy of the late Eocene to early Oligocene type Bastendorff Formation, near Coos Bay, Oregon, *in* Weaver, D. W., Hornaday, G. R., and Tipton, A., eds., *Paleogene symposium and selected technical papers: Conference on future energy horizons of the Pacific Coast*: Long Beach, Calif.: Pacific Sections, AAPG-SEPM-SEG, p. 563–585.
- Toenges, A. L., Dowd, J. J., Turnbulol, L. A., Schopf, J. M., Cooper, H. M., Abernethy, R. E., Yancey, H. F., and Geer, M. R., 1948, Minable reserves, petrography, chemical characteristics, and washability tests of coal occurring in the Coos Bay coal field, Coos County, Oregon: U.S. Bureau of Mines Technical Paper 707, 56 p.
- Turner, F. E., 1938, Stratigraphy and mollusca of the Eocene of western Oregon: *Geological Society of America Special Paper* 10, 130 p.
- Walker, G. W., and McLeod, N. S., 1991, Geologic map of Oregon: U.S. Geological Survey, Washington, D.C., scale 1:500,000. http://ngmdb.usgs.gov/Prodesc/prodesc_16259.htm
- Warren, A. D., and Newell, J. H., 1981, Calcareous plankton biostratigraphy of the type Bastendorff Formation, Southwest Oregon, *in* Armentrout, J. M., ed., *Pacific Northwest Cenozoic biostratigraphy: Geological Society of America Special Paper* 184, p. 105–112.
- Weaver, C. M., 1945, Stratigraphy and paleontology of the Tertiary formations at Coos Bay, Oregon: *Seattle, University of Washington, Publications in Geology*, v. 6, p. 31–62.
- Wells, R., Bukry, D., Friedman, R., Pyle, D., Duncan, R., Haeussler, P., and Wooden, J., 2014, Geologic history of Siletzia, a large igneous province in the Oregon and Washington Coast Range: Correlation to the geomagnetic polarity time scale and implications for a long-lived Yellowstone hotspot: *Geosphere*, v. 10, p. 692–719.
- Wells, R. E., Jayko, A. S., Niem, A. R., Black G., Wiley, T., Baldwin, E., Molenaar, K. M., Wheeler, K. L., DuRoss, C. B., and Givler, R. W., 2000, Geologic map and database of the Roseburg 30 × 60' quadrangle, Douglas and Coos Counties, Oregon: U.S. Geological Survey Open-File Report 00-376, 1:100,000, 55 p. <http://pubs.er.usgs.gov/publication/ofr00376>
- Wentworth, C. K., 1922, A scale of grade and class terms of clastic sediments: *Journal of Geology*, v. 30, p. 377–392.
- Wiley, T. J., 2008, Preliminary geologic maps of the Corvallis, Wren, and Marys Peak 7.5' quadrangles, Benton, Lincoln, and Linn, Counties, Oregon: Oregon Department of Geology and Mineral Industries Open-File Report O-08-14, 1:24,000, 13 p. <http://www.oregongeology.org/pubs/ofr/O-08-14.zip>
- Wiley, T. J., and Black, G. L., 1994, Geologic map of the Tenmile quadrangle, Douglas County, Oregon: Oregon Department of Geology and Mineral Industries Geologic Map Series GMS-86, 1:24,000, 5 p. <http://www.oregongeology.org/pubs/gms/GMS-086.pdf>
- Wiley, T. J., McClaughry, J. D., and D' Allura, J., 2011, Geologic database and generalized geologic map of Bear Creek Valley, Jackson County, Oregon: Oregon Department of Geology and Mineral Industries Open-File Report O-11-11, 75 p., scale 1:63,360. <http://www.oregon-geology.org/pubs/ofr/p-O-11-11.htm>
- Wiley, T. J., McClaughry, J. D., Ma, L., Mickelson, K. A., Niewendorp, C. A., Stimely, L. L., Herinckx, H. H., and Rivas, J., 2014, Geologic map of the southern Oregon coast between Port Orford and Bandon, Curry and Coos Counties, Oregon: Oregon Department of Geology and Mineral Industries Open-File Report O-14-01, 1:24,000, geodatabase, 66 p. <http://www.oregongeology.org/pubs/ofr/p-O-14-01.htm>
- Witter, R. C., Kelsey, H. M., and Hempill-Haley, E., 2003, Great Cascadia earthquakes and tsunamis of the past 6700 years, Coquille River estuary, southern coastal Oregon: *Geological Society of America Bulletin*, v. 115, p. 1289–1306.
- Witter, R. C., Zhang, Y., Wang, K., Priest, G. R., Goldfinger, C., Stimely, L. L., English, J. T., and Ferro, P. A., 2011, Simulating tsunami inundation at Bandon, Coos County, Oregon, using hypothetical Cascadia and Alaska earthquake scenarios: Oregon Department of Geology and Mineral Industries Special Paper 43, 57 p., scales 1:63,360 and 1:10,000. <http://www.oregongeology.org/pubs/sp/p-SP-43.htm>

APPENDIX—GEOGRAPHIC INFORMATION SYSTEMS (GIS) DATABASE

This appendix describes the digital databases included with this publication.

Geodatabase specifications

Digital data compiled for the southern Oregon coast are stored in an Esri-format geodatabase. The following information describes the overall database structure, feature classes, and supplemental tables.

The data are stored in an Esri-formatted geodatabase and were created using ArcGIS version 10.1 (SP 1). The geodatabase contains two feature data sets: **GeologicMap** and **Relationships** (Figure A1). **GeologicMap** contains all of the spatially oriented data (feature classes) created for this project. The **Relationships** feature data set is used to hold all of the relationships created to connect or relate the supplemental tables to each other or to the MapUnitPolys feature class.

Figure A2 shows the relationships between the tables and the MapUnitPolys feature class. All supplemental tables eventually relate to the *tblMapUnit*, through either a direct or indirect relationship. The *tblMapUnit* table is the only table with a relationship to the MapUnitPolys feature class.

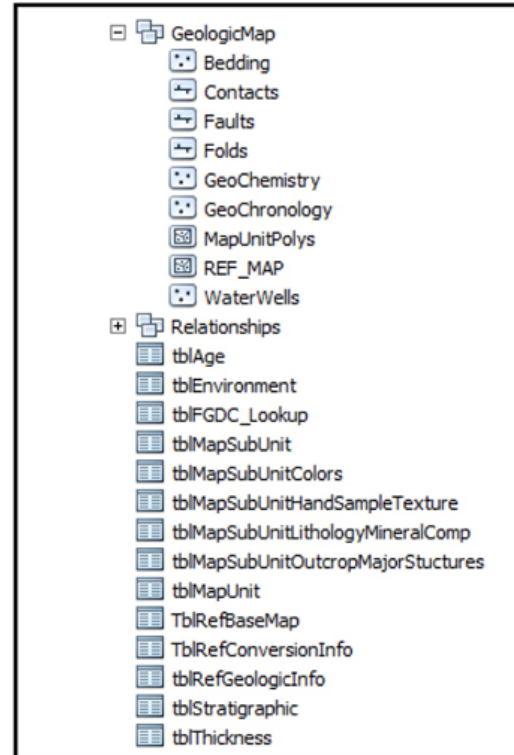


Figure A1. Southern Oregon coast geodatabase feature data sets.

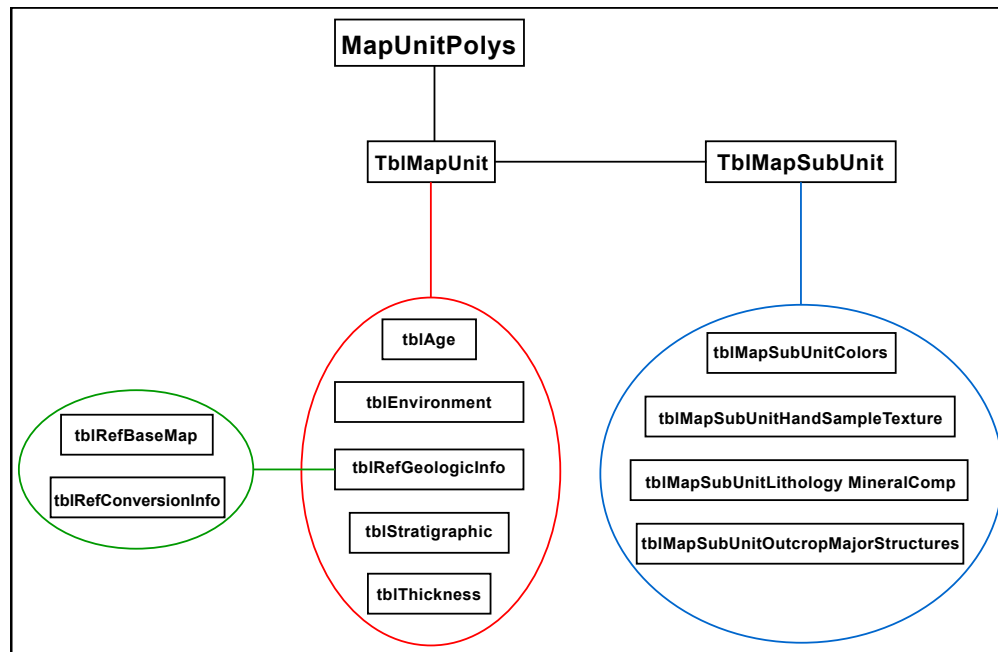


Figure A2. Relationships between tables and MapUnitPolys feature class in the geodatabase.

Geodatabase feature class specifications

Each feature class within the geodatabase has detailed metadata to accompany the data. Please see the metadata for detailed information such as process descriptions, accuracy specifications, and entity attribute descriptions. Figure A3 is provided as a summary description for each feature class.

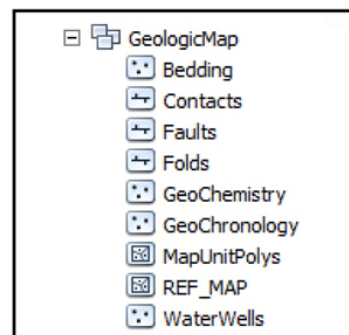
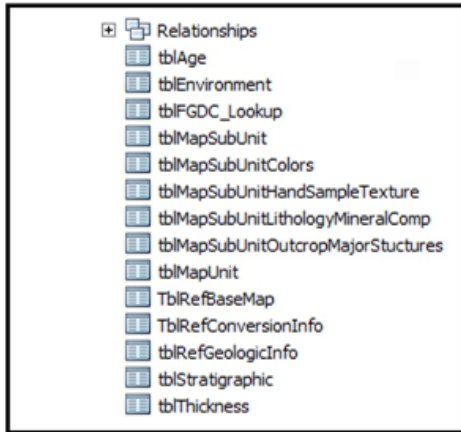


Figure A3. Southern Oregon coast geodatabase feature classes.

| Feature Class Name | Description |
|--------------------|---|
| Bedding | This feature class represents point locations where bedding measurements were made, or were compiled from previous studies, along the southern Oregon coast during the course of this study. These data are also contained in the bedding (strike and dip) database described in more detail below. |
| Contacts | The vector lines in this feature class denote confidence in position and nature of boundaries between rock types. Unconcealed contacts were used along with unconcealed faults to create map unit polygons. |
| Faults | These vector lines represent known fault locations along the southern Oregon coast. The existence and location confidence for the faults are provided in the feature class attribute table. Unconcealed faults were combined with unconcealed contacts to create map unit polygons. |
| Folds | These vector lines represent known fold axis locations along the southern Oregon coast. The existence and location confidence for the fold axes are provided in the feature class attribute table. |
| GeoChemistry | This feature class represents point locations where whole-rock samples have been analyzed by X-ray fluorescence (XRF) techniques. Includes data collected by the authors during the course of this study or compiled from previous studies along the southern Oregon coast. These data are also contained in the geochemistry database described in more detail below. |
| GeoChronology | This feature class represents point locations where $^{206}\text{Pb}/^{238}\text{U}$ (zircon) or other $^{40}\text{Ar}/^{39}\text{Ar}$, K/Ar, ^{14}C , uranium series, and thermoluminescence (TL) isotopic ages have been obtained for rock samples along the southern Oregon coast. Includes data collected by the authors during the course of this study or compiled from previous studies. These data are also contained in the geochronology database described in more detail below. |
| MapUnitPolys | A polygon feature class representing the geologic map units as defined by the authors. |
| REF_MAP | This feature class depicts the southern Oregon coast study area. |
| WaterWells | This feature class represents point locations where water wells were located along the southern Oregon coast. Includes data obtained by the authors from the Oregon Department of Water Resources (OWRD). These data are also contained in the water well database described in more detail below. |

Geodatabase table specifications**Figure A4.** Southern Oregon coast geodatabase relationships.

| Table Name | Description |
|--|--|
| <i>tblAge</i> | Contains information about the stratigraphic and radiometric age of the map unit; relates to the <i>tblMapUnit</i> table. |
| <i>tblEnvironment</i> | Contains information about the genetic environment and landform and whether or not information exists for geochemistry, paleontology, or petrology; relates to the <i>tblMapUnit</i> table. |
| <i>tblFGDC_Lookup</i> | Contains descriptions for the reference codes used to attribute the line and point features. Codes are defined in the FGDC Digital Cartographic Standard for Geologic Map Symbolization (http://www.fgdc.gov/standards/projects/FGDC-standards-projects/geo-symbol). |
| <i>tblMapSubUnit</i> | Contains information about the components, or subunits, of the reference map unit; relates to the <i>tblMapUnit</i> table. |
| <i>tblMapSubUnitColors</i> | Lists colors of the fresh and weathered rock surfaces for a subunit; relates to the <i>tblMapSubUnit</i> table. |
| <i>tblMapSubUnitHandSampleTexture</i> | Contains information about the texture or appearance of a subunit at a hand sample level; relates to the <i>tblMapSubUnit</i> table. |
| <i>tblMapSubUnitLithologyMineralComp</i> | Contains information of mineral or composition descriptors for a subunit; relates to the <i>tblMapSubUnit</i> table. |
| <i>tblMapSubUnitOutcropMajorStructures</i> | Contains information about the structure of a subunit when viewed at the outcrop level; relates to the <i>tblMapSubUnit</i> table. |
| <i>tblMapUnit</i> | Contains all of the map units defined for the southern Oregon coast; includes the map unit geologic symbol and unit name; relates to the MapUnitPolys feature class. |
| <i>tblRefBaseMap</i> | Contains information about the base map; relates to the <i>tblGeologicInfo</i> table. |
| <i>tblRefConversionInfo</i> | Contains information about the conversion process to digital data; relates to the <i>tblRefGeologicInfo</i> table. |
| <i>tblRefGeologicInfo</i> | Contains the general bibliographic information about the map or database; relates to the <i>tblMapUnit</i> table. |
| <i>tblStratigraphic</i> | Contains formal or informal stratigraphic classification and names of the map units; relates to the <i>tblMapUnit</i> table. |
| <i>tblThickness</i> | Contains information about the total thickness of the mapped unit; relates to the <i>tblMapUnit</i> table. |

Geodatabase projection specifications

All spatial data are stored in the Oregon Statewide Lambert Conformal Conic projection. The datum is NAD83 HARN. The linear unit is international feet. See detailed projection parameters below:

Projection: Lambert_Conformal_Conic

False_Easting: 1312335.958005

False_Northing: 0.000000

Central_Meridian: -120.500000

Standard_Parallel_1: 43.000000

Standard_Parallel_2: 45.500000

Latitude_Of_Origin: 41.750000

Linear Unit: Foot (0.304800)

Geographic Coordinate System:

GCS_North_American_1983_HARN

Angular Unit: Degree (0.017453292519943299)

Prime Meridian: Greenwich (0.000000000000000000)

Datum: D_North_American_1983_HARN

Spheroid: GRS_1980

Semimajor Axis: 6378137.000000000000000000

Semiminor Axis: 6356752.314140356100000000

Inverse Flattening: 298.257222101000020000

Geologic maps

Plates 1–4 are geologic maps at a scale of 1:24,000 displaying the geology of the map area.

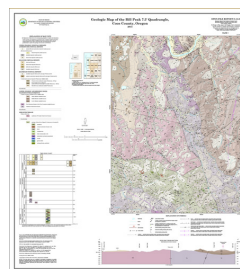


Plate 1: Geologic map of the Bill Peak 7.5' quadrangle, Coos County, Oregon

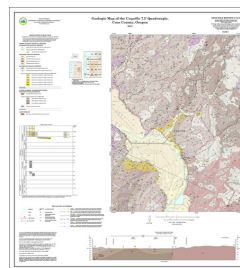


Plate 2: Geologic map of the Coquille 7.5' quadrangle, Coos Counties, Oregon

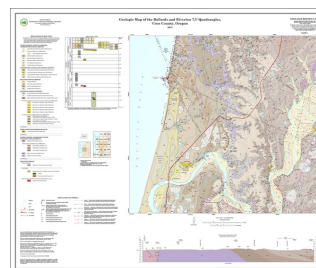


Plate 3: Geologic map of the Bullards and Riverton 7.5' quadrangles, Coos County, Oregon

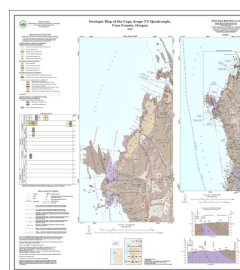


Plate 4: Geologic map of the Cape Arago 7.5' quadrangle, Coos County, Oregon

Geochemical analytical methods

Geologic mapping along the southern Oregon coast was supported by several new X-ray fluorescence (XRF) geochemical analyses of whole-rock samples of igneous rocks. Descriptive rock unit names for igneous rocks are based on normalized major element analyses plotted on the total alkalis ($\text{Na}_2\text{O} + \text{K}_2\text{O}$) versus silica (SiO_2) diagram (TAS) of Le Bas and others (1986), Le Bas and Streckeisen (1991), and Le Maitre and others (1989). New and compiled XRF geochemical analyses are included in the main geodatabase, as a separate shapefile named SC2015_Geochemistry, and are also provided in a Microsoft Excel® spreadsheet named SC2015_Geochemistry.xls. A readme file explaining fields listed in the spreadsheet can be found below. The locations of all geochemical samples are given in five coordinate systems: UTM Zone 10 (datum = NAD 27, NAD 83, units = meters), Geographic (datum = NAD 27, NAD 83, units = decimal degrees), and Oregon Lambert (datum = NAD 83, HARN, units = international feet).

Samples denoted by lab abbreviation F & M were analyzed by XRF at the Department of Geosciences, Franklin and Marshall College, Lancaster, Pennsylvania, under the direction of S. A. Mertzman. Detailed analytical procedures for the Franklin and Marshall X-ray laboratory were described by Boyd and Mertzman (1987) and Mertzman (2000) and are available online at <http://www.fandm.edu/earth-environment/laboratory-facilities/xrf-and-xrd-lab>. Notes for spreadsheet: nd, no data.

Readme file for southern Oregon coast geochemical database spreadsheet columns

| Field | Description |
|------------|--|
| SAMPLE_NO | A unique number identifying the sample. E.g., 78 SCJ 13. |
| MAP_NO | A unique number identifying the sample on the map plates. |
| QUADRANGLE | The USGS 7.5' quadrangle in which the sample is located. E.g., Bullards. |
| ELEV_FT | Elevation of sample location in feet. E.g., 20. |
| UTMN_NAD27 | Meters north in NAD 27 UTM projection, zone 10. |
| UTME_NAD27 | Meters east in NAD 27 UTM projection, zone 10. |
| LAT_NAD27 | Latitude in NAD 27 geographic coordinates. |
| LONG_NAD27 | Longitude in NAD 27 geographic coordinates. |
| UTMN_NAD83 | Meters north in NAD 83 UTM projection, zone 10. |

| | |
|-------------------------|--|
| UTME_NAD83 | Meters east in NAD 83 UTM projection, zone 10. |
| LAT_NAD83 | Latitude in NAD 83 geographic coordinates. |
| LONG_NAD83 | Longitude in NAD 83 geographic coordinates. |
| N_83HARN | Feet north in Oregon Lambert NAD 83, HARN, international feet. |
| E_83HARN | Feet east in Oregon Lambert NAD 83, HARN, international feet. |
| TERRANE_GR | Geologic group that the sample is assigned to. See GeologicMap , MapUnitPolys in the geodatabase. |
| FORMATION | Geologic formation that the sample is assigned to. See GeologicMap , MapUnitPolys in the geodatabase. |
| MEMBER | Geologic member that the sample is assigned to. See GeologicMap , MapUnitPolys in the geodatabase. |
| MAP_UNIT_N | Geologic unit that the sample is assigned to. See GeologicMap , MapUnitPolys in the geodatabase. E.g., Intrusive rocks. |
| MAP_UNIT_L | Unique label identifying the geologic unit that the sample is assigned to. See GeologicMap , MapUnitPolys in the geodatabase. E.g., Tbi. |
| TAS_LITHOLOGY | Rock name assigned based on the total alkalis ($\text{Na}_2\text{O} + \text{K}_2\text{O}$) versus silica (SiO_2) diagram (TAS) of Le Bas and others (1986), Le Bas and Streckeisen (1991), and Le Maitre and others (1989). E.g., Basalt, Rhyolite. |
| MAJOR ELEMENTS | SiO_2 , Al_2O_3 , TiO_2 , FeO^* , MnO, CaO, MgO, K_2O , Na_2O , P_2O_5 . In wt.%. |
| TRACE ELEMENTS | Ni, Cr, Sc, V, Ba, Rb, Sr, Zr, Y, Nb, Ga, Cu, Zn, Pb, La, Ce, Th, U, Co, Nd. In ppm. |
| LOI | Value for loss on ignition as reported by lab. |
| Fe_2O_3 | Iron (III) oxide or ferric oxide reported in original analysis. |
| FeO | Iron (II) oxide or ferrous oxide reported in original analysis. |
| REFERENCE | Publication reference, keyed to the reference list in this report. |
| METHOD | Analytical method used by laboratory that analyzed the sample. E.g., XRF. |
| LABORATORY | Analytical laboratory that analyzed the sample. E.g., F & M. |
| NOTES | Special information (e.g., alteration) about certain samples. |

Geochronology analytical methods

Several new $^{206}\text{Pb}/^{238}\text{U}$ radiometric age determinations, derived from detrital zircons in sandstones, were prepared and analyzed under the direction of Joshua Schwartz at California State University, Northridge. Zircon dating was performed by laser ablation-inductively coupled plasma-mass spectrometry (LA-ICP-MS), following the sample preparation and data analysis techniques outlined by Chang and others (2006). Original data for new $^{206}\text{Pb}/^{238}\text{U}$ isotopic ages are located in the Appendix on this CD. Several other K/Ar ages for igneous rocks adjacent to the map area and ^{14}C and Thermoluminescence (TL) ages reported for Quaternary surficial units, have also been compiled for the area (Fiebelkorn and others, 1983; Sloan and others, 2003; Witter and others, 2003; Peterson and others, 2007; Ricker and Niewendorp, 2013). Please note that K-Ar ages, determined with decay constants prior to 1977, have not been recalculated for this report. The geochronological data points are included in the geodatabase, as a separate shapefile named SC2015_Geochronology, and are also provided as a Microsoft Excel® spreadsheet named SC2015_Geochronology.xls. A readme file explaining fields listed in the spreadsheet can be found below. The locations of radiometric ages are given in five coordinate systems: UTM Zone 10 (datum = NAD 27, NAD 83, units = meters), Geographic (datum = NAD 27, NAD 83, units = decimal degrees), and Oregon Lambert (datum = NAD 83, HARN, units = international feet). Notes for spreadsheet: na, not applicable; nd, no data.

Readme file for southern Oregon coast geochronology database spreadsheet columns

| | |
|------------|--|
| SAMPLE_NO | A unique number identifying the sample. E.g., 14 SCJ 14. |
| CORE_ID | A unique number identifying a drill core from which the sample was obtained. |
| QUADRANGLE | The USGS 7.5' quadrangle in which the sample is located. E.g., Bullards. |
| ELEV_FT | Elevation of sample location in feet. E.g., 22. |
| UTMN_NAD27 | Meters north in NAD 27 UTM projection, zone 10. |
| UTME_NAD27 | Meters east in NAD 27 UTM projection, zone 10. |
| LAT_NAD27 | Latitude in NAD 27 geographic coordinates. |
| LONG_NAD27 | Longitude in NAD 27 geographic coordinates. |
| UTMN_NAD83 | Meters north in NAD 83 UTM projection, zone 10. |
| UTME_NAD83 | Meters east in NAD 83 UTM projection, zone 10. |
| LAT_NAD83 | Latitude in NAD 83 geographic coordinates. |

| | |
|--|--|
| LONG_NAD83 | Longitude in NAD 83 geographic coordinates |
| N_83HARN | Feet north in Oregon Lambert NAD 83, HARN, international feet |
| E_83HARN | Feet east in Oregon Lambert NAD 83, HARN, international feet |
| TERRANE_GR | Geologic group that the sample is assigned to. See GeologicMap , MapUnitPolys in the geodatabase. E.g., Sixes terrane. |
| FORMATION | Geologic formation that the sample is assigned to. See GeologicMap , MapUnitPolys in the geodatabase. E.g., Fulmar subterrane |
| MEMBER | Geologic member that the sample is assigned to. See GeologicMap , MapUnitPolys in the geodatabase. |
| MAP_UNIT_N sandstone of Fivemile Point | Geologic unit that the sample is assigned to. See GeologicMap , MapUnitPolys in the geodatabase. |
| MAP_UNIT_L | Unique label identifying the geologic unit that the sample is assigned to. See GeologicMap , MapUnitPolys in the geodatabase. E.g., Tefm |
| LITHOLOGY | Rock type analyzed. E.g., sandstone. |
| POLARITY N, R, I | Natural remanent magnetization of the sample analyzed. |
| AGE_MA | Age determined for the sample in millions of years. |
| ERROR_MA | Error in age determination in millions of years. |
| AGE_KA | Age determined for the sample in thousands of years. |
| ERROR_KA | Error in age determination in thousands of years. |
| REP_AGE_YBP | Calendar age for sample, where age is determined by the radiocarbon dating (^{14}C) method. Reported age in thousands of years. |
| REP_ERROR | Error in age determination in years before present. |
| METHOD | Analytical method used by laboratory that analyzed the sample. E.g., $^{206}\text{Pb}/^{238}\text{U}$. |
| MATERIAL_DATED | Type of material analyzed. E.g., detrital zircon. |
| REFERENCE | Publication reference, keyed to the reference list in this report. |
| LABORATORY | Analytical laboratory that analyzed the sample. E.g., CSUN |
| NOTES | Special information (e.g., alteration) about certain samples. |

Bedding (strike and dip)

Strike and dip measurements of inclined bedding were taken along the southern Oregon coast during the course of this study by traditional compass and clinometer methods. Additional measurements have been compiled from previous workers. Strikes and dips are reported in both quadrant format (e.g., N30W, 15NE) and azimuthal format using the right-hand rule (e.g., 330, 15NE, American convention). Field-measured bedding is coded by its appropriate Federal Geographic Data Committee (FGDC) reference number for geologic map symbolization. The measured point data are included in the geodatabase, a separate shapefile named SC2015_Bedding, and are also provided as a Microsoft Excel® spreadsheet named SC2015_Bedding.xls. A readme file explaining fields listed in the spreadsheet can be found below. The locations of these point data are given in five coordinate systems: UTM Zone 10 (datum = NAD 27, NAD 83, units = meters), Geographic (datum = NAD 27, NAD 83, units = decimal degrees), and Oregon Lambert (datum = NAD 83, HARN, units = international feet). Strike and dip symbols can be properly drawn by the Esri ArcMap product by opening the layer properties, categorizing by type, choosing the appropriate symbol, and rotating the symbol based on the “Strike_Azi” field. (The advanced button allows you to select the rotation field.) The rotation style should be set to geographic in order to maintain the right-hand rule property. Azimuths are given in true north; an additional clockwise correction of about 1.6 degrees is needed to plot strikes and dips properly on the Oregon Lambert conformal conic projection in this area. Notes for spreadsheet: nd, no data.

Readme file for southern Oregon coast strike and dip database spreadsheet columns

| | |
|------------|---|
| STRUCTURE | Type of geologic structure from which feature was determined. E.g., Inclined bedding. |
| FGDC_REF | An attribute code assigned to each feature, derived from the Federal Geographic Data Committee (FGDC) digital standard for geologic map symbolization. E.g., 6.2. |
| QUADRANGLE | The USGS 7.5' quadrangle in which the sample is located. E.g., Bullards. |
| ELEV_FT | Elevation of data location in feet. E.g., 22. |
| UTMN_NAD27 | Meters north in NAD 27 UTM projection, zone 10. |
| UTME_NAD27 | Meters east in NAD 27 UTM projection, zone 10. |
| LAT_NAD27 | Latitude in NAD 27 geographic coordinates. |

| | |
|-------------|--|
| LONG_NAD27 | Longitude in NAD 27 geographic coordinates. |
| UTMN_NAD83 | Meters north in NAD 83 UTM projection, zone 10. |
| UTME_NAD83 | Meters east in NAD 83 UTM projection, zone 10. |
| LAT_NAD83 | Latitude in NAD 83 geographic coordinates. |
| LONG_NAD83 | Longitude in NAD 83 geographic coordinates. |
| N_83HARN | Feet north in Oregon Lambert NAD 83, HARN, international feet. |
| E_83HARN | Feet east in Oregon Lambert NAD 83, HARN, international feet. |
| TERRANE_GR | Geologic group that the sample is assigned to. See GeologicMap , MapUnitPolys in the geodatabase. E.g., Sixes terrane. |
| FORMATION | Geologic formation that the sample is assigned to. See GeologicMap , MapUnitPolys in the geodatabase. E.g., Fulmar subterrane. |
| MEMBER | Geologic member that the sample is assigned to. See GeologicMap , MapUnitPolys in the geodatabase. |
| MAP_UNIT_N | Geologic unit that the sample is assigned to. See GeologicMap , MapUnitPolys in the geodatabase. E.g., sandstone of Fivemile Point. |
| MAP_UNIT_L | Unique label identifying the geologic unit that the sample is assigned to. See GeologicMap , MapUnitPolys in the geodatabase. E.g., Tefm . |
| STRIKE_QUAD | Strike direction of the inclined plane, stated in a north-directed quadrant format. E.g., N35E. |
| DIP | Amount of dip, degrees from horizontal, with direction. E.g., 45SE. |
| STRIKE_AZI | Strike direction of the inclined plane, as determined by employing the right-hand rule (American convention). E.g., 035. |
| DIP_AZIMUTH | Azimuthal direction of dip. E.g., 125. |
| DIP_AMOUNT | Amount of dip, degrees from horizontal. E.g., 45. |
| REFERENCE | Publication reference, keyed to the reference list in this report. |
| NOTES | Special information (e.g., alteration) about certain samples. |

Water well logs

The well log database is derived from written drillers' logs provided by Oregon Department of Water Resources (OWRD). Well logs vary greatly in completeness and accuracy, therefore locally limiting the utility of subsurface interpretations based upon these data. Water well logs compiled and used for interpretation during the course of this study were not field located. The approximate locations were estimated using tax lot maps, street addresses (coordinates obtained from Google Earth™), and aerial photographs to plot locations on the map. Location accuracy ranges widely, from errors of one-half mile possible for wells located only by section and plotted at the section centroid to a few tens of feet for wells located by address or tax lot number on a city lot with bearing and distance from a corner. At each mapped location the number of the well log is indicated. This number can be combined with the first four letters of the county name (e.g., CURR 5473), to retrieve an image of the well log from the OWRD web site (http://apps.wrd.state.or.us/apps/gw/well_log/).

The measured point data are included in the geodatabase, as a separate shapefile named SC2015_WaterWells and are also provided as a Microsoft Excel® spreadsheet named SC2015_WaterWells.xls. A readme file explaining fields listed in the spreadsheet can be found below. The locations of water well point data are given in six coordinate systems: UTM Zone 10 (datum = WGS 84, NAD 27, NAD 83, units = meters), Geographic (datum = NAD 27, NAD 83, units = decimal degrees), and Oregon Lambert (datum = NAD 83, HARN, units = international feet).

Well intervals listed in the well log database sometimes alternate between consolidated and unconsolidated lithologies and may be listed as alternating between bedrock and surficial geologic units. This may occur where bedrock units are soft (lower Pleistocene and Miocene units), where paleosols or weak zones (mélange) lie within bedrock, and, most commonly, where cemented or partly cemented zones alternate with unconsolidated zones in surficial deposits.

Readme file for southern oregon coast well log database

Lithologic abbreviations used (alphabetical by group)

| UNCONSOLIDATED SURFICIAL UNITS | |
|--------------------------------|---|
| a | ash |
| bd | boulders |
| c | clay |
| ch | clay, hard (often logged as claystone but probably not bedrock) |
| g | gravel |

| | |
|--------------------------|--------------------------------------|
| gc | cemented gravel |
| gs | gravel and sand (also sandy gravel) |
| m | mud |
| s | sand |
| sg | sand and gravel (also gravelly sand) |
| st | silt |
| ROCK, sedimentary | |
| a | argillite |
| bc | breccia |
| cg | conglomerate |
| cs | claystone |
| pbs | pebbly sandstone |
| sh | shale |
| sts | siltstone |
| ss | sandstone |
| ROCK, igneous | |
| an | andesite |
| b | basalt |
| ba | basaltic andesite |
| cd | cinders |
| pu | pumice |
| d | diorite |
| gb | gabbro |
| gr | granite |
| l | lava |
| r | rhyolite |
| sc | scoria |
| t | tuff |
| v | volcanic, undivided |
| vb | volcanic breccia |
| Rock, metamorphic | |
| mv | meta-volcanic rocks, undivided |
| ms | meta-sedimentary rocks, undivided |
| grn | greenstone |
| gn | gneiss |
| p | peridotite |
| ph | phyllite |
| sch | schist |
| slt | slate |
| sp | serpentine |
| OTHER | |
| af | artificial fill |
| cl | coal (lignite) |
| dg | decomposed granite |

| | |
|----|---|
| o | other (drillers unit listed in notes column of spreadsheet) |
| rk | rock |
| sl | soil |
| u | unknown (typically used where a well has been deepened) |

Water well log spreadsheet columns

| Field | Description and Example |
|------------|--|
| TRS | One digit for township, two digits for range, and section; negative if township is south of Willamette baseline. E.g., -10931. |
| COUNTY | Coos County. E.g., COOS. |
| GRID | Well log number for wells. Wells in Coos County preceded by acronym COOS (e.g., COOS 53799). E.g., 53779. |
| WELL_EL_FT | Wellhead elevation in feet as given by Google Earth™ at corresponding WGS 84 location. E.g., 100. |
| LOCATED_BY | Google Earth™ elevation for cursor location at a given address. E.g., Google. |
| | Google Earth™ elevation at house in vicinity of given address. E.g., House. |
| | Pad identifying approximate well location, visible in air photo. E.g., Pad. |
| | Approximate taxlot centroid or other best guess for well location using a combination of taxlot maps and aerial photographs. E.g., Taxlot. |
| | Owner name. E.g., Owner. |
| | Wells located by Oregon Water Resources Department (OWRD) using handheld GPS. E.g., OWRD. |
| | GPS coordinates of wellhead included with well log. E.g., GPS. |
| | Approximate quarter-quarter-section centroid. E.g., qq. |
| | Approximate quarter-section centroid. E.g., q. |
| | Approximate fit to sketch map included with well log. E.g., map |
| LITHOLOGY | Best interpretation of driller's log using abbreviations above. E.g., g. |
| BASE_FT | Record base of driller's interval or, if lithology abbreviation would not change, similar intervals, in feet below wellhead. E.g., 17. |
| TOP_FT | Calculated top of driller's interval or similar intervals, in feet below wellhead. E.g., 14. |

| | |
|--|---|
| TOP_EL_FT | Calculated elevation at top of driller's interval, or similar intervals, in feet above sea level. E.g., 86. |
| BASE_EL_FT | Calculated elevation at base of driller's interval, or similar intervals, in feet above sea level. E.g., 83. |
| BEDRK_LITH | Lists bedrock lithologies, when encountered, abbreviations listed above. E.g., ss. |
| BEDRK_ELEV | Calculated elevation at which bedrock or soil over bedrock was first encountered, in feet above sea level. E.g., 83. |
| TAX_LOT | Taxlot number. Where it is determined that a taxlot number is used more than once in the section then the appropriate subdivision of the section is indicated in the notes field. E.g., 800. |
| NOTES | Notes about the stratigraphic interval as originally described by the well driller. |
| MAP_UNIT_L | Geologic unit interpreted in subsurface on the basis of drillers log and designated by map unit label used in accompanying geodatabase. Intervals labeled "suna" (surface unit not applicable) are those where the lithology as interpreted by the original drillers' log do not correspond; also denotes intervals in the subsurface where a precise unit label cannot be applied. E.g., Tefm . |
| QUADRANGLE | The USGS 7.5' quadrangle in which the sample is located. E.g., Bullards. |
| <i>*Well location given in six coordinate systems calculated by reprojecting original WGS 84 UTM, zone 10 locations.</i> | |
| UTMN_WGS84 | Meters north in WGS84 UTM projection, zone 10. |
| | |
| UTME_WGS84 | Meters east in WGS84 UTM projection, zone 10. |
| UTMN_NAD27 | Meters north in NAD 27 UTM projection, zone 10. |
| UTME_NAD27 | Meters east in NAD 27 UTM projection, zone 10. |
| LATITUDE_NAD27 | Latitude in NAD 27 geographic coordinates. |
| LONGITUDE_NAD27 | Longitude in NAD 27 geographic coordinates. |
| UTMN_NAD83 | Meters north in NAD 83 UTM projection, zone 10. |
| UTME_NAD83 | Meters east in NAD 83 UTM projection, zone 10. |
| LATITUDE_NAD83 | Latitude in NAD 83 geographic coordinates. |
| LONGITUDE_NAD83 | Longitude in NAD 83 geographic coordinates. |
| N_83HARN | Feet north in Oregon Lambert NAD 83, HARN, international feet. |
| E_83HARN | Feet east in Oregon Lambert NAD 83, HARN, international feet. |